Exelon®
Nuclear

# Exelon Nuclear
# Pre-Submittal Meeting

Proposed Relaxation Request
from
First Revised Order EA-03-009
Byron Station Unit 2

February 13, 2008

Exelon Nuclear

# Agenda

Introduction – Pat Simpson

Background and Inspection Results – Scot Greenlee

Boat Sample Results – Jean Smith

Growth and Probabilistic Assessments – Guy DeBoo

Fall 2008 Inspection Plans– Scot Greenlee

Evaluation Conclusions – Rich Hall

Proposed Relaxation Request – Dave Chrzanowski

Closing Remarks - Scot Greenlee

Exelon Nuclear

# Introduction

Patrick Simpson

Manager - Licensing

Exelon Nuclear

# Meeting Purpose

- ✓ Convey Exelon Nuclear's plans regarding the Byron Unit 2 reactor pressure vessel (RPV) head
- ✓ Obtain NRC feedback
  - Relaxation request submittal
  - Inspection scope

Exelon Nuclear

# Background and Inspection Results

Scot Greenlee

Byron Station Engineering Director

Exelon Nuclear

# Background

- ✓ Unit 2 RPV head
  - Westinghouse 4-loop NSSS design
  - Head penetration nozzles were provided by B&W Tubular Products
  - The RPV head fabrication and penetration nozzle installation were by B&W
- ✓ Unit 2 commercial operation – August 1987
- ✓ Unit 2 is a T-Cold Head (550°F)
  - 2.2 Effective Degradation Years (EDY)
- ✓ Prior to the Spring 2007 refueling outage (B2R13), Bare Metal Visual (BMV) examinations were performed in:
  - Fall 2002 (B2R10)
  - Fall 2005 (B2R12)

Exelon Nuclear

# Inspection Results

- ✓ Industry - no defects found
  - U.S. – 1560 RPV upper head penetrations inspected
    - Head temperatures ≤ 561°F
    - One remaining low-susceptibility head inspection in Spring 2008
  - U.S. – 804 RPV bottom mounted penetrations
  - International – More than 1600 bottom mounted penetrations inspected
- ✓ Byron and Braidwood Stations
  - 100% BMV – no indications
  - 100% volumetric ultrasonic testing (UT) – Byron Unit 2 penetration 68 axial indication
  - Leak path assessment did not detect any leaks
- ✓ Unit 2 penetration 68 results
  - UT exam revealed 50% through-wall axial indication ~0.52" long
  - Subsequent dye penetrant (PT) exam of J-groove weld identified one rounded and one linear indication

# Inspection Results (continued)

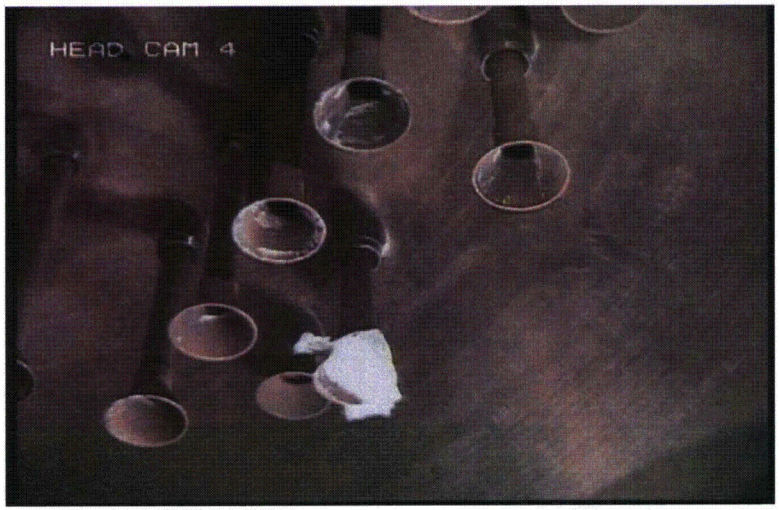


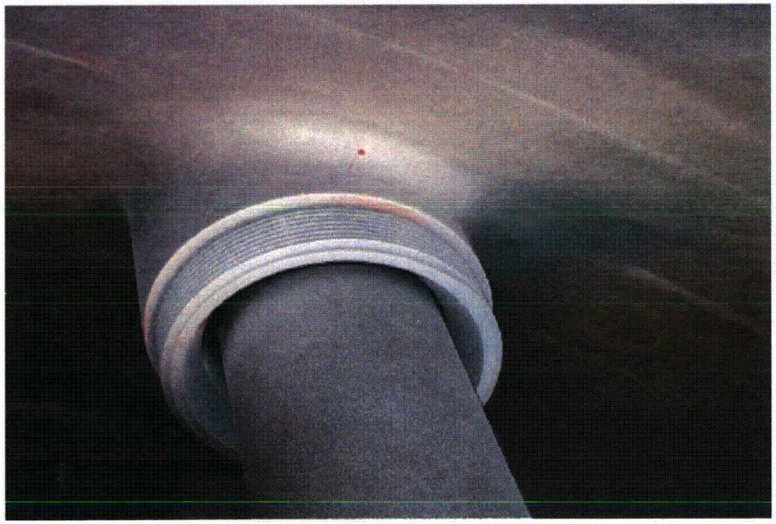

Exelon Nuclear

# Boat Sample Results

Jean Smith
Senior Materials Engineer
Corporate Asset Management

# Boat Sample Results

- ✓ Rounded subsurface defect captured by the boat sample identified as lack of fusion between the weld and tube surfaces
  - Incipient cracks were observed emanating from the defect
  - Weld defect produced during original fabrication process
- ✓ Linear indication exhibited multiple defect/crack morphologies including lack of fusion, hot cracking, and PWSCC
  - In the weld, the direction of PWSCC propagation was from the subsurface location toward the wetted surface
  - In the tube material, none of the PWSCC was connected to the outer surface of the tube below the J-groove and/or fillet weld

Cut surface of boat sample

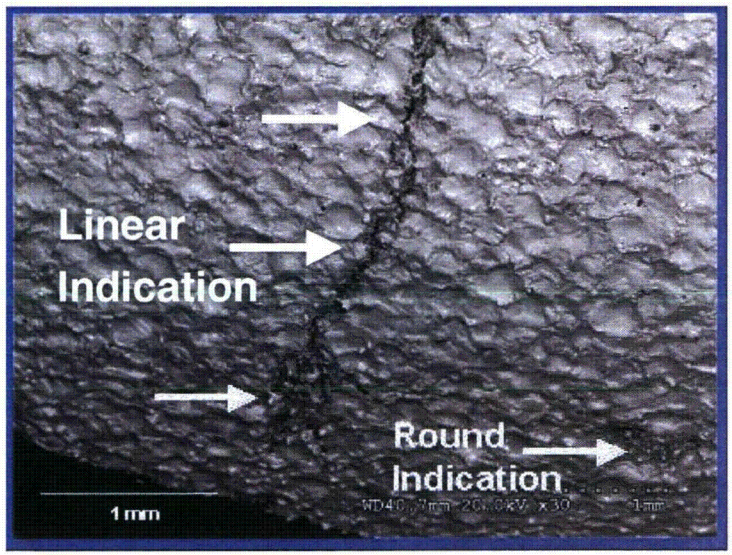


SEM Image of inset area above

# Boat Sample Results (continued)

- ✓ Subsurface linear defect is connected to the lack-of-fusion defect
- ✓ Evidence indicates a high probability that the rounded PT indication not captured by the boat sample was connected below the surface to the lack-of-fusion defect
- ✓ A surface flaw the size of the rounded indication would have been considered acceptable by ASME Code of fabrication for Byron Station
- ✓ Heavy grinding in this area may have masked the indication during fabrication exams

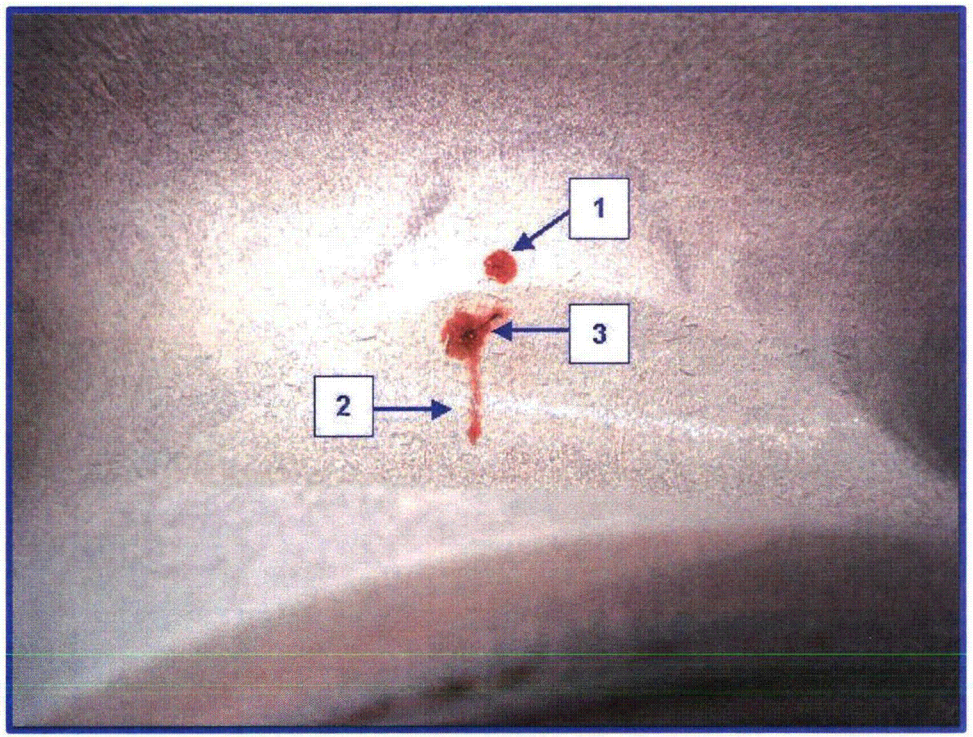


1. Rounded PT indication
2. Subsurface portion of axial indication
3. Subsurface linear defect connected to lack of fusion

Exelon Nuclear

# Boat Sample Results(continued)

- ✓ Three elements must be present simultaneously for PWSCC initiation
  - Susceptible Metallurgical Condition
    - Susceptibility is related to grain boundary carbide coverage (GBCC)
    - Nozzle 68 Heat 80054 considered to have good GBCC - 29 other nozzles from the same heat have been inspected with no indications
  - Tensile Stress
    - Includes residual welding stresses and operating pressures
    - Unit 2 penetration 68 is not the location of highest stress
  - Critical Corrosive Environment
    - PWSCC has strong temperature dependence
    - Below 570°F (as in Unit 2), PWSCC initiation and growth are very slow processes
- ✓ Necessary conditions for the initiation of PWSCC would not have been simultaneously met without the presence of the original fabrication weld defects, which created a critical corrosive environment

Exelon Nuclear

# Growth Projections and Probabilistic Assessment

Guy DeBoo
Senior Staff Engineer
Corporate Asset Management

Exelon Nuclear

# Probabilistic Assessment

Probabilistic evaluations based on Monte Carlo simulations determined:

- ✓ Probability of a 50% through-wall crack occurring in Unit 2 after 20 years of service is three orders of magnitude below the probability expected for flaw initiation and growth due to typical PWSCC
- ✓ The observed flaw did not occur in the most susceptible Unit 2 penetration location (i.e., penetration 72 is 4 to 6 times more likely to initiate a flaw)
- ✓ The flaw in penetration 68 is not due to normal flaw initiation and growth by PWSCC in the Alloy 600 base metal

Exelon Nuclear

# Growth Projections

- ✓ Performed analyses to determine the PWSCC project growth rates for RPV head penetrations
  - Growth studies for five RPV head penetration groups (0°, 25.4°, 42.8°, 43.8° and 47°)
  - Growth based on operational plus weld residual stresses
  - PWSCC growth rates per MRP-55 Rev 1 for Alloy 600 tube material
  - Postulated flaw sized at the limit of UT detection, 0.075" by 0.150"
  - Postulated flaw located at highest stressed locations on the uphill and downhill sides of the penetration
  - Growth limited to the top of the J-groove where pressure boundary leak would initiate

Exelon Nuclear

# Growth Projections (continued)

- ✓ Minimum time for undetected flaw to initiate a leak path is greater than 9 years or 6 fuel cycles

- ✓ A modified inspection interval for Unit 2 (not every outage) is adequate to detect flaws prior to initiating a leak path

Exelon Nuclear

# Fall 2008 Inspection Plans

Scot Greenlee

Byron Station Engineering Director

Exelon Nuclear

# Fall 2008 Inspection Plans

- ✓ In accordance with NRC Order EA-03-009, Fall 2008 (B2R14) examinations will include:
  - Volumetric examination of all 79 penetrations
  - Leak path assessment of the RPV penetration to RPV low-alloy steel annulus
  - Surface examination (dye penetrant) examination of the penetration 68 weld overlay
  - 100% BMV of the external RPV head surface

Exelon Nuclear

# Evaluation Conclusions

Rich Hall

Manager – Corporate Asset Management

Exelon Nuclear

# Evaluation Conclusions

- ✓ Unit 2 head penetration flaw required welding defects, present from fabrication, to initiate PWSCC
- ✓ UT examinations demonstrate any potential flaws in other Unit 2 penetrations are less than the threshold of detection
- ✓ PWSCC growth studies determined a minimum of 9 years or 6 fuel cycles is needed for postulated flaw to initiate a leak path
- ✓ A modified inspection frequency is sufficient to detect flaws prior to initiating a leak path

Exelon Nuclear

# Proposed Relaxation Request

David Chrzanowski

Corporate Licensing Engineer

Exelon Nuclear

# Proposed Relaxation Request

- ✓ Exelon will submit a relaxation request from NRC Order EA-03-009 proposing an alternative inspection frequency based on unique circumstances
- ✓ Justification will include:
  - Results of boat sample evaluation
  - Results of the flaw growth analysis
  - Industry experience
  - Uniqueness of penetration 68 indication
- ✓ Approval will be targeted before Unit 2 Spring 2010 (B2R15 ) refueling outage

Exelon Nuclear

# Proposed Relaxation Request (continued)

- ✓ Proposed inspection frequency
  - Volumetric examination every fourth refueling outage
  - Following examination in Fall 2008 – next volumetric in Fall 2014
  - No additional surface examinations of penetration 68
  - BMV examination every third refueling outage
  - Consistent with the requirements for a low susceptibility head

Exelon Nuclear

# Closing Remarks

Scot Greenlee

Byron Station Engineering Director

Exelon Nuclear

# Closing Remarks

- ✓ Unit 2 RPV head penetration 68 indication is unique
  - Inspection results
  - Boat sample evaluations
- ✓ Modified inspection frequency appropriate for Unit 2 RPV head
- ✓ Plan to submit Order relaxation request in near future requesting NRC approval

# BYRON UNIT 2 – TECHNICAL BASIS FOR REACTOR PRESSURE VESSEL HEAD INSPECTION RELAXATION

*Document Number AM-2007-011*
*Revision 1*
*September 27, 2007*

Corporate Engineering Department
Exelon Nuclear

PREPARED BY: JEAN L. SMITH DATE: _____

REVIEWED BY: GUY H. DEBOO DATE: _____

INDEPENDENT REVIEWER: JAMES J. CIRILLI DATE: _____

APPROVED BY: RICHARD R. HALL DATE: _____
(DATE ISSUED)

## Executive Summary

The U.S. Nuclear Regulatory Commission (NRC) issued Order EA-03-009 in February 2004 to all U.S. pressurized water reactor (PWR) licensees to address the potential for primary water stress corrosion cracking (PWSCC) in the penetration nozzles and related welds of the reactor pressure vessel (RPV) head. During B2R13 in April 2007, Byron Unit 2 conducted an inspection of the penetration nozzles in compliance with the Order.

The inspections revealed an indication in penetration Nozzle 68. A metallurgical examination of a boat sample removed from Nozzle 68 concluded that a lack-of-fusion weld defect created during the manufacturing of the head had caused the initiation of PWSCC. The NRC Order requires any head that has observed PWSCC to follow the inspection interval for a high susceptibility head for subsequent outages; the Order does not specifically address the inspection frequency when the source of crack initiation is not PWSCC. Therefore, a series of evaluations were completed to determine a technically justified frequency for future examinations.

A detailed probabilistic evaluation was carried out to determine the probability of developing a PWSCC crack of the size found in Nozzle 68. The evaluation showed that the probability of having a PWSCC flaw of this size would be about three orders of magnitude less than the probability corresponding to cracking which has been observed in plants. This finding further supports the conclusions of the metallurgical failure analysis report which states that the crack initiation was due to an extenuating circumstance, namely the lack-of-fusion weld defect.

The probabilistic evaluation was also used to determine the effect of inspection frequency on the probability of leakage due to PWSCC initiation and growth. It was found that an inspection frequency of six years, which is consistent with the frequency required for low susceptibility plants, led to a very low probability of leakage.

A statistical treatment of all the available inspection results for head penetrations was completed to estimate the probability that flaws would be found in the future as a function of inspection frequency. For the base case chosen, the results show there is approximately a one percent chance of cracking in the next cycle and about a five percent chance in the next six years.

Although the likelihood of a crack existing is low, a deterministic analysis of crack growth rates was completed. In the study, a flaw, which had not been found by the inspection methods used, was postulated to exist and was allowed to grow according to the accepted industry model. Flaws in a range of shapes and orientations were considered, and the results showed that each flaw would remain within the Code acceptance limits for at least six years.

In summary, it was demonstrated that the flaw found in Byron Unit 2 Nozzle 68 did not originate from PWSCC. Two complementary approaches have shown that a six year inspection frequency results in a very low probability of the development of cracks in the future. Even if a flaw had been below the threshold of detection at B2R13, calculations show that it would remain acceptable to the ASME Code criteria for at least six years. Based on these analyses, an inspection frequency for Byron Unit 2 that is consistent with a low susceptibility head would not significantly increase the probability of a through-wall crack and subsequent leakage on top of the RPV head; therefore, the low susceptibility inspection frequency is acceptable.

# TABLE OF CONTENTS

# 1 Introduction

The U.S. Nuclear Regulatory Commission (NRC) issued Order EA-03-009[1] in February 2004 to all U.S. pressurized water reactor (PWR) licensees to address the potential for primary water stress corrosion cracking (PWSCC) in the penetration nozzles and related welds of the reactor pressure vessel (RPV) head. The Order recognizes that the susceptibility of RPV head penetrations to PWSCC appears to be strongly linked to the operating time and temperature of the RPV head. Accordingly, the necessary RPV head inspections required by the Order are dependent on the value of effective degradation years (EDY), which are calculated using an equation defined in the Order.

The equation for EDY is a function of time at temperature and is normalized to a reference temperature of 600°F. At the time of Byron Unit 2 Refueling Outage 13 (B2R13) in April 2007, the value for Unit 2 was 2.2 EDY, which is considered by the Order to be in the low susceptibility category. Based on the low value of EDY, Byron Unit 2 was not expected to have initiated PWSCC by B2R13.

The following report describes the inspections performed in accordance with the NRC Order at Byron Unit 2 during B2R13, and it discusses the indications that were detected during the inspections. The report highlights the outlier nature of this finding relative to the numerous inspections that have been performed in the industry according to the Order.

A summary of the metallurgical failure analysis that was performed on a boat sample removed from Byron Unit 2 describes the discovery of an original fabrication weld defect, which created the environment necessary for PWSCC. A discussion of the requirements for the initiation of PWSCC is included to illustrate the uniqueness of the conditions at Byron Unit 2 and their effect on the detected flaw.

A probabilistic analysis of the occurrence of PWSCC in Byron Unit 2 after 20 years of service is presented along with a probabilistic evaluation to determine the effect of inspection frequency on the probability of leakage. The analysis provides further evidence that PWSCC would have been highly unlikely without the existence of an extenuating factor such as the original fabrication weld defect. A statistical treatment of all the available inspection results is used to estimate the probability as a function of inspection frequency that flaws would be found in the future.

Based on an initial flaw size at the threshold of detection by current inspection techniques, a crack growth study is presented that indicates the inspection frequency prescribed by the Order for a low susceptibility head is appropriate for Byron Unit 2 despite the discovery of PWSCC.

# 2 Reactor Pressure Vessel Head Inspections

This section reports the results of the inspections conducted by Byron Unit 2 and the industry in accordance with NRC Order EA-03-009. A discussion of the inspection techniques and their reliability is included.

## 2.1 Byron and Braidwood Inspection Results

Byron and Braidwood first implemented bare metal visual (BMV) examinations of the reactor pressure vessel head starting in 2002 to meet the requirements of NRC Bulletin 2002-02[2]. The following dates are for completion of the first BMV exams:

- Braidwood 1 - Spring 2003
- Braidwood 2 - Spring 2002
- Byron 1 - Fall 2003
- Byron 2 -Fall 2002

The initial BMV and all subsequent exams (both Byron and Braidwood) have not detected any evidence of boric acid in the annulus region of the CRDM nozzle-to-head interface. With the issuance of NRC Order EA-03-009 in February 2004, specific criteria were established for frequency of BMV and the requirement for a volumetric examination was added. Both Byron and Braidwood established a three-year frequency of examination for the BMV starting with the initial BMVs performed to meet Bulletin 2002-02.

In accordance with NRC Order EA-03-009, each reactor vessel head (CRDM nozzles) must be examined per the order by February 2008. Byron and Braidwood have used volumetric examination of the CRDM nozzle tube by use of a blade probe for the CRDM nozzles with thermal sleeves installed and an open probe for nozzles without thermal sleeves. Each of the two exam methods has both ultrasonic exam (UT) and eddy current exam (ET) capabilities. The main exam is completed using the UT probe with supplementary EC probes also taking data. The exam of the CRDM nozzles is completed from the ID of the tube for the full wall thickness and approximately 10% of the J-Groove weld being examined.

Both Byron and Braidwood have completed these exams on all four units, and the total population inspected to date is 312 CRDM nozzles and four 1" vent line connections. Of these four units only Byron Unit 2 has found an unacceptable condition in one nozzle.

## 2.2 Byron Unit 2 Inspection Results

During Refueling Outage B2R13 in Spring 2007, Byron Unit 2 was required to meet the requirements of NRC Order EA-03-009. As a low susceptibility head plant, Byron was

required to complete a volumetric exam of all 78 CRDM nozzles and the one 1" vent line connection. All 78 CRDM nozzles and the vent connection were examined. During this examination CRDM Nozzle 68 had an indication detected. This indication was reflective of PWSCC, and the decision was made to obtain a confirmatory boat sample. Subsequent metallurgical analysis identified a lack-of-fusion weld defect, which was responsible for the initiation of the observed PWSCC. The examination also identified 39 Parent Tube Indications (PTI). Each one of the PTIs was evaluated in accordance with WesDyne procedure WDI-UT-013[3] and was dispositioned as No Detectable Defect (NDD), which equates to no evidence of PWSCC.

### 2.2.1 Penetration 68

After identification of the indication on Penetration 68, additional examinations were undertaken to determine the exact nature of the indication. The first exam completed was the Dye Penetrant (PT) examination of the exterior surface of the J-Groove weld. The PT exam identified two indications, one rounded and one linear.[4]

After retrieval of the boat sample, a PT of the excavation was completed; Reference 5 contains the details of the inspection.[5] Following the PT exam, the excavated area was repaired, and an overlay of the CRDM nozzle and J-groove weld was completed. The overlay was then inspected using a PT exam to ensure no surface defects existed.[6, 7]

With the identification of PWSCC on Penetration 68, Byron Unit 2 was categorized as a "High Susceptibility" head in accordance with the NRC Order. Byron initiated and completed a 100% Bare Metal Visual Examination during the outage as required by the NRC Order. No evidence of any leakage was found.

### 2.2.2 Other Tube Indications

The RPVH CRDM inspection was analyzed using WesDyne procedure WDI-UT-013 Rev. 12. The inspection probe employed was the Trinity design, which contains an axial shooting time-of-flight diffraction (TOFD) pair optimized for OD initiated flaws, a 0 degree probe for leak path detection, and an eddy current probe. The UT TOFD method was demonstrated through the MRP/EPRI protocol, as documented in MRP-89.[8]

The UT TOFD method is inherently very sensitive to crack tip diffraction signals. However, it is also equally sensitive to a myriad of other signal sources, most of which are associated with the machining and welding fabrication processes associated with the J-groove weld. The technique is sufficiently sensitive to respond to the grain structure change going from the nozzle base metal into the weld metal. These signals are broadly characterized as weld interface indications (WII). Because of local grinding and weld repairs, this interface often is not a straight line and the signals can take on some characteristics of a crack tip diffraction response. The vast majority of signals detected have not been associated with PWSCC.

The analysis procedure has detailed flow charts (Figures 2-1, 2-2, and 2-3) which specify a step-by-step process for distinguishing actual PWSCC response from manufacturing artifacts. Initially, any suspect response is categorized as a parent tube indication (PTI). Then the overall shape of the response is evaluated to determine if the response is a linear crack-like response or more like a diffuse surface response associated with metallurgical changes. Linear responses are categorized as special interest (SI) while surface-type responses are dispositioned as no detectable degradation (NDD). This analysis process differs slightly for indications that are entirely within the elevation of the weld (Figure 2-2) or outboard of the weld (Figure 2-3) because additional inferences can be drawn for the OD back wall that are not possible at the weld location.

Penetration 68 had a PTI indication within the weld zone that was analyzed as linear and given a 'special interest' designation. The SI designation then allows for additional confirmatory testing be eliminate potential false positives by determining if the indication is connected to a wetted surface, which is a requisite condition for initiation of PWSCC. In this case PT was performed on the J-groove weld surface and both a rounded and linear indication were detected coincident with the SI location.

The same process was followed for each of the 78 nozzles. There were 39 PTI designations initially. Other than Nozzle 68, all the other indications were evaluated as surface type responses and were dispositioned as NDD.

## ET/UT: ID INDICATION SCREENING

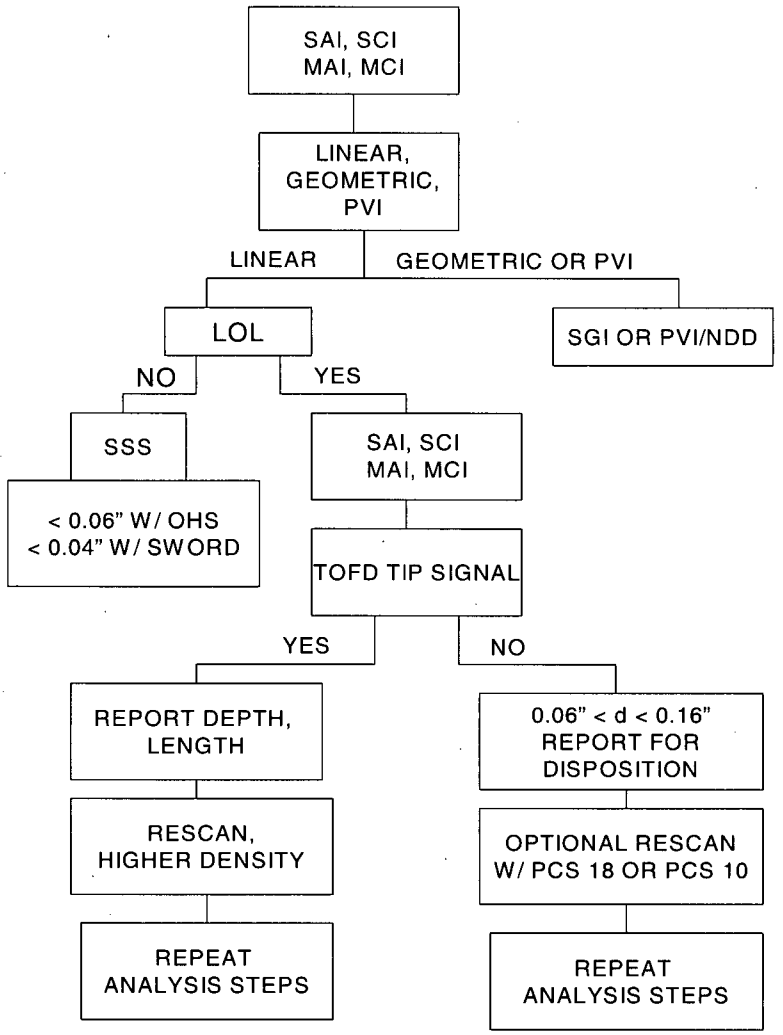


**Figure 2-1:** ET/UT: ID Indication Screening Flowchart (Ref. 3)

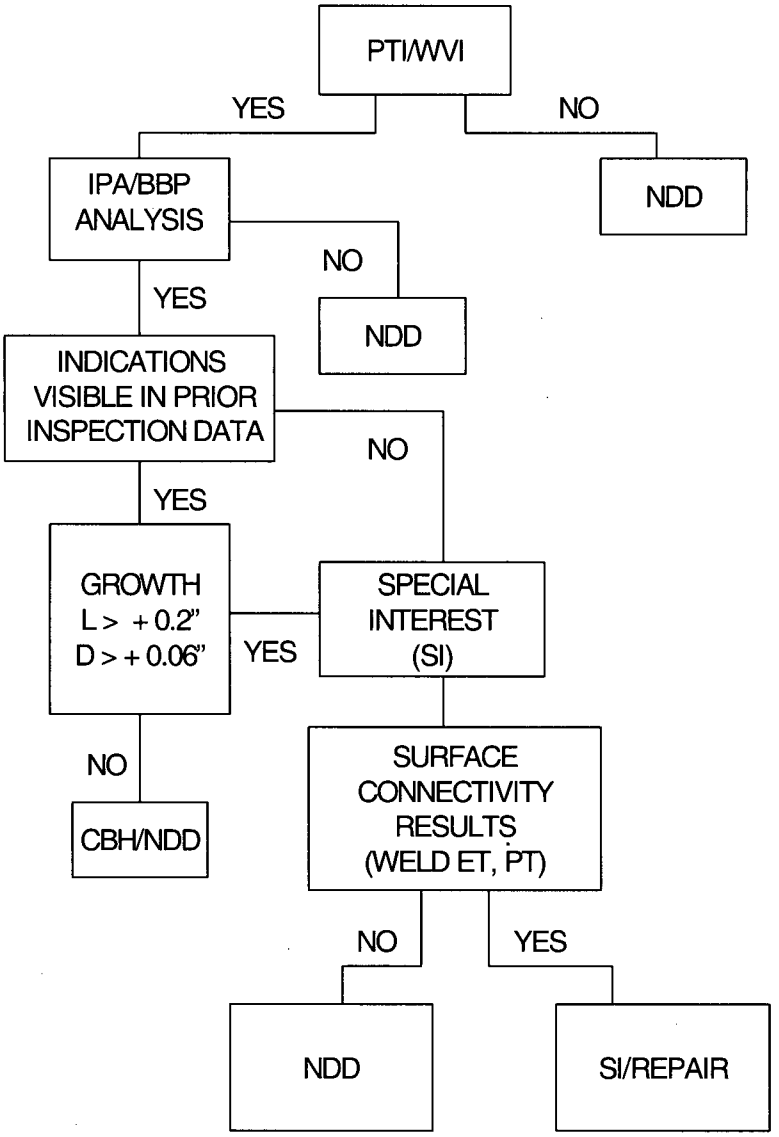


**Figure 2-2:** UT: OD Indication Screening Within Weld Zone Flowchart (Ref. 3)

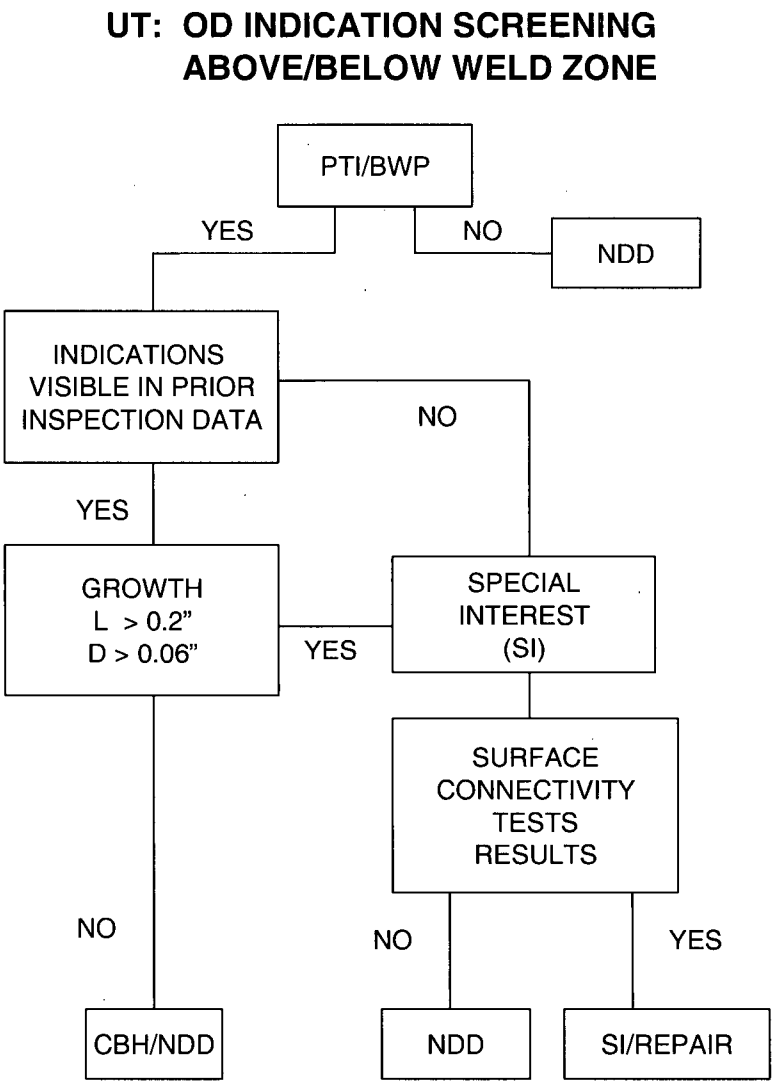


**Figure 2-3:** UT: OD Indication Screening Above/Below Weld Zone Flowchart (Ref. 3)

## 2.3 Industry Inspection Results

As of the end of the Spring 2007 outage season, only three plants categorized as low susceptibility by the NRC Order had yet to be inspected. Over the period of 2004 through 2007, approximately 1404 upper head penetrations have been inspected, and with the exception of Byron Unit 2 CRDM Nozzle 68, no detectable defects have been observed. The plants that have been inspected are listed in Table 2-1, and the table includes only plants with reported head temperatures of 561°F or less. Approximately ten additional plants at slightly higher head temperatures could be added to the table; however, the represented group was selected to ensure conservatism. The listed units are all of the Westinghouse cold head design, and all have 78 penetrations per head.

Another large database of low temperature head penetrations is the bottom head penetrations. The U.S. inspection results are shown in Table 2-2. A total of 15 plants have been inspected representing approximately 804 penetrations. The number of penetrations is not the same for every plant, and in some cases, the inspected penetration population was affected by other outage related considerations. In addition, these results do not include South Texas 2, which was found to have two leaking bottom penetrations in April 2003. Foreign results are also not included in the table; although, results to date indicate more than 1600 bottom mounted nozzles have been inspected in France, Sweden, Belgium, and Japan with no indications found.

**Table 2-1**
**Inspections Completed on Cold Head Plants to Date**

| | Number of Penetrations |
|---|---|
| **Spring 2005** | |
| Byron 1 | 78 |
| Braidwood 2 | 78 |
| Comanche Peak 2 | 78 |
| **Spring 2006** | |
| Shearon Harris | 78 |
| Braidwood 1 | 78 |
| **Fall 2006** | |
| Vogtle 1 | 78 |
| Seabrook | 78 |
| Wolf Creek | 78 |
| McGuire 2 | 78 |
| Catawba 1 | 78 |
| V. C. Summer | 78 |
| South Texas 1 | 78 |
| Sequoyah 2 | 78 |
| **Spring 2007** | |
| Byron 2 | 78 |
| Vogtle 2 | 78 |
| McGuire 1 | 78 |
| Callaway | 78 |
| Millstone 3 | 78 |

| Table 2-2<br>Bottom Head Penetrations Inspected to Date | |
|---|---|
| | **Findings** |
| **2004** | |
| Callaway | NDD |
| Catawba 2 | NDD |
| Surry 1 | NDD |
| Turkey Point 3 | NDD |
| **2005** | |
| McGuire 2 | NDD |
| Byron 1 | NDD |
| Surry 2 | NDD |
| Catawba 1 | NDD |
| Wolf Creek | NDD |
| Diablo Canyon 1 | NDD |
| Turkey Point 4 | NDD |
| **2006** | |
| Diablo Canyon 2 | NDD |
| Indian Point 2 | NDD |
| Vogtle 1 | NDD |
| **2007** | |
| Vogtle 2 | NDD |

## 2.4 Reliability of Inspection Techniques

The volumetric examination equipment has completed a detailed demonstration as described in MRP-89, "Demonstrations of Vendor Equipment and Procedures for Inspection of Control Rod Drive Head Mechanisms".[8]

The second phase of demonstration, which began in August 2002, employs mockups containing manufactured flaws of accurately known size and location. The MRP Inspection and Assessment Committees conducted joint meetings to identify the scope of the demonstrations and to design the demonstration mockups. The demonstration protocol is listed in MRP document MRP-89 Section 8.

The scope of the demonstration was to:

- Quantify detection limits of ID and OD connected flaws from the ID of the penetration tube
- Document sizing capabilities of the ID and OD connected flaws from the ID of the penetration tube

- Evaluate capabilities to detect defects on the wetted surface of the RVHP attachment weld

- Investigate the capability to detect flaws approaching the weld-to-tube interface (triple point) using UT inspection from the ID surface of the penetration tube.

Based on the mockup design criteria, flaw manufacturing processes were selected as appropriate for the NDE methods employed by inspection vendors. The NDE methods employed are pulse-echo ultrasonic (UT), forward scatter time-of-flight diffraction (TOFD) UT, and eddy current techniques (ET) for the tube inside surface.

The morphology of the manufactured flaws in the MRP-89 Phase II demonstrations is based on the metallurgical investigations of tube and weld flaws removed from Oconee Nuclear Plant Units 1 and 3. The UT and ET responses of the manufactured flaws used in the demonstrations have been shown to be comparable to responses from service-induced PWSCC. A wide range of flaw sizes and locations were included in the mockups to quantify the performance of the demonstrated inspection techniques throughout the inspection volume.

WesDyne displayed a very high confidence of detection and sizing in their demonstration activities. Mockup (J) was the OD-flawed mockup used in the demonstration. Of the numerous flaws in this mockup, only one flaw (8% of the wall thickness) was missed during one inspection, and the flaw size was under the size used for the crack growth analysis in this report, i.e. 0.075" deep by 0.15" in length. WesDyne also has examined approximately 5,000 nozzles during 62 outage campaigns and to date all nozzles returned to service as NDD have not leaked. There has been only one case where an indication resolved as NDD subsequently grew during the next cycle.

WesDyne's procedure also provides additional confidence with redundant analysis of any parent tube indication (PTI). The inspection procedure requires that any indication greater than 10% be identified as a PTI. The 10% limit is based on the manufacturing process whereby in process "modifications" do not exceed 10% wall removal into the nozzle. Since there is progressive PT during welding, some grinding and repair welding may be performed. A manufacturing repair is only documented if it occurs after the final PT, so everything prior to that is not considered a repair. Therefore, based on this cutoff, the demonstrated detection was 100%.

The inspection data analysis process uses two production analysts who report indications greater than 10%, and afterward a resolution analyst resolves the reported indication as having flaw/non-flaw characteristics. For example, if each analyst had a POD of 80%, their combined POD is 96%. With the third analyst, also with a POD of 80%, the combined POD would then be 99%. Therefore, with three looks at the data and 100% detection, the POD for the process should be extremely high.

# 3 Metallurgical Examination of Byron Unit 2 Nozzle 68

After the indication was detected in Nozzle 68, the decision was made to collect a boat sample to gain a better understanding of the nature of the indication. This section presents the results of the metallurgical examination of the boat sample, discusses the factors involved in the initiation of PWSCC, and compares the occurrence of PWSCC in Byron Unit 2 to other reported cases of PWSCC in RPV head penetrations.

## 3.1 Metallurgical Examination Results

In order to evaluate the indications that were found during the UT and PT examinations, a "boat" sample was removed from the Nozzle 68 tube and J-groove weld by electrode discharge machining (EDM). The laboratory analysis of the boat sample was conducted at BWXT in Lynchburg, VA, and the metallurgical failure analysis report[9] was prepared by Exelon PowerLabs. Figure 3-1 illustrates the two dye penetrant indications (denoted by arrows) on the surface of the J-groove weld on Nozzle 68. The axial indication corresponded to the approximate location of the axial ultrasonic reflector, and the J-groove weld toe extended beyond the axial indication. A rounded indication approximately 0.050" diameter was also detected.

After the boat sample was removed, a PT exam was conducted on the excavation site. The PT exam uncovered an angled, subsurface linear defect that intersected the original axial indication; the subsurface defect was partially captured by the boat sample. The PT exam also showed that the deepest portion of the original surface axial indication was not captured by the boat sample nor was the original rounded surface PT indication. The post-excavation PT exam results are shown in Figure 3-2.

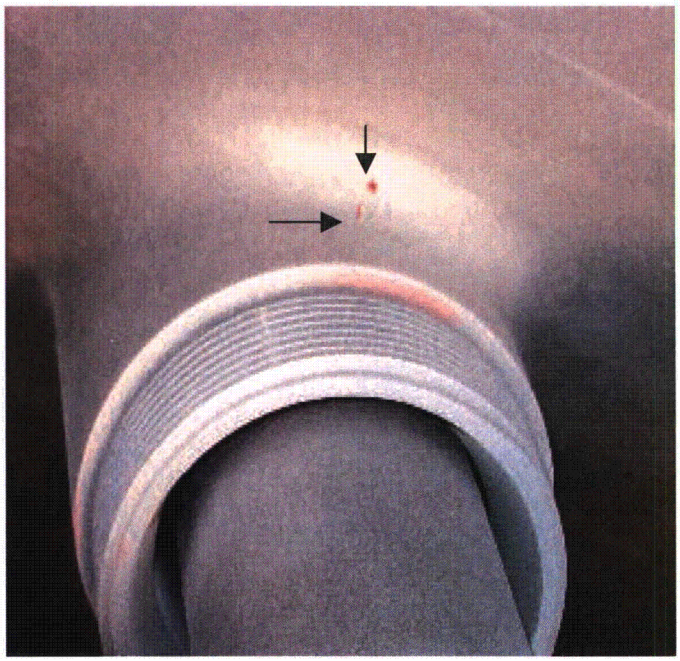

**Figure 3-1:** A photograph of the two dye penetrant indications on the surface of the J-groove weld on CRDM 68.

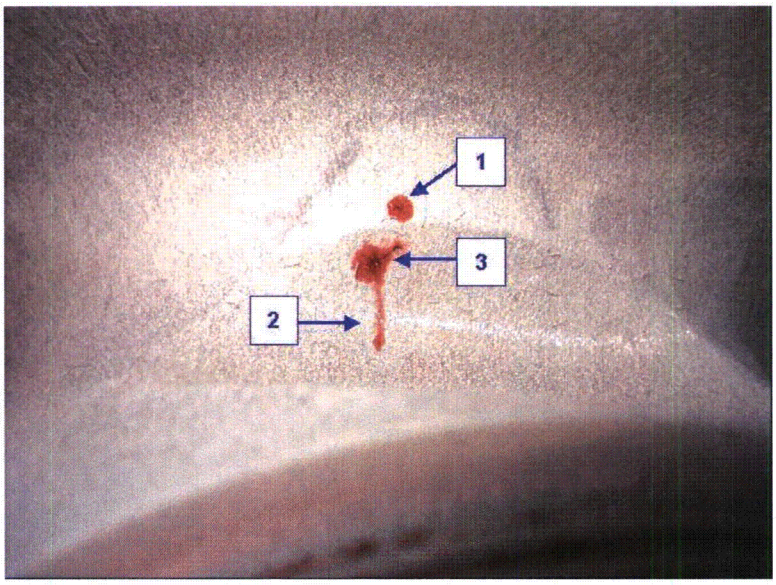


**Figure 3-2:** A photograph of the field dye penetrant results of the excavation site after the boat sample was removed. The excavation uncovered an angled, subsurface linear defect (#3) that intersected the subsurface portion of the original axial linear defect (#2). The original rounded indication (#1) remained in the penetration.

The boat sample measured approximately 1.5" long by 0.75" wide and had a maximum thickness of 0.375". The boat sample can be seen in Figure 3-3. The front surface is the wetted J-groove weld; the back surface is the EDM cut surface. Heavy grinding marks can easily be seen on the weld surface.

The horizontal cut between Sections A and B was below the axial indication on the wetted surface of the boat sample; however, it intersected the axial indication on the EDM surface. A metallurgical mount was prepared of this surface on Section B. The tube base metal contained branched, intergranular cracking typical of PWSCC. The crack branches had sharp tips and contained little oxidation. There was limited interdendritic cracking into the weld as shown in Figure 3-4. Within the Section B mount, none of the cracking in the tube extended to the wetted surface of the boat sample.

The horizontal cut face in Section B was also used to determine the hardness properties. The results of the hardness tests were considered typical for mill annealed Alloy 600 tubing and Inconel 182 weld metal; although, an area of relatively high hardness was present on the heavily ground (cold worked) surface layer of the weld. Section C, shown in Figure 3-3, was used to determine the weld metal and tube metal chemistries, which were found to be consistent with Inconel 182 filler metal and the original heat fabrication records, respectively.

In the laboratory, Section A was subjected to bending along the axial indication to reveal the crack growth surface. The exposed crack surface of the tube material was reflective with an intergranular appearance (Figure 3-5). There were no clear indications of crack age in the tube material; however, a thumbnail-shaped region emanating from the EDM cut surface appeared to be more oxidized than the remainder of the sample.

The exposed surface of the weld exhibited characteristics typical of both PWSCC and hot cracking. Lack of fusion between weld passes, which was parallel to the fusion line, could be seen on the exposed weld surface (Figure 3-6), and within the weld there were several cracks that were connected to the lack of fusion defect. Dimpled voids, which are indicative of ductile tearing, were present at various locations in the weld. It is likely that the ductile tearing regions were small intact ligaments that failed when the crack surface was broken open in the lab. In general, there were more ductile tearing regions adjacent to the wetted surface of the sample (also seen in Figure 3-6).

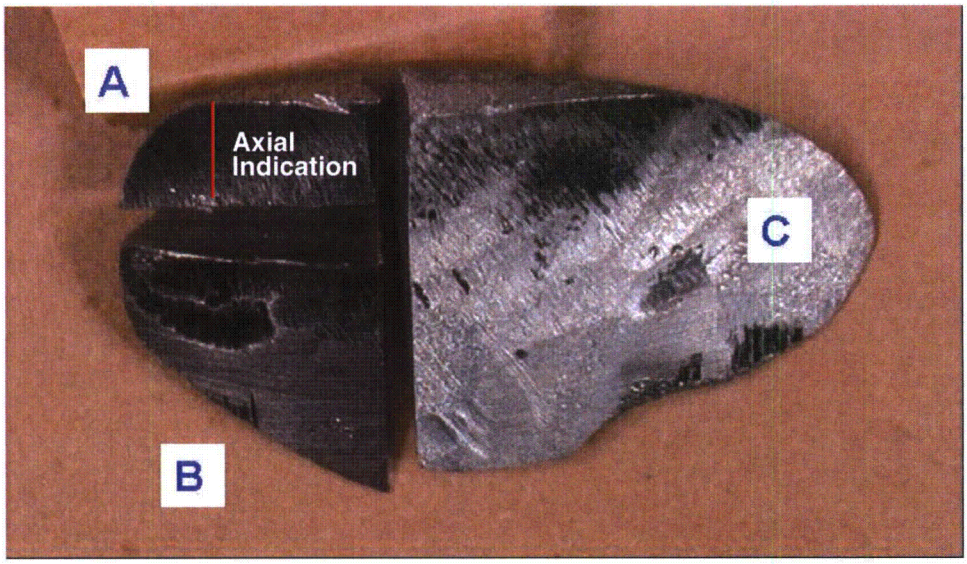


**Figure 3-3:** A photograph of the boat sample after initial sectioning in the laboratory. The front surface is the wetted surface of the J-groove weld; the back surface is the EDM cut surface.

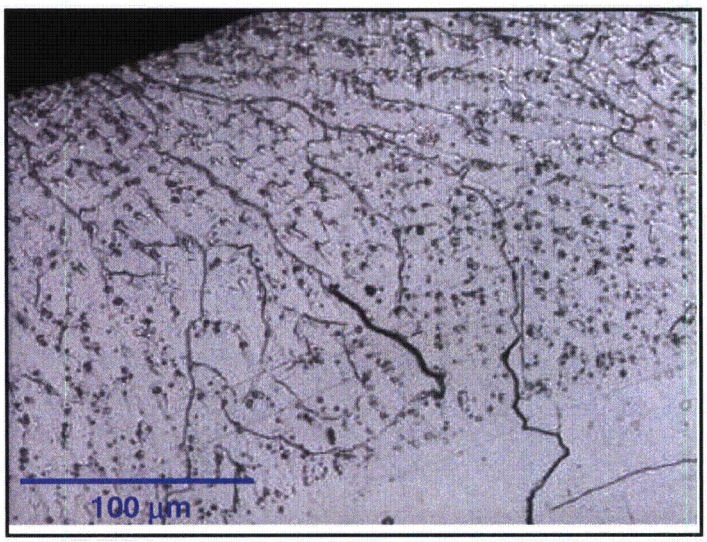


**Figure 3-4:** Photomicrograph of the metallurgical mount prepared from the horizontal cut face in Section B. The direction of crack growth is from the tube material into the weld. (Original magnification 375X; electrolytic phosphoric-nital dual etch)

**Figure 3-5:** A stereoscope view of the exposed surface of the axial indication from Section A. The weld is toward the left side of the sample.

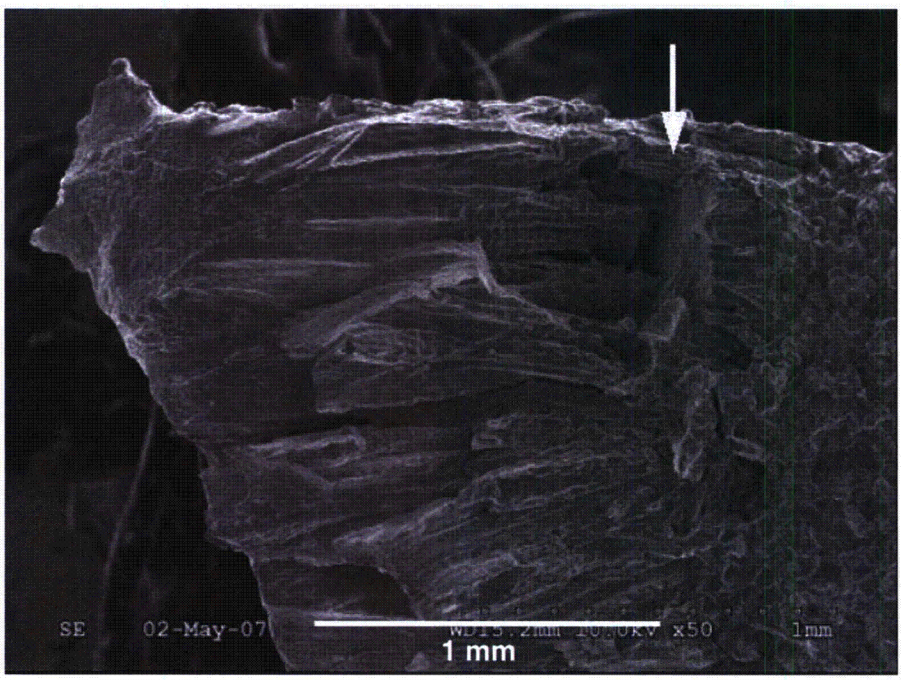


**Figure 3-6:** A scanning electron micrograph of the exposed surface of the axial indication from Section A. The arrow points to the lack of fusion between the weld passes. A ductile region can be seen in the upper left corner of the sample. (Original magnification 50X)

Based on the general characteristics of the weld defects, interdendritic weld separations, direction of crack branching, and local ductile tearing, it was concluded that the primary direction of propagation within the weld was toward the wetted surface of the boat sample. These characteristics suggest the PWSCC did not initiate from the wetted surface of the boat sample.

A portion of the subsurface angled defect was captured in the boat sample; the defect had the appearance of a rounded defect and was visible on the EDM cut surface of Section A. A metallurgical mount was prepared on a cross-sectional plane adjacent to the indication. After a series of grind-polish-examine steps, the indication was identified as a weld lack-of-fusion defect between the outer surface of the tube and the weld. (Figure 3-7)

After repolishing the sample in preparation for an SEM exam, a porous inclusion near the edge of the lack-of-fusion crevice was uncovered as seen in Figure 3-8. Several incipient interdendritic cracks had initiated from the edge of the inclusion and the lack-of-fusion crevice. Most of the cracks appeared to be hot cracks; however, the angular appearance of two cracks appeared similar to incipient PWSCC.

The large inclusion and most of the smaller inclusions contained titanium, nitrogen, and oxygen. The lack-of-fusion crevice contained oxidized metallic particles from the EDM cutting tool and base metal debris. No measurable fluorine or other potentially corrosive elements were identified in the incipient cracks or the lack-of-fusion crevice.

The laboratory evaluations identified the axial indication as a combination of PWSCC and welding defects including lack of fusion and hot cracking. The subsurface defect was identified as lack of fusion between the outer diameter of the tube and the J-groove weld. Within the boat sample, the cracking characteristics indicated the PWSCC initiated at a subsurface location on the tube OD, propagated in an axial/radial direction into the tube, and propagated toward the wetted surface of the J-groove weld fillet leg.

The source of the original rounded indication on the weld wetted surface, which was not captured by the boat sample, cannot be determined. However, based on the presence of welding defects in the boat sample, the most probable cause is considered a welding imperfection that was not detectable or an indication that was considered acceptable per the fabrication inspection requirements. The Byron Unit 2 reactor head was fabricated by Babcock & Wilcox in 1977; the applicable code was the 1971 Edition of the ASME Section III, Summer 1973 Addenda. Per the 1971 edition of ASME Section III, NB-5000, an isolated 3/16" rounded dye penetrant indication would be considered acceptable. At 0.050", the rounded indication on the J-groove weld surface of CRDM #68 was well within this limitation.

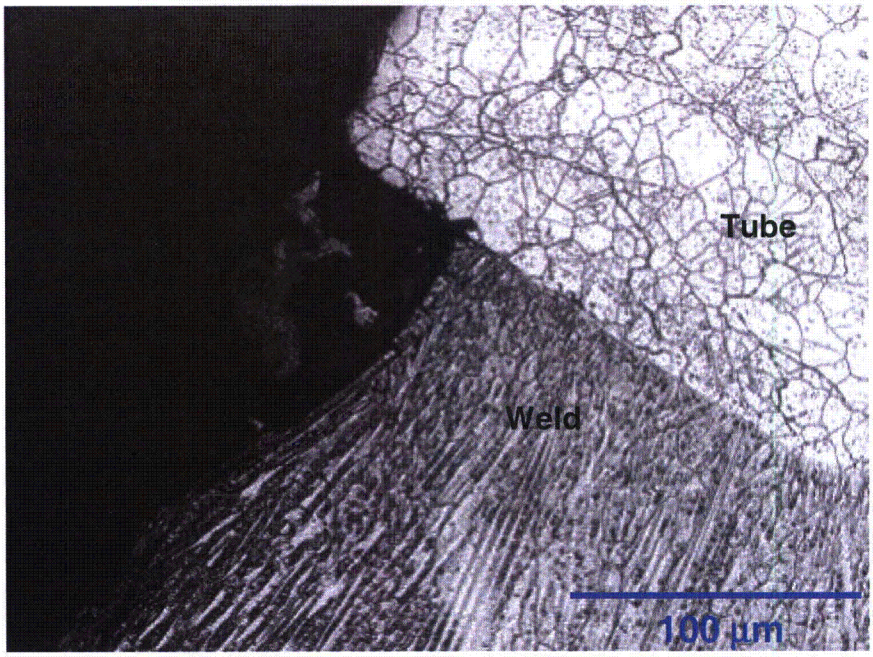


**Figure 3-7:** An etched view of the lack-of-fusion defect contained in Section A. Also note the flat interface at the fusion line, which indicates there was little penetration at this location. (Original magnification 190X, electrolytic phosphoric-nital dual etch)

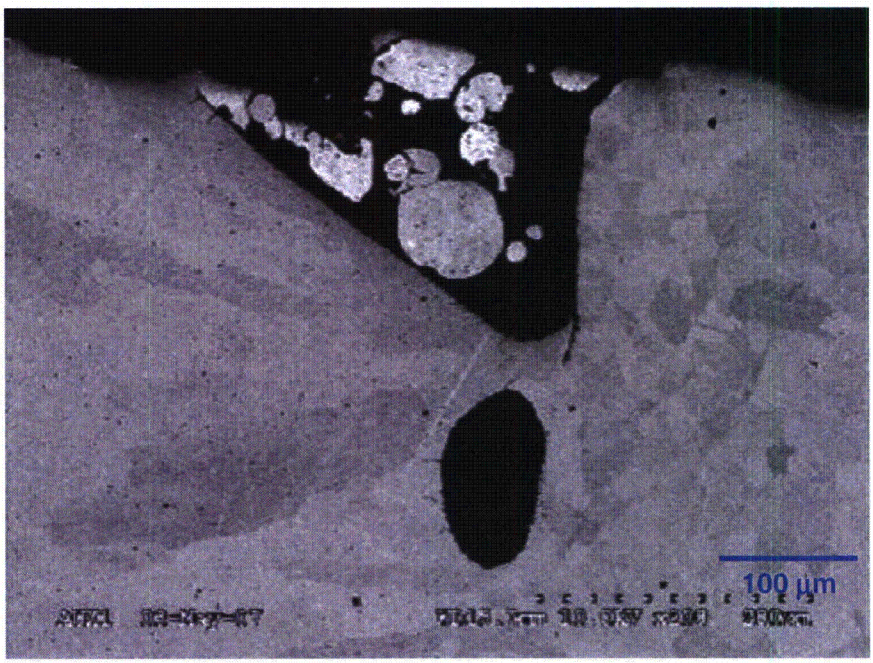


**Figure 3-8:** A scanning electron micrograph of the lack-of-fusion defect after repolishing, which revealed the large inclusion. (Original magnification 200X)

The CRDM J-groove welds were fabricated with multiple weld passes. For Nozzle 68, grinding was performed throughout the weld to remove indications, and no weld repairs were reported for this penetration. A final fabrication dye penetrant examination was performed, and it is possible that the rounded indication was less than the minimum relevant size.

At the time of B2R14, the presence of PWSCC in Byron Unit 2 was unexpected based on the categorization of Unit 2 as a low susceptibility plant per the methodology of NRC Order EA-03-009. The conclusion drawn in the boat sample failure analysis report is that the PWSCC was not the result of exposure of the Alloy 600 tube material to the bulk primary water environment; rather, the premature initiation of PWSCC is attributed to a series of weld defects, which created a conducive crevice corrosion environment in the high stress region of the J-groove weld.

## 3.2 PWSCC Requirements

Stress corrosion cracking (SCC) is the term given to crack formation of susceptible alloys under the influence of a tensile stress of sufficient magnitude exposed to a system-specific corrosive environment. Most alloys are susceptible to SCC in at least one environment; although, pure metals are generally resistant to SCC. The three key elements that must be present simultaneously for SCC to occur are a susceptible metallurgical condition, a tensile stress, and a critical corrosive environment. The elimination of any one of these three elements or the reduction of one of these three elements below some "threshold" level can mitigate SCC.

### 3.2.1 Metallurgy

SCC may be either transgranular or intergranular; however, the crack follows a macroscopic path that is generally normal to the tensile component of stress. The intergranular failure mode (IGSCC) suggests an inhomogeneity at the grain boundaries. Primary water stress corrosion cracking (PWSCC) refers to IGSCC in the primary water environment of PWRs. Alloy 600 is a high nickel austenitic alloy containing approximately 72 weight percent nickel that is prone to PWSCC. In Alloy 600, the susceptibility to PWSCC is increased by a lack of contiguous coverage of chromium carbides at the grain boundary. Grain boundary coverage is dependent on the heat treating history and carbon content of the material.

### 3.2.2 Stress

The reactor pressure vessel (RPV) head in a PWR has numerous penetrations for instrumentation and control rod drive mechanisms (CRDMs). The penetrations are held in place by a J-groove weld. Due to residual weld stresses and operational pressures, a number of high tensile stress regions exist in both the J-groove weld and the outer

diameter of the penetration tube. These tensile stresses can be above the threshold required to initiate and propagate PWSCC provided the material is susceptible and the environment is conducive to PWSCC.

### 3.2.3 Environment

PWSCC of Alloy 600 and its weld metals (e.g., Alloys 182 and 82) is primarily affected by material properties and loading parameters; however, the fact that IGSCC of Alloy 600 occurs in an apparently innocuous environment such as deaerated high-purity water indicates a secondary effect by environmental factors on both PWSCC initiation and propagation. The environmental parameters that can affect PWSCC include lithium, boron, and zinc concentrations; pH at temperature; temperature; and dissolved hydrogen concentration[10] with the largest impact being made by temperature and dissolved hydrogen.

Temperature is an environmental variable that strongly affects PWSCC crack initiation and propagation in Alloy 600. Temperature dependence has been represented according to an Arrhenius plot with an apparent activation energy. The propensity of PWSCC initiation and subsequent crack propagation increases with increasing temperature; however, at temperatures below 570°F (300°C) as is the case at Byron Unit 2, the high value of the apparent activation energy indicates that both crack initiation and propagation become very slow processes.[11]

The main effect produced by an increase in partial pressure of hydrogen is the lowering of the corrosion potential to a more anodic value where SCC susceptibility is higher. While this effect may be significant, a statistical evaluation of PWSCC initiation data indicates that the effect of hydrogen on PWSCC is not especially strong in the normal operating range of 25 to 50 cc/kg (2.2 to 4.5 ppm) dissolved hydrogen.[11]

## 3.3 PWSCC in Byron Unit 2

This section considers the three key elements of PWSCC as applied to Nozzle 68. The mill annealed Alloy 600 material is known to be susceptible to PWSCC, and susceptibility is related to grain boundary carbide coverage. The Alloy 600 material from B&W Heat 80054 contained in the boat sample had grain boundary carbide coverage in excess of 50%[12], which is considered to be a significant level of coverage.

The downhill side of the J-groove weld is a high tensile hoop stress region due to residual welding stresses and operating pressure;[13] although, it will be shown in Section 4 that Nozzle 68 does not represent the location with the highest probability for initiating PWSCC.

The low operating temperatures in the upper RPV head at Byron Unit 2 do not constitute an environment that is conducive to PWSCC during a life cycle of 2.2 EDY. At this temperature, an extenuating factor must be involved for the primary water

environment to become a key element of SCC. In Nozzle 68, the extenuating factor was the crevice created by the lack-of-fusion defect. The local changes in the environment caused by the presence of a crevice are known to facilitate PWSCC initiation.

For PWSCC to initiate at a subsurface location and to propagate towards the wetted surface, the initiation site (i.e., the lack-of-fusion weld defect) would need to be wetted by the primary water. In Nozzle 68, the wetted path from the bulk primary water environment to the subsurface initiation site is believed to have consisted of a series of weld defects starting with the rounded surface indication and including lack of fusion between weld passes and between the tube and hot cracks within the weld. This conclusion is supported by the incipient cracks seen adjacent to the lack-of-fusion defects that were present between weld passes and between the weld and tube materials.

### 3.4 PWSCC Initiation and Chromium Depletion

In an effort to understand the mechanisms of degradation affecting materials in light water reactors, EPRI has prepared the report *Status Review of Initiation of Environmentally Assisted Cracking and Short Crack Growth*[14] to provide a status review of current knowledge of SCC initiation and short crack growth in nickel base alloys, austenitic stainless steels, and carbon and low alloy steels exposed to typical PWR and BWR aqueous environments. The report illustrates that in deaerated high temperature water, the oxidation of Ni-Fe-Cr alloys leads to the formation of a multilayered oxide that is well crystallized and that may contain some nickel hydroxides. The inner, Cr-rich oxide layer is assumed to be protective. The external layer consists of relatively large crystallites spread over the surface and is much lower in chromium or even chromium-free. The overall thickness of this oxide is much greater than the passive layers formed near room temperature. It is not well established if only part of the inner oxide layer is truly protective, and the thickness of the inner layer is not known. Relatively recently, it has been demonstrated that the metal substrate can also undergo two types of damage during oxidation in high temperature water: 1) penetration of oxygen at the grain boundaries, and 2) selective oxidation of chromium resulting in a Cr-depleted layer. This damage has been observed on Ni-base alloys such as Alloy 600.

The presence of a Cr-depleted layer on the surface and possibly at the grain boundaries may increase susceptibility to PWSCC. As stated by EPRI, this degradation mechanism warrants further investigation. Projecting the potential effects of chromium depletion to Byron Unit 2 does not reconcile the occurrence of PWSCC in Nozzle 68. Chromium depletion on the wetted metal surface would presumably facilitate crack initiation on the wetted surface with crack propagation proceeding towards the interior of the weld or tube material. In the case of Nozzle 68, the direction of crack propagation was from a subsurface location towards the wetted surface of the J-groove weld.

## 3.5 Other Industry PWSCC Experiences

### 3.5.1 Palisades

Background

Palisades is a Combustion Engineering (CE) unit that began commercial operation in December 1971. During refueling outage (RFO) 17 in October 2004, Palisades conducted full volumetric UT examinations of the RPV head penetrations per NRC Order EA-03-009. At that time, Palisades was a moderate susceptibility head with an EDY ~9. The ultrasonic inspections revealed leak path indications in CRDM Penetrations 29 and 30. A bare metal visual examination was performed on the exterior of the RPV head, and no evidence of leakage was visible. Dye penetrant testing on the two penetrations showed minor surface indications that required further evaluation. Grinding operations on Penetration 29 revealed a ¼" axial indication perpendicular to the fusion line of the J-weld and butter and on Penetration 30 revealed a circumferential crack approximately 1" long adjacent to the fusion line of the J-weld and the butter. The cracks were small and tight with no visible evidence of leakage. Although, a boat sample was not removed from either penetration, the bottom portion of each nozzle was cut and removed. New half nozzles were inserted and welded to the upper portion of the existing nozzles and to the RPV head. The unit was placed back into service.

Without a metallurgical analysis, Palisades did not have the basis to seek relaxation or relief from the inspection requirements of the Order. As such, Palisades is now classified as a high susceptibility head per the Order. Full volumetric UT and BMV examinations were conducted at the subsequent refueling outage (RFO 18 in Spring 2005), and no indications were found.

Comparison to Byron Unit 2

The initiation point for PWSCC at Palisades was not determined; however, observations made during the in-situ exploratory grinding operations performed on the surface suggest that the direction of crack propagation was from the external wetted surface towards the interior. In contrast, the PWSCC in Byron Unit 2 originated at a subsurface location and progress towards the external wetted surface. Palisades also had a higher value of EDY than Byron Unit 2, so the effect of time at temperature was greater at Palisades.

### 3.5.2 Oconee Unit 1

Background

Oconee Unit 1 is a Babcock & Wilcox (B&W) unit that began commercial operation in July 1973. As of February 2001, the estimated EDY for Oconee Unit 1 was 22.1, which is in the high susceptibility category. During refueling outage 19 in November 2000, a visual inspection on the top surface of the RPV head was performed as part of the

normal shutdown surveillance. The visual inspection and subsequent video inspections showed evidence of boric acid crystals on the vessel head surface around five thermocouple nozzles and CRDM Nozzle 21. An eddy current inspection of CRDM Nozzle 21 performed by Framatome ANP did not identify any indications that suggested a through-wall leak path. An ultrasonic examination of Nozzle 21 was performed in an attempt to locate evidence of OD surface cracking or lack of bond condition. The initial 0° weld profile scan showed evidence of a region of lack of bond between the tube OD surface and the J-groove weld; however, a rescan of the nozzle indicated no lack of bond condition existed.

The thermocouple nozzles were each found to contain large axial, crack-like indications originating on the inside of the nozzles above the weld. These cracks were determined to be the leakage pathway for the thermocouples. A boat sample was removed from CRDM Nozzle 21 to determine the cause of the observed radial cracking and to reconcile the UT signal reflection anomalies detected between the nozzle wall and the attachment weld. PWSCC was determined to be the primary mechanism of crack propagation in the weld and CRDM housing base metal. There was some evidence of hot cracking; however, this crack morphology appears to be secondary to the PWSCC. The destructive examination did not reveal any cracks or other discontinuities at the interface between the weld and the tube material that would explain the anomalous UT signal from this region.

Comparison to Byron Unit 2

Based on EDY, Oconee Unit 1 was a high susceptibility unit at the time of the inspection. The PWSCC observed in CRDM Nozzle 21, and presumably the thermocouple nozzles, was due to exposure of the susceptible material to the corrosive environment in a region of high tensile stress. The occurrence of PWSCC in this unit was not unforeseen based on time at temperature and was not initiated by any identified anomaly.

### 3.5.3 Ohi Power Station Unit 3 – Kansai Electric Power Company

Background

Ohi Power Station Unit 3 is a Mitsubishi Heavy Industries unit, which began commercial service in 1991. During the 10$^{th}$ periodical inspection in April 2004 boric acid was detected near the root of CRDM Penetration 47. Leakage from this nozzle was found, and subsequent visual inspections of the remaining 69 locations revealed boric acid deposits on Penetration 67, a thermocouple penetration. At the time of the inspection, the value of effective degradation years (EDY) for this unit was 4.8, which is considered low susceptibility.

Penetration 67 was examined using eddy current testing, UT, and a helium leak test, and no significant signal indications were found. A review of the records of previous inspections showed leakage of primary coolant from the conoseal cover around the

upper part of Penetration 67 during trial operation. Previous reports suggested that the leaked boric acid was not properly removed from the nozzle at the time of commissioning, and it has remained in place since that time.

Penetration 47 was examined using eddy current testing, and no significant indications of flaws were observed in the interior of the nozzle. Using the advanced Grooveman with low frequency, two signal indications of cracking were identified in the J-groove weld. Ultrasonic testing revealed no significant signal indications in either the base metal of the nozzle or in the vicinity of the nozzle. Dye penetrant test indications were found on the J-groove weld in the same region as detected using eddy current testing. No helium gas was detected during a leakage test of the interior of the nozzle; however, helium gas was detected during a test of the J-groove weld and vicinity.

A boat sample was not removed; however, in-situ metallurgical replicas were prepared. Linear cracks were identified on the J-groove weld surface in the same region as the ET and PT indications. The cracks were observed mainly along the dendrite boundary of the weld metal in the area where PT found indications. Subsequent surface grinding and replication revealed longer, branched cracks along the grain boundaries of the weld metal. After the exam, the J-weld portion of Penetration No. 47 was repaired by weld overlay using Alloy 690. Circumferential abrasions, which were presumed to be grinder marks, were observed in the vicinity of the indications, but marks indicative of buffing, which was required under the normal manufacturing procedures, were not observed. Mock-up experiments suggest that the lack of buffing on the J-groove weld left the surface under residual tensile stress. The findings indicate that the combination of residual tensile stress, material, and environmental conditions led to the initiation of stress corrosion cracking and the propagation of a through-wall crack.

Comparison to Byron Unit 2

Like Byron Unit 2, Ohi Unit 3 was a low susceptibility head based on EDY. The conclusion drawn by the owner, Kansai Electric Power Company, was that the PWSCC was precipitated by a high level of tensile residual stress attributed to the failure to perform a buffing step during the welding procedure. While a boat sample was not taken, in-situ metallurgical replicas characterized the cracking as typical of PWSCC and laboratory mock-up testing verified that high residual tensile stresses could result from the lack of buffing. The cause of the PWSCC at Ohi Unit 3 is not the same as Byron Unit 2; however, both were isolated occurrences. In both cases, a situation existed in the effected nozzle that made the circumstances unique and increased the susceptibility to PWSCC. Byron Unit 2 and Ohi Unit 3 illustrate that widespread PWSCC is not likely in a low susceptibility head without a unique set of extenuating conditions.

# 4 Probabilistic Assessment of PWSCC in Byron Unit 2

As reported above, the occurrence of PWSCC in Byron Unit 2 after only 2.2 effective degradation years was not expected, and the three factors necessary to initiate PWSCC

would not have been met without the presence of the identified weld defects. To illustrate the uniqueness of the PWSCC event, an assessment of primary water stress corrosion cracking in head penetration Nozzle 68 was conducted by employing probabilistic and structural reliability tools. Included in the assessment as a comparison was Nozzle 72, which, at a 47° angle to the reactor head, represents a location more prone to PWSCC. To calculate the probability of failure of an Alloy 600 vessel head penetration as a function of operating time (t), structural reliability models were used with Monte Carlo simulation methods. This section describes these structural reliability models and their basis for the primary failure mode of crack initiation and growth due to PWSCC, the assessment results, and the conclusions.

## 4.1 Probabilistic Models for PWSCC Assessment

The models used for the probabilistic evaluation of head penetration nozzles[15] were developed in 1997 and applied to the vessel head penetrations in 41 Westinghouse plants for their response to NRC Generic Letter 97-01. At that time, these probabilistic models had already been verified in the following ways:

1. Calculated stresses compare well with measured stresses (see Figure 4-1).

2. Crack growth rates agree with measured field data (see Figure 4-2).

3. All models have been independently reviewed by APTECH Engineering[16], and an improved model was developed for the effect of monotonic yield strength on time to initiation.

4. A wide range (both high and low values) of calculated probabilities is consistent with actual plant observations that were available in 1997 (Table 4-1).

**Table 4-1**
**1997 Comparison of VHPNPROF Calculated Probabilities with Plant Observations**

| Parameters | Almaraz 1 | D. C. Cook 2 | Ringhals 2 | North Anna 1 |
|---|---|---|---|---|
| Hours of Operation | 85,400 | 87,000 | 108,400 | 91,000 |
| Setup Angle (°) | 42.6 | 50.5 | 38.6 | * |
| Temperature (°F) | 604.3 | 598.5 | 605.6 | 600.0 |
| Yield Strength (ksi) | 37.5 | 58 | 51.2 | 51.2 |
| Percent GBC | 57.0 | 44.3 | 3.0 | 2.0 |
| Flaw Depth/Wall | 0.10 | 0.43 | 0.25 | 0.10 |
| Initiation Probability | 1.1% | 41.4% | 37.6% | 15.3% |
| Failure Probability** | 1.1% | 38.1% | 34.6% | 15.3% |
| Penetrations with Reported ISI Indications | 0 | 1 | 3 (2 with scratches) | 0 |

Notes:

* Calculations performed at an equivalent setup angle for the second-highest stress location since it could be inspected.

** Defined here as the probability of reaching the specified flaw depth for the individual penetration.

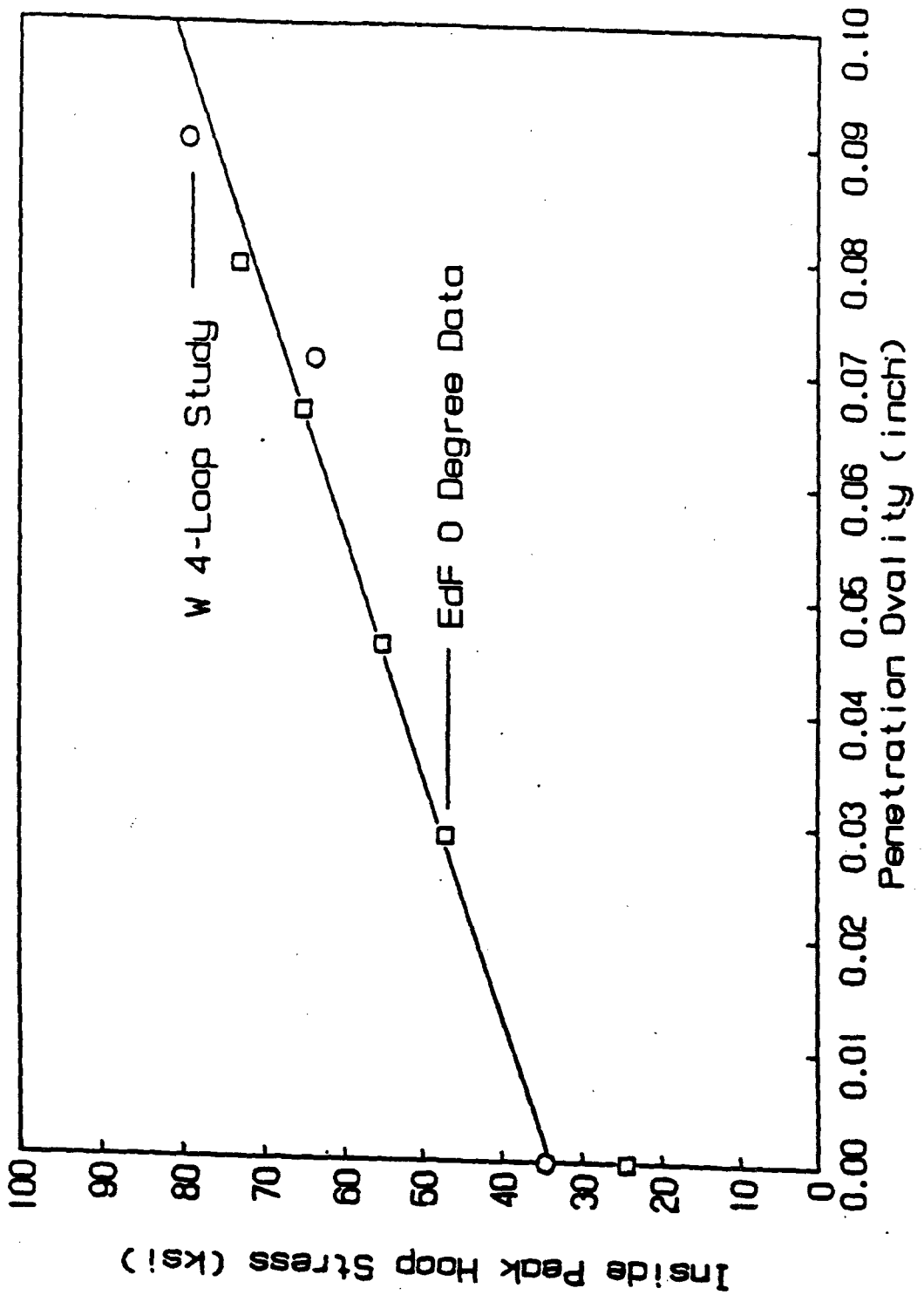


**Figure 4-1:** Vessel Head Penetration Stresses From WOG Four-Loop Plant Study [Ref. 21]

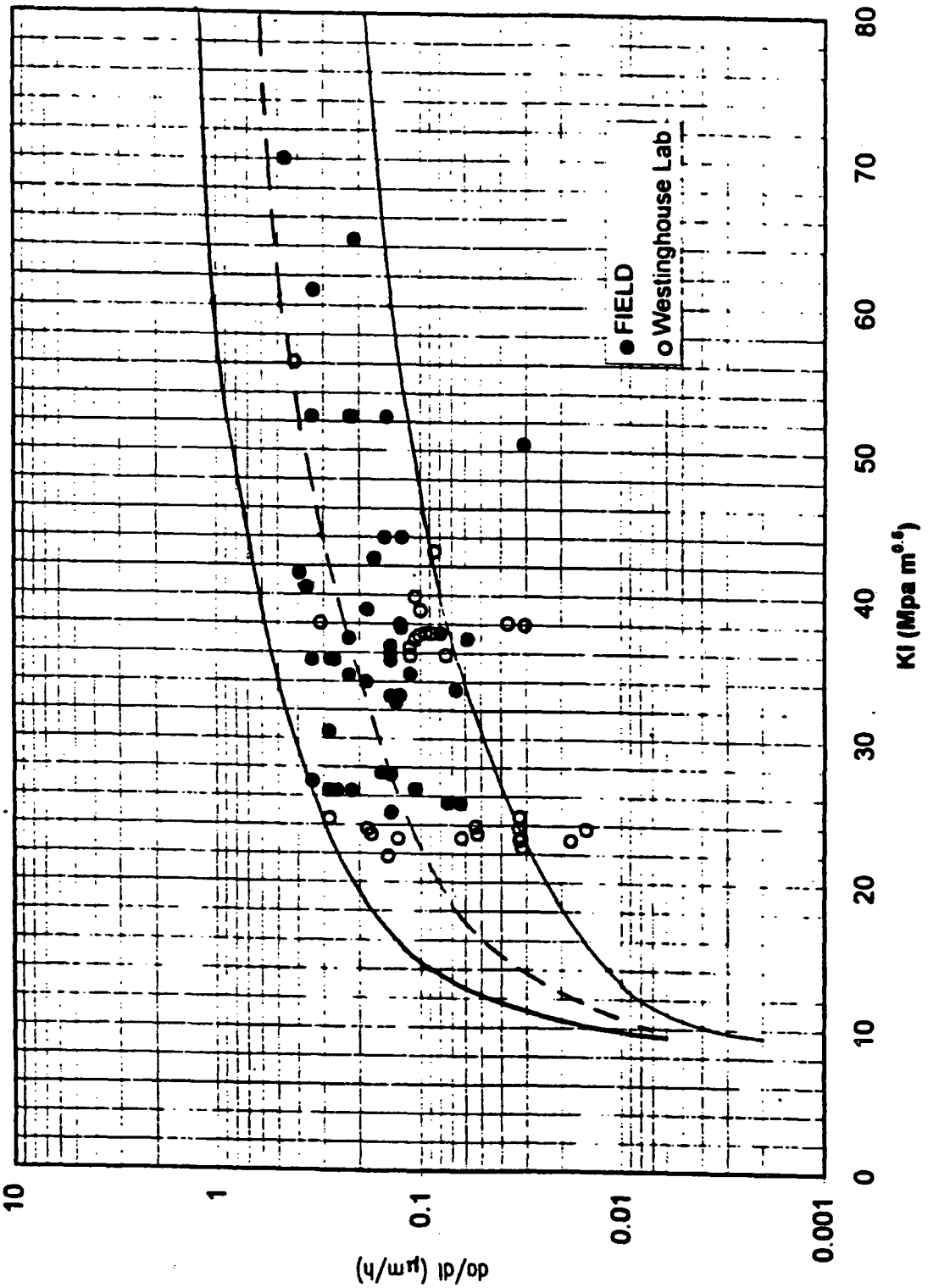


**Figure 4-2:** Comparison of Recent Alloy 600 Data With the Crack Growth Rate Model

As results of further nozzle inspections became available in 2003, the 1997 probability calculations were reevaluated and still found to be consistent with these observations (Table 4-2). In the models for PWSCC assessment, the most important parameter for estimating the failure probability is the time to failure, $t_f$ in hours. It is defined as follows:

$$t_f = t_i + (a_f - a_0) / (da/dt) \qquad (4\text{-}1)$$

where:

$t_i$ = time to initiation in hours

$a_f$ = failure crack depth in inches

$a_0$ = crack depth at initiation in inches*

da/dt = crack growth rate in inch/hour

**Table 4-2**
**2003 Comparison of VHPNPROF Calculated Probabilities with Plant Observations**

| Parameters | Beaver Valley 1 | Farley 2 |
|---|---|---|
| 1997 WCAP Report | 14913 (Ref. 31) | 14906 (Ref. 32) |
| Years of Operation | 27 | 22 |
| Setup Angle (°) | 38.6 | 42.6 |
| Temperature (°F) | 607.0 | 596.9 |
| Yield Strength (ksi) | 48.5 | 48.5 |
| Percent GBC | 23.0 | 23.0 |
| Flaw Depth/Wall | 0.75 | 0.75 |
| Probability of Flaw of This Depth | 43.9% | 27.6%** |
| Penetrations with Reported ISI Indications in 2002 | 4 (~50% through wall) | 0 |
| ** Note: Probabilities do not reflect any reduction due to several years of operation with Zinc Addition | | |

1. _____

* $a_o$, the crack depth at initiation is 1.5 mm or 0.059 inches for consistency with previous assessments.

In Equation (4-1), both the crack depths at failure and initiation may be specified as a fraction of the penetration wall thickness (w). The failure depth $a_f$ depends upon the failure mode being calculated. Since the failure mode of concern is axial cracks in the penetration that are deeper than the structural limit of 75 percent of the penetration wall thickness (w), it would be specified as:

$$a_f = 0.75\ w \tag{4-2}$$

The constant 0.75 in equation (4-2) can be replaced with other values for different failure modes, such as 0.10 for crack initiation, 0.50 for an observed flaw half-way through the wall or 0.995 for a through-wall flaw that could result in a small leak.

The time to PWSCC crack initiation, $t_i$ in hours, is consistent with that developed for PWSCC susceptibility by Rao[17] as updated by Begley and Woodman of APTECH[16]:

$$t_i = \frac{C_1(1+C_2P_{GBC})}{\sigma^{n_1}S_y^{n_2}}\exp\left(\frac{Q_1}{RT}\right) \tag{4-3}$$

$C_1$ = the initiation coefficient, which was based upon the data of Hall and others[18] for forged Alloy 600 pressurizer nozzles, with only the uncertainty in a log-normal distribution based upon the data of Gold and others[19],

$C_2$ = coefficient for the effect of grain boundary carbide coverage, which is based upon the data of Norring and others[20],

$P_{GBC}$ = percentage grain boundary carbide coverage in the penetration material,

$\sigma$ = the maximum residual and operating stress level derived from the detailed elastic-plastic finite-element analysis from the WOG study of Ball and others[21] as shown in Figure 4-1, with its normally distributed uncertainty being derived from the variation in ovality from Duran and others[22] as shown in Figure 4-3, which is a trigonometric function of the penetration diameter and setup angle (local angle between the head and longitudinal axis of penetration),

$S_y$ yield strength of the penetration material,

$n_1, n_2$ = exponents on stress and yield strength, respectively ($n_1 = 4$, $n_2 = 2.5$),

$Q_1$ = the activation energy for crack initiation, which is normally distributed,

R = universal gas constant and

T = the penetration absolute temperature, which is uniformly distributed based upon the calculated variation of the nominal head operating temperature.

Either data from field replication, as was done for Beznau Unit 2[23] or the correlation model by Rao[24] can be used to determine the percent grain boundary carbide coverage, $P_{GBC}$ in Equation (4-3). The model developed by Rao is a statistical correlation of measured values with the certification parameters for 39 commercial heats of Alloy 600 head penetration nozzle materials. For Byron Unit 2, this model was used to calculate the percentage grain boundary carbide coverage in B&W Heat 80054 for Nozzle 68 and B&W Heat 90704 for penetration Nozzle 72 in the same row (highest initiation probability of all nozzles) for the PWSCC assessments. Table 4-3 compares the tensile and chemistry values for these material heats with the range of values that were used to develop the correlation model (Ref. 24). For Heat 80054 in cracked Nozzle 68, chemistry values were available from both the heat certification[25] as well as the metallurgical evaluations of the boat sample by Exelon (Ref. 9).

**Table 4-3**

**Comparison of Material Properties for Byron Unit 2 Head Penetrations and Model Correlation for PGBCC***

| Heat No. (Nozzle) | Data Source (Ref.) | YS* (Ksi) | UTS* (Ksi) | Carbon (%) | Manganese (%) | Nickel (%) |
|---|---|---|---|---|---|---|
| 80054 (68) | CMTR* (25) | 36.5 | 94.6 | 0.029 | 0.27 | 76.23 |
| 80054 (68) | Boat Sample (9) | N/A | N/A | 0.023 | 0.14 | 76.00 |
| 90704 (72) | CMTR* (25) | 40.3 | 90.4 | 0.024 | 0.24 | 75.34 |
| Minimum | Model (24) | 30.5 | 83.5 | 0.028 | 0.16 | 73.66 |
| Maximum | Model (24) | 54.5 | 104.3 | 0.100 | 0.88 | 85.20 |

* Abbreviations: PGBCC = percent grain boundary carbide coverage
YS = 0.2% offset yield strength
UTS = ultimate tensile strength
CMTR = certified material testing report
N/A = not available

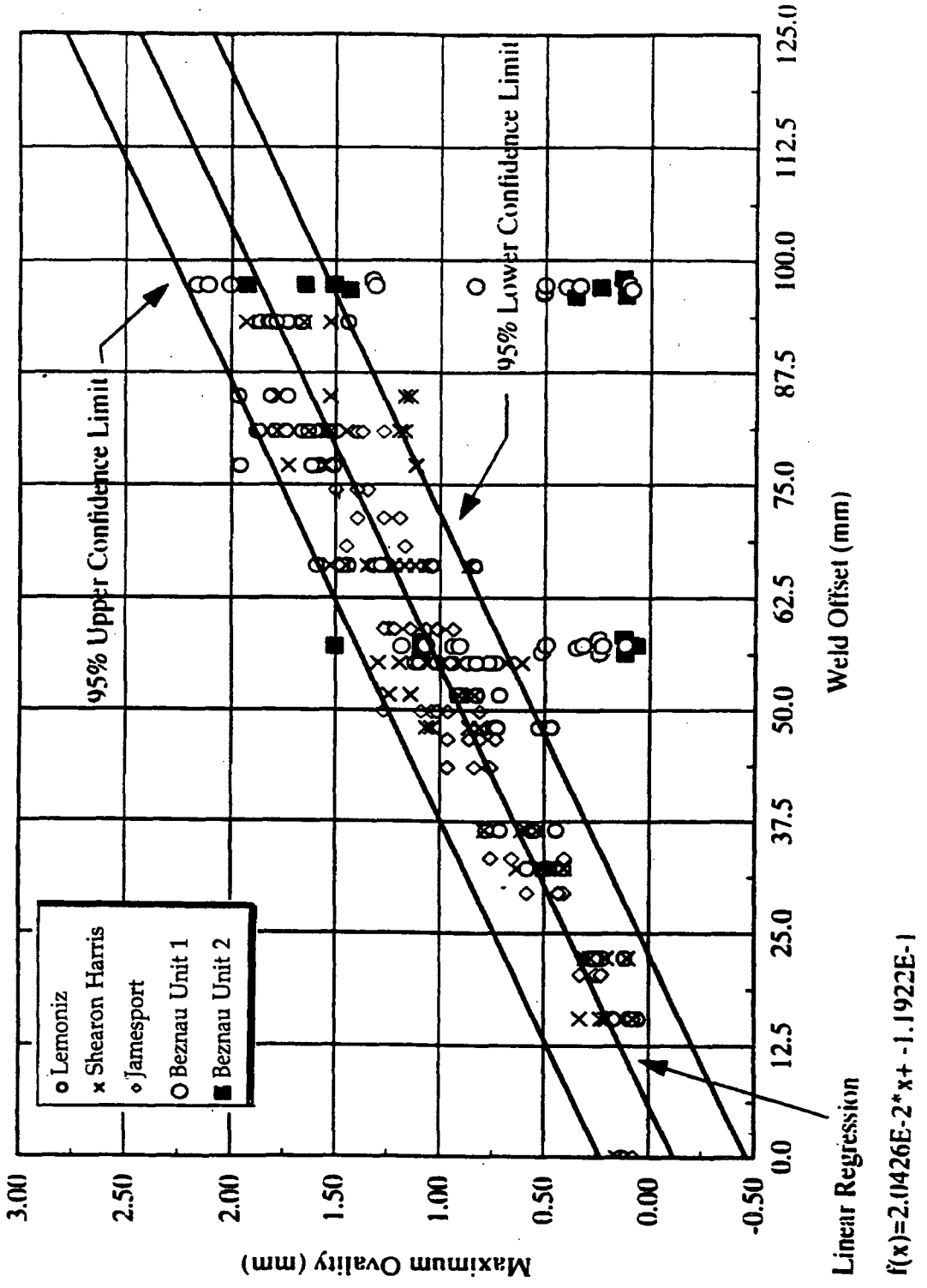


**Figure 4-3:** Measured Vessel Head Penetration Ovality Data and Regression Results [Ref. 22]

The hours at temperature per operating cycle (one year), which are normally distributed, are used to check if crack initiation has occurred. Even though the operating cycle for Byron Unit 2 is 18 months or 1.5 years, a one-year cycle is used for the PFM calculations, because this value was previously requested by the regulatory reviewers. Once the crack has initiated, it is assumed to have a depth of $a_0$ and its growth rate, da/dt, is calculated by the Peter Scott model, which matches the latest Westinghouse and French data and the previous data given in the WOG report on the industry Alloy 600 PWSCC growth rate testing results[26]. The crack growth rate is given by:

$$\frac{da}{dt}=C_3(K_I-K_{TH})^{1.16}\exp\left(\frac{-Q_2}{RT}\right) \quad (4\text{-}4)$$

$C_3$ = a log-normally distributed crack growth rate coefficient (see Figure 4-2)

$K_I$ = the stress intensity factor conservatively calculated assuming a constant stress through the penetration wall for an axial flaw at the inside surface with a length six times its depth using the following form of the Raju and Newman equations[27]:

$$K_I=0.982+1.006(a/w)^2\sigma(\pi a)^{0.5} \quad (4\text{-}5)$$

$Q_2$ = activation energy for PWSCC crack growth, which is also normally distributed, and

$K_{TH}$ = threshold stress intensity factor for crack growth.

The probability of failure of the Alloy 600 vessel head penetration as a function of operating time t, is calculated directly for each set of input values using Monte Carlo simulation. Monte Carlo simulation is an analytical method that provides a histogram of failures with time in a given number of trials (simulated life tests). The area under the simulated histogram increases with time due to PWSCC. The ratio of this area to the total number of trials is approximately equal to the probability of failure at any given time. In each trial, the values of the specified set of random variables are selected according to the specified distribution. A mechanistic analysis is performed using these values to calculate if the penetration will fail at any time during its lifetime (e.g., 20, 40 or 60 years). This process is repeated many times (e.g., 60,000) until a sufficient number of failures is achieved (e.g., ten per year) to define a meaningful histogram, which is an approximation of the lower tail of the true statistical distribution in time to failure (see Figure 4-4). The shape of the distribution depends upon the input median values and specified distributions of the random variables. For the worst penetration in one plant, the mean time to failure was greater than 160 years but its uncertainty was so large that the normalized area under the histogram (estimated probability) at 60 years was 8 percent.

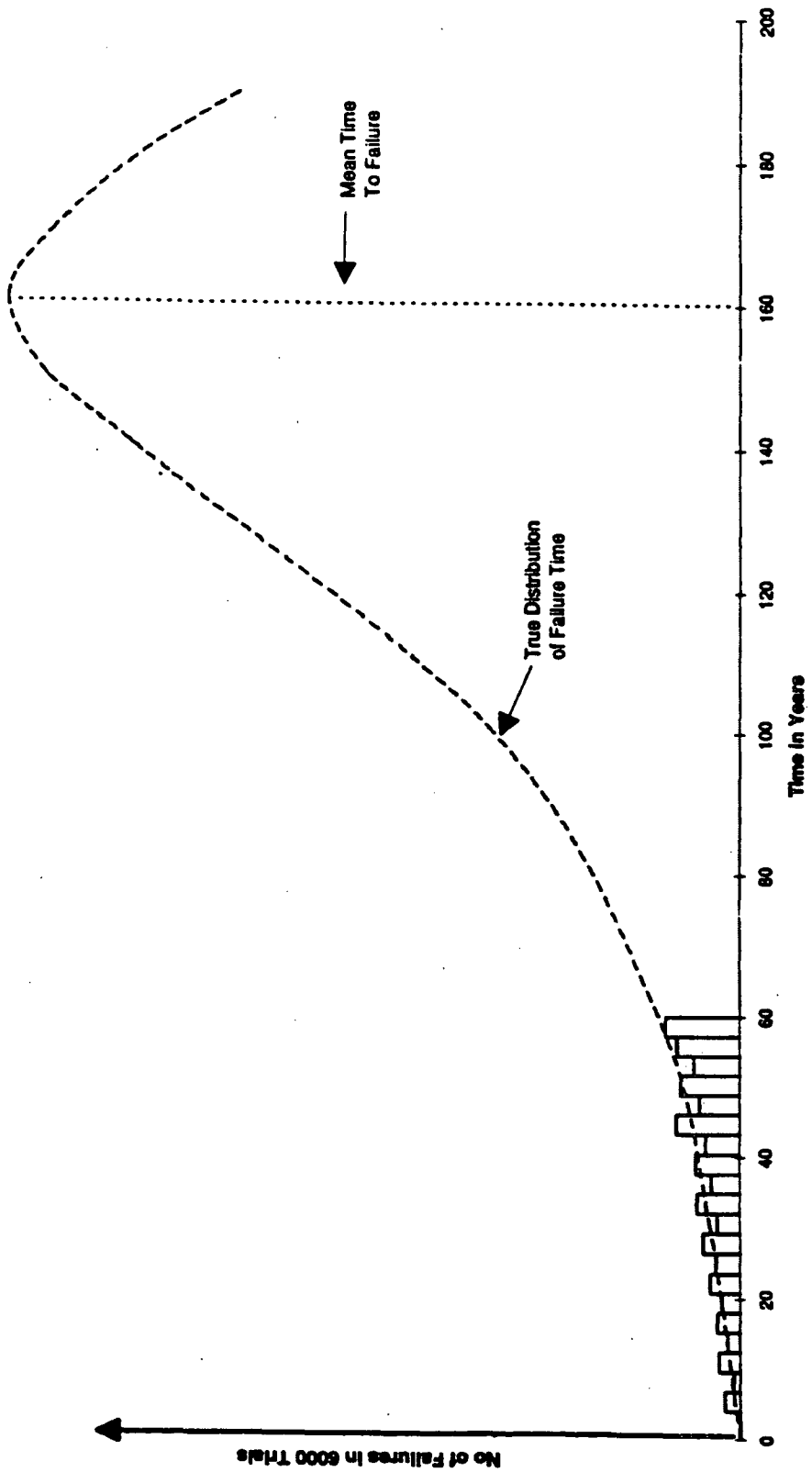


**Figure 4-4:** Example Histogram of Failures From Monte Carlo Simulation

To apply the Monte Carlo simulation method for vessel head penetration nozzle (VHPN) failure, the existing PROF (probability of failure) object library in the Westinghouse Structural Reliability and Risk Assessment (SRRA) software system was combined with the PWSCC structural reliability models. This system provides standard input and output, including plotting and probabilistic analysis capabilities (e.g., random number generation, importance sampling). The result was program VHPNPROF for calculation of head penetration failure probability with time. Descriptions of the 21 VHPNPROF input variables are given in Table 4-4. This table also indicates the type of statistical distribution that was used to simulate the uncertainty in each random variable. The uncertainty in those variables with a constant distribution was not simulated in the current PWSCC assessment.

The Westinghouse SRRA Software System has been verified by hand calculation for simple models and alternative methods for more complex models[28]. Also, the application of this same Westinghouse SRRA methodology to the WOG-sponsored pilot program for piping risk-based inspection has been extensively reviewed and verified by the American Society of Mechanical Engineers (ASME) Research Task Force on Risk-Based Inspection (RBI) Guidelines[29] and other independent NRC contractors. Table 4-5 provides a summary of the wide range of parameters that were considered in this comprehensive benchmarking study that compared the Westinghouse-calculated probabilities from the analysis (labeled SRRA) with those from the pc-PRAISE program[30]. As shown in Figure 4-5, the comparison of calculated probabilities after 40 years of operation is excellent for both small and large leaks and full breaks, including those reduced due to taking credit for leak detection.

As indicated previously, the VHPNPROF Program calculated probabilities of getting a given crack depth due to PWSCC were compared for four plants where sufficient head penetration information and inspection results were available in 1997. The four plants are identified in Table 4-1 along with the values of the key input parameters and calculated failure probabilities. This table also shows the agreement between the inspection results available in 1997 and the VHPNPROF predicted failure trends due to PWSCC.

Almost five years later, the 1997 VHPNPROF results were found to predict the latest Beaver Valley and Farley inspection results. As shown in Table 4-2, the four head penetration nozzles (50 to 53) with deep cracks at Beaver Valley Unit 1[31] were predicted to have very high probability of a flaw 75% through the wall after 27 years of operation. For Farley Unit 2[32], the same material that cracked at Beaver Valley was in almost all the head penetrations but no cracking was observed after 22 years of operation. In both cases, the percent grain boundary carbide coverage was not a predicted value, but a measured value from field replication. The lack of cracking was predicted at Farley Unit 2 because it had operated about five years less that Beaver Valley Unit 1 at a head temperature about 10°F lower. It also operated for several years with Zinc Addition, which is a PWSCC mitigation measure whose effects were not reflected in the probabilities of Table 4-2. Large cracks were never observed at Farley Unit 2 because the vessel closure head and its penetration nozzles were replaced before they could

occur. Therefore, it can be concluded that the probability ranges are 34% to 44% for expected failure and 0% to 33% for unexpected failure.

**Table 4-4**
**Variables for Structural Reliability Model of Reactor Vessel Head Penetration Nozzle (VNPNPROF)**

| No. | Name | Description of Input Variable | Distribution |
|---|---|---|---|
| 1 | ANGLE-P | Penetration setup angle (degrees) | Constant |
| 2 | C0-SIGR | Peak hoop stress at 0 degrees (ksi) | Normal |
| 3 | C1-SIGR | Change in stress with angle (ksi) | Constant |
| 4 | PTEMP-F | Penetration material temperature (F) | Uniform |
| 5 | S-YIELD | Material monotonic yield strength (ksi) | Normal |
| 6 | NCY-ISI | Cycles between inservice inspections | Constant |
| 7 | D05-ISI | Depth at 5% detection probability (in.) | Constant |
| 8 | D50-ISI | Depth at 50% detection probability (in.) | Constant |
| 9 | HRS@T/CY | Hours at temperature per operating cycle | Normal |
| 10 | C0-TINIT | Initiation coefficient at 0 PGBCC (hr) | Log-Normal |
| 11 | PGBCC-TI | Percent grain boundary carbide coverage | Normal |
| 12 | Q-TINIT | Initiation activation energy (cal/mole) | Normal |
| 13 | SEXP-TI | Stress exponent for initiation time | Constant |
| 14 | C1-TINIT | Initiation time change with PGBCC (hr) | Constant |
| 15 | C-GRATE | Crack growth rate coefficient (in./hr) | Log-Normal |
| 16 | KITH-GR | Threshold stress intensity (ksi-in.^.5) | Constant |
| 17 | Q-GRATE | Growth rate activation energy (cal/mole) | Normal |
| 18 | KEXP-GR | Growth rate stress intensity exponent | Constant |
| 19 | DEPTH-L | Crack depth at Initiation (in.) | Normal |
| 20 | DEPTH-L | Limit on crack depth (fraction of wall) | Constant |
| 21 | TH-WALL | Penetration wall thickness (in.) | Normal |

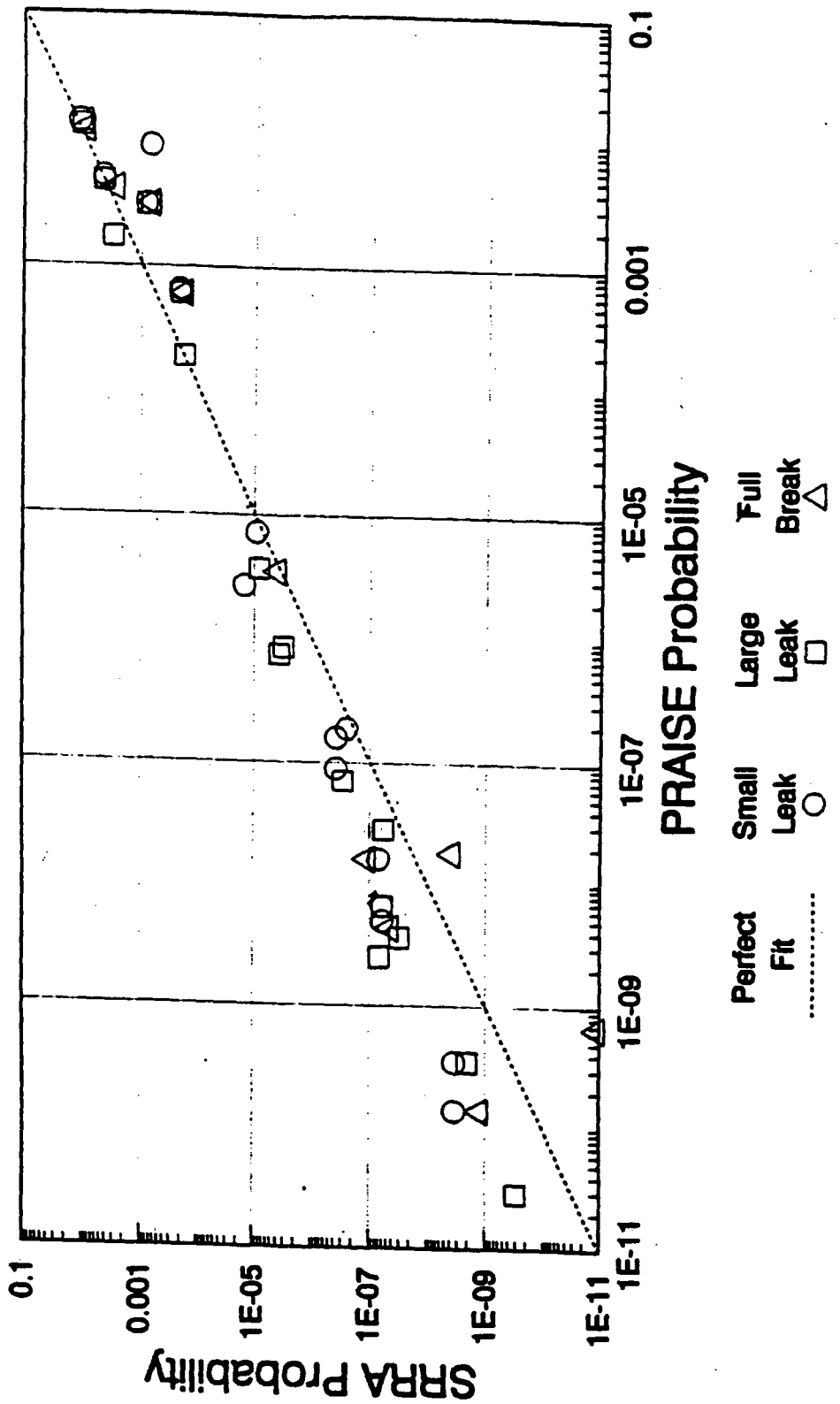


**Figure 4-5:** Comparison of Calculated Piping Probabilities

| Table 4-5<br>Parameters Used for the pc-Praise Benchmarking Study | | |
|---|---|---|
| **Type of Parameter** | **First Value** | **Second Value** |
| Pipe Material | Ferritic | Stainless steel |
| Pipe Geometry | 6.625" OD<br>0.562" Wall | 29.0" OD<br>2.5" wall |
| Failure Modes | Small leak<br>(through-wall crack) | Full break<br>(unstable fracture) |
| Last-Pass Weld Inspection | No 4-ray | Radiographic |
| Pressure Loading | 1000 psi | 2235 psi |
| Low-Cycle<br>Loading | 25 ksi range<br>10 cycles/year | 50 ksi range<br>20 cycles/year |
| High-Cycle*<br>Loading | 1 ksi range<br>0.1 cycles/min. | 20 ksi range<br>1.0 cycles/sec. |
| Design Limiting Stress | 15 ksi | 30 ksi |
| Disabling Leak Rate | 50 gpm | 500 gpm |
| Detectable Leak Rate | None | 3 gpm |
| * Note: Mechanical vibration (1st value of stress range and 2nd value of frequency) for small pipe, thermal fatigue (2nd value of stress range and 1st value of frequency) for large pipe. | | |

## 4.2 PWSCC Assessment Results

The probabilistic PWSCC assessment results of the vessel head penetrations nozzle (VHPN) numbers 68 and 72 in Byron Unit 2 are summarized in Table 4-6. This table provides the probability of initiating a flaw due to PWSCC as well as propagating it 50 percent (observed in Nozzle 68) and 100 percent through the wall at the end of 20 years (1987 through 2007) of operation at a head temperature of 551° F. The small differences in the minimum and maximum values of probability for head penetration Nozzle 68 are due to the difference in the predicted value of grain boundary carbide coverage for the two sets of chemistry values for the VHPN material heat 80054 that are reported in Table 4-3.

The probabilities based on the occurrence of 50% through-wall crack in VHPN number 68 that was observed after 20 years in Table 4-6, are significantly lower (approximately three orders of magnitude) than the values predicted for observed cracking due to PWSCC initiation and growth in Tables 4-1 and 4-2. The 20-year probabilities reported in Table 4-6 also indicate that crack initiation and growth due to PWSCC is four to six times more likely to occur in VHPN Number 72 than VHPN Number 68, where it was

observed in Byron Unit 2. This probability further indicates that another factor (namely, lack of fusion in the weld) facilitated the initiation of PWSCC in Nozzle 68.

**Table 4-6**
**Summary of Byron Unit 2 RVHP Probabilities at 20 Years**

| Penetration No. | Failure Mode | Probability |
|---|---|---|
| 68 (Minimum) | Initiation | 1.90 E-04 |
| | 50% Through Wall | 4.49 E-05 |
| | 100% Through Wall | 2.06 E-05 |
| 68 (Maximum) | Initiation | 1.97 E-04 |
| | 50% Through Wall | 4.66 E-05 |
| | 100% Through Wall | 2.15 E-05 |
| 72 | Initiation | 1.20 E-03 |
| | 100% Through Wall | 8.03 E-05 |

## 4.3 Effects of In-Service Inspections

The beneficial effects of in-service inspection (ISI) were modeled and calculated in the same way as was done in the PFM models for piping RI-ISI (Ref. 28) and in the NRC sponsored pc-PRAISE Code (Ref. 30) for PFM analysis of piping welds. Specifically, only the flaws remaining after an ISI exam are left to cause failures (larger flaw depth of concern) later in life, because flaws that are detected are assumed to be repaired or removed. Existing fabrication or initiated flaws that were not detected in the initial examination would remain in the nozzle and be subject to potential crack growth due to PWSCC. If the undetected crack grows, then the chance of its being detected during a subsequent inspection will increase. The input to these PFM models for the effects of ISI should be selected to represent the inspection accuracy and frequency for the inspection that have been, or will be, performed in accordance with the requirements for reactor vessel head penetration nozzles.

For Byron Unit 2, penetration Nozzle 68 was inspected after 20 years of operation and the fabrication-induced flaw from which PWSCC initiated and slowly propagated at the relatively low head temperatures was detected and subsequently repaired. As noted previously, during this same inspection no flaws were detected in Nozzle 72, which had a higher probability of flaw initiation and growth than for Nozzle 68. This was as expected since Table 4-6 shows that the probability of initiating a flaw due to PWSCC after 20 years of operation is only 0.12%. Since this probability and the probability of having a through wall flaw, which is the primary concern because it could result in a small leak of boric acid, both increase with operating time, Nozzle 72 was selected for

evaluation of the effects of ISI after the initial inspection after 20 years. ISI frequencies of 3, 6 and 9 years (2, 4 and 6 operating cycles) were evaluated to determine an acceptable frequency based upon the probability of a through-wall flaw after 60 years of operation.

The probability of detection (POD) that was used in the evaluation of ISI effects was linearly proportional to (a/t), where a is flaw depth and t is the penetration nozzle wall thickness. For this POD of flaws due to PWSCC, there would only be a 10% probability of detecting a flaw depth 10% through the wall and a 50% probability of detecting a flaw depth half way through the wall. This is very conservative because it minimizes the benefit of ISI. In addition, the PWR Materials Reliability Program (MRP) inspection demonstration for Alloy-600 head penetration nozzles (Ref. 8) showed a very high POD for flaw depths equal to or greater than 10% of the wall thickness.

The effects of ISI frequency for Byron Unit 2 head penetration Nozzle 72 for inspections after 20 years of operation are shown in Table 4-7. As can be seen in this table, the effect of subsequent ISI is to decrease the probability of a through-wall flaw after 60 years of operation from 2.4% with no ISI to 0.065% with ISI every 6 years (a factor of ~37 reduction). Any of the ISI frequencies that were evaluated, 3, 6, or 9 years (2, 4, or 6 cycles), would be acceptable. These ISI frequencies provide significant improvement over the no ISI case, and the difference between inspection intervals is a factor of three or less.

**Table 4-7**
**Effect of ISI on Cumulative Probability of Through Wall Flaw in Byron Unit 2 Nozzle 72 for First ISI at 20 Years**

| End of Year | Without Any ISI | ISI Every 3 Years | ISI Every 6 Years | ISI Every 9 Years |
|---|---|---|---|---|
| 20 | 8.03E-05 | 8.03E-05 | 8.03E-05 | 8.03E-05 |
| 25 | 4.42E-04 | 1.66E-04 | 2.28E-04 | 2.28E-04 |
| 30 | 1.33E-03 | 2.00E-04 | 3.92E-04 | 5.24E-04 |
| 35 | 3.33E-03 | 2.12E-04 | 5.42E-04 | 7.89E-04 |
| 40 | 5.86E-03 | 2.13E-04 | 6.12E-04 | 1.02E-03 |
| 45 | 8.95E-03 | 2.13E-04 | 6.34E-04 | 1.12E-03 |
| 50 | 1.29E-02 | 2.13E-04 | 6.43E-04 | 1.18E-03 |
| 55 | 1.84E-02 | 2.13E-04 | 6.46E-04 | 1.22E-03 |
| 60 | 2.41E-02 | 2.13E-04 | 6.47E-04 | 1.24E-03 |

## 4.4 Probabilistic Assessment Summary and Conclusions

1. PWSCC probabilistic failure assessments were made by employing Westinghouse crack initiation and growth models that were benchmarked in 1997 with cracking

observations in four plants and confirmed six years later with cracking observations in two additional plants.

2. The results of the probabilistic assessments showed that the probability of having the observed 50% through-wall flaw in Nozzle 68 after 20 years of service were three orders of magnitude below those expected (34% to 44%) for flaw initiation and growth due to PWSCC in Byron Unit 2.

3. The results of the PWSCC probabilistic assessments also showed that the observed 50% through-wall flaw did not occur in the most likely nozzle location in Byron Unit 2.

4. The conclusion of these probabilistic calculations is that the 50% through-wall flaw depth observed in vessel head penetration Nozzle 68 of Byron Unit 2 is not due to normal flaw initiation and growth by PWSCC in the Alloy 600 base metal. Additional conditions, such as those identified in the boat sample metallurgical analysis, are needed to initiate and grow a PWSCC flaw in Nozzle 68.

5. This conclusion is further supported by inspection results from cold head plant upper head penetrations and bottom mounted penetration nozzles, as described in Section 2.3.

6. The effect of in-service inspection after 20 years of operation is to reduce the probability of a through-wall flaw due to initiation and growth by PWSCC after 60 years of operation by a factor of about 37 for an inspection interval of six years.

7. Based on these analyses, an inspection frequency for Byron Unit 2 that is consistent with a low susceptibility head would not significantly increase the probability of a through-wall crack and subsequent leakage on top of the RPV head; therefore, the low susceptibility inspection frequency is acceptable.

## 4.5 Weibull Analysis of Cold Head RVHP Inspection Results

In order to determine the probability of developing repairable indications for future outage intervals, a statistical analysis of available industry experience for Alloy 600 reactor vessel head penetrations (RPVH) was conducted for reactor heads with a temperature similar to Byron Unit 2. The goal of this work is to determine the probability of occurrence of repairable indications for future inspection outages. RVHP inspection data available for 18 four-loop cold head plants is summarized in Section 2.3. The effective degradation years (EDY) at the time of inspection for these plants range from about 1.9 to 2.5. An effective degradation year is equivalent to one effective full power year at 600°F. The Byron 2 inspection occurred at 2.2 EDY.

The statistical model is designed to provide probabilistic predictions of the number of RVHP nozzle surfaces that will develop a recordable flaw similar to that discovered at Byron Unit 2 in the interval between the B2R13 and B2R14 inspection outages. The results of the base case are summarized in Table 4-8. The predicted probability of

flaws requiring repair developing in one or more penetrations during that interval is 1%. Restated, if a thousand heads were observed over the interval of interest, 99% of these heads are expected have head penetrations without flaws; equivalently, 1% of the heads would have one or more flawed RVHP.

One assumption of this analysis is that, within the population of cold head plants, the occurrence of a flaw on one penetration at a point in time is independent of (uncorrelated with) the occurrence or non-occurrence of a flaw on another penetration. This assumption is supported by the unique set of factors that caused the flaw found in Nozzle 68 at Byron Unit 2 (refer to Section 3).

### 4.5.1 Description of Steps Taken in Developing the Statistical Model

*Step 1: Specify a failure model:*

The Weibull distribution is the most popular statistical model of corrosion-related failure. The Weibull cumulative probability of failure (in this case, "detectable indications") by the time of the last inspection ($t_c$) for the $i^{th}$ penetration in a specified group is:

$$p = 1 - \exp(-(t_c / \alpha)^{\beta}) \qquad (4\text{-}6)$$

The alpha ($\alpha$) parameter is the "characteristic life" of a penetration. Due to data limitations, the beta ($\beta$) shape parameter must be inferred from other studies. Statistical analyses of PWSCC in Alloy 600 materials[33,34] suggest a shape value of 2.0 to 3.0. A value of 2.5 is assumed for the base case analysis; the basis for this assumption is provided below.

*Step 2: Estimation of characteristic life (alpha):*

If failures exist in the data set of interest, then the value of alpha is [35]:

$$\hat{\alpha} = \frac{t_{15}}{(-\ln(1-(x/N)^{1/\beta}} \qquad (4\text{-}7)$$

*Step 3: Predict the unconditional probability of $i^{th}$ penetration failure between the last (EDY=$t_{13}$) and next inspection (EDY=$t_{14}$):*

$$q = \exp(-(t_{13} / \hat{\alpha})^{\beta}) - \exp(-(t_{14} / \hat{\alpha})^{\beta}) \qquad (4\text{-}8)$$

An indication is defined as having one or more recordable, detectable flaws in the base metal of the penetration surface of interest. This is the probability of indications in the time interval of interest before it is known if the penetration has survived to the last inspection.

*Step 4: Predict the conditional probability of the $i^{th}$ penetration failing between the last and next inspection, given that it survived to the last inspection:*

$$\pi = \frac{q}{1-p} \qquad (4\text{-}9)$$

This step adjusts for the fact that the penetration has survived, without detectable degradation, to the last inspection. If a nozzle surface has not survived but has been repaired, as is the case for Byron Unit 2 Nozzle 68, then the surface for that nozzle is assumed to be impervious to PWSCC for the time interval of interest here (one refueling cycle).

*Step 5: Predict the probability of x>0 for the N penetrations failing between the two inspections:*

probability (1 or more VHPN with flaws) = 1- Binomdist(0, N, π) (4-10)

In Excel®, binomdist(0, N, π) is the function for the binomial distribution calculating the probability of zero "failures" in N trials given the probability of failure on any given trial is π. Thus Equation 4-9 calculates the probability of one or more VHPN with indications as one minus the probability of zero ID indications. Probabilities of any surfaces with flaws up to N can also be calculated using this distribution.

*Step 6: Calculate the probability distribution describing the predicted number of penetrations having one or more recordable flaws in the Byron 2 reactor vessel head by the next inspection:*

The probabilities of finding 0, 1, 2, ...et cetera nozzles with one or more flaws are calculated using the binomial function shown on the right side of Equation 4-10. Note that the prediction is for the number of penetrations that have one or more flaws (there may be more than one flaw, usually called an "indication" in NDE parlance, on a penetration, but this is not counted here).

### 4.5.2 Weibull Shape Parameter

Since only one detectable defect has been found out of 1,404 cold head RVHP inspections, a shape parameter must be assumed in order to determine the Weibull "characteristic life" or scale parameter (β). The pattern of the failure rate over time determines the appropriate Weibull shape parameter. The failure rate is defined as the frequency with which a component experiences a failure at time (t) given that it has survived to that time. It is expressed as failures per unit time. A shape parameter of β<1 implies a decreasing failure rate over time consistent with component "infant mortality". A shape parameter of β=1 implies a failure rate which is constant over time or "random" failures. When β=2, it implies a failure rate which increases linearly with time. Shape parameter values between 1 and 2 imply an increasing failure rate with a

decreasing rate of increase. Shape parameters greater than 2 imply increasing failure rates with increasing rates of increase.

Statistical analyses of PWSCC in Alloy 600 materials (References 33 and 34) suggest a shape value of 2.0 to 3.0. The base case Weibull analyses are based on an assumed value of 2.5. Sensitivity results are provided for shape parameters of 2.0 and 3.0.

### 4.5.3 Results of the Statistical Analysis

For the assumed base case Weibull shape parameter of 2.5, the calculated scale parameter is 35.2 EDY. This represents the time at which 63.2 percent of RVHP cold head locations would be repaired. With an increase of 0.1 EDY per calendar year of plant operation, this would be equivalent to about 352 years of operation. Table 4.8 indicates that based on these Weibull parameters, the projected mean repairs at B2R14 are 0.018% or 0.018 penetrations out of 77 RVHP. This is consistent with a 1.41% probability that one or more RVHP repairs would be required. If the next RVHP inspection is during B2R17, these values would increase to mean repairs 0.085% or 0.065 penetrations out of 77 RVHP with a 5.00% probability that one or more RVHP repairs would be required.

**Table 4-8**
**Weibull Analysis Base Case**
**(Weibull Shape Parameter = 2.5 and Weibull Scale Parameter = 34.5)**

| Outage # | 14 | 17 | 21 |
|---|---|---|---|
| EDY at Outage | 2.35 | 2.80 | 3.40 |
| Mean Repairs (%) | 0.018% | 0.085% | 0.202% |
| Mean Repairs (out of 77 RVHP) | 0.014 | 0.065 | 0.156 |
| Probability Of Repair(*) | 1.41% | 5.00% | 8.65% |

### 4.5.4 Sensitivity of Results to the Assumed Shape Parameter

Sensitivity results presented in Tables 4.9 and 4.10 for assumed Weibull shape parameters from 2.0 and 3.0 indicate projected mean repairs at B2R14 between 0.013% and 0.024% or between 0.010 and 0.019 penetrations out of 77 RVHP. This is consistent with a 1.03% to 1.85% probability that one or more RVHP repairs would be required. For the next RVHP inspection during B2R17 these values would increase to mean repairs between 0.059% and 0.117% or between 0.046 and 0.090 penetrations out of 77 RVHP with a 3.46% to 6.93% probability that one or more RVHP repairs would be required.

**Table 4-9**
**Sensitivity Results for Assumed Shape Parameter**
**(Weibull Shape Parameter = 2.0 and Weibull Scale Parameter = 71.2)**

| Outage # | 14 | 17 | 21 |
|---|---|---|---|
| EDY at Outage | 2.35 | 2.80 | 3.40 |
| Mean Repairs (%) | 0.013% | 0.059% | 0.133% |
| Mean Repairs (out of 77 RVHP) | 0.010 | 0.046 | 0.102 |
| Probability Of Repair | 1.03% | 3.46% | 5.50% |

**Table 4-10**
**Sensitivity Results for Assumed Shape Parameter**
**(Weibull Shape Parameter = 3.0 and Weibull Scale Parameter = 21.3)**

| Outage # | 14 | 17 | 21 |
|---|---|---|---|
| EDY at Outage | 2.35 | 2.80 | 3.40 |
| Mean Repairs (%) | 0.024% | 0.117% | 0.297% |
| Mean Repairs (out of 77 RVHP) | 0.019 | 0.090 | 0.229 |
| Probability Of Repair | 1.85% | 6.93% | 12.98% |

### 4.5.5 Comparison with MRP-105 Weibull Analysis Results for RPV Head Cracking

MRP-105 performed a Weibull analysis based on inspection results for 30 of 69 U. S. PWRs which had performed NDE by the end of the Spring 2003 outage season. This analysis included both hot and cold head plants, and 14 of the 30 plants had detected leakage or some form of cracking. The plants with leaks or cracking operated with head temperatures between 593.7° F and 605.0° F and had EDYs between 11.2 and 23.7 at the time of inspection. The resulting Weibull scale parameter from this study was 62.3 EDY for an assumed shape parameter of 3.0.

The projection of repairs presented in Table 4.11 indicates results lower than those in Table 4.10 for the cold head analysis by a factor of over 20.

**Table 4-11**
**Comparison with MRP-105 Weibull Analysis**
**(Weibull Shape Parameter = 3.0 and Weibull Scale Parameter = 62.3)**

| Outage # | 14 | 17 | 21 |
|---|---|---|---|
| EDY at Outage | 2.35 | 2.80 | 3.40 |
| Mean Repairs (%) | 0.001% | 0.005% | 0.012% |
| Mean Repairs (out of 77 RVHP) | 0.001 | 0.004 | 0.009 |
| Probability Of Repair | 0.07% | 0.28% | 0.55% |

### 4.5.6 Comparison with Weibull Analysis Results for Bottom Head Penetration Cracking

Inspection results for bottom head penetrations presented in Section 2.3 indicate that out of 1,600 inspections, only two leaking penetrations were found at the South Texas plant in Spring 2003. For an assumed Weibull shape parameter of 2.5, the calculated scale parameter is 27.5 EDY. Table 4.12 presents summary results for Byron 2 RVHP if this scale parameter is taken as representative of repairable flaws in lower temperature head penetrations. This would indicate that projected mean repairs at B2R14 are 0.032% or 0.025 penetrations out of 77 RVHP. This is consistent with a 2.46% probability that one or more RVHP repairs would be required, as shown in Table 4-12. For the next RVHP inspection during B2R17 these values would increase to mean repairs 0.149% or 0.115 penetrations out of 77 RVHP with a 8.62% probability that one or more RVHP repairs would be required. These results are just slightly higher than those presented in Table 4.10 for the RVHP analysis with an assumed shape parameter of 3.0.

**Table 4-12**
**Results for Scale Parameter for Repairable Flaws**
**(Weibull Shape Parameter = 2.5 and Weibull Scale Parameter = 27.5)**

| Outage # | 14 | 17 | 21 |
|---|---|---|---|
| EDY at Outage | 2.35 | 2.80 | 3.40 |
| Mean Repairs (%) | 0.032% | 0.149% | 0.355% |
| Mean Repairs (out of 77 RVHP) | 0.025 | 0.115 | 0.273 |
| Probability Of Repair | 2.46% | 8.62% | 14.70% |

### 4.5.7 Summary of Weibull Analyses

Based on the Weibull analysis of cold head RVHP and low temperature bottom head penetration inspection and failure data presented in this section, the projected RVHP failures at Byron Unit 2 at the next outage (B2R14) is very low with the probability of repair of one or more penetrations at approximately 1%. These values increase over time but remain low with an expected value of repair at about 5% in six years for the base case.

## 5 Byron Unit 2 PWSCC Growth Projections and Flaw Tolerance

This section reviews the PWSCC crack growth rates and flaw tolerance of RPV head penetrations. It summarizes the evaluation methods and residual stress fields used in the nozzle crack growth studies. The evaluation results and crack growth projections

are summarized and used to establish the recommended inspection intervals for the Byron Unit 2 reactor vessel head nozzles.

## 5.1 PWSCC Crack Growth Rates

PWSCC crack growth rates for Alloy 600 material used in these growth projections have been defined in MRP-55[36] and accepted by the industry in ASME Section XI, Appendix O[37]. The PWSCC growth rates have been determined to be directly dependent on temperature, i.e. increasing temperature increases the crack growth rate.

Temperature monitoring of the Byron Unit 2 reactor vessel head has demonstrated the operating temperature is below 558°F. Two Reactor Vessel Level Indication System (RVLIS) Probes were installed for determination of the vessel water level during an accident condition. The RVLIS Probes contain 8 thermocouple sensors. Two of these sensors, the upper sensors, are located in the head area above the Upper Internal Support Plate[38]. Sensor 1 is located as close as possible to the top of the head and the next lower sensor, Sensor 2, is located just above the Upper Internal Support Plate. Additionally, the two upper sensors have limited interaction with the lower sensors by way of a divider disk[39]. This separation ensures that a true representation of head temperature is measured. Measurements from Sensors 1 and 2 since startup of Unit 2 Cycle 14 (current operating cycle) are presented in Figure 5-1. The maximum average temperature for the head based on these measurements is 545°F. These measurements confirm that using a temperature of 558°F is conservative when calculating crack growth in the head nozzles.

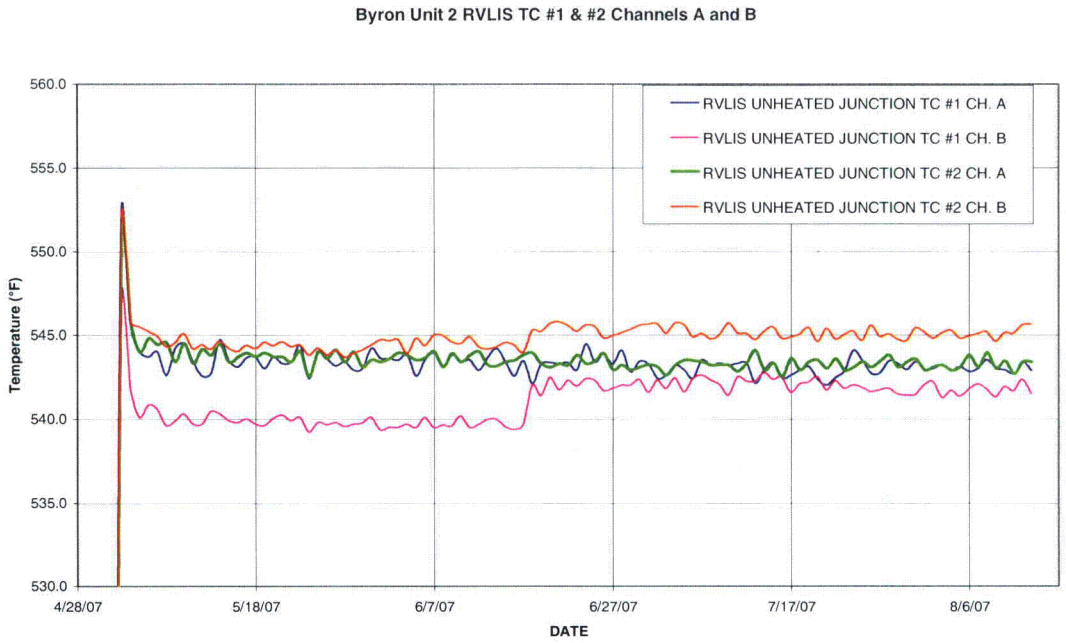


**Figure 5-1:** Byron Unit 2 Reactor Vessel Head Operating Temperature for Fuel Cycle 14

The following equation was taken from the ASME code, Reference 37, and is used for the crack growth projections.

$$\dot{a} = \exp\left[-\frac{Q_g}{R}\left(\frac{1}{T}-\frac{1}{T_{ref}}\right)\right]\alpha\left(K_I - K_{th}\right)^{\beta} \qquad (5\text{-}1)$$

where

$\dot{a}$ = the crack growth rate at temperature, T, in m/s
$Q_g$ = Thermal activation energy for crack growth, 130 kJ/mole
$R$ = universal gas constant, 8.314 x $10^{-3}$ kJ/mole-°K
$T$ = Absolute operating temperature, °K
$T_{ref}$ = absolute reference temperature used to normalize data, 598.15°K
$\alpha$ = crack growth rate coefficient,2.67 x 10-12 for units of m/s and stress intensity factor units of MPa√m
$K_I$ = crack tip stress intensity factor, MPa√m
$K_{th}$ = crack tip stress intensity factor threshold for SCC, 9 MPa√m
$\beta$ = exponent, 1.16

Using this equation, comparisons of the crack growth rates for the Byron Unit 2 head temperature of 545°F, the 558°F head temperature used for the crack growth predictions, and a typical hot head temperature of 600°F can be performed. Figure 5-2 presents these comparisons for a range of stress intensity factors. Based on the magnitude of the weld residual stresses driving PWSCC cracks and the crack sizes that can be detected, the stress intensity factor would be expected to range from 20 to 60 MPa√m.

From these comparisons, the crack growth rate for a typical hot reactor head temperature of 600°F is three times greater than the rate used in these crack growth predictions at a temperature of 558°F for a given $K_I$. It should also be noted that the crack growth rate at 558°F is approximately 1.43 time greater than the rate at 545°F, the Byron Unit 2 measured head temperature.

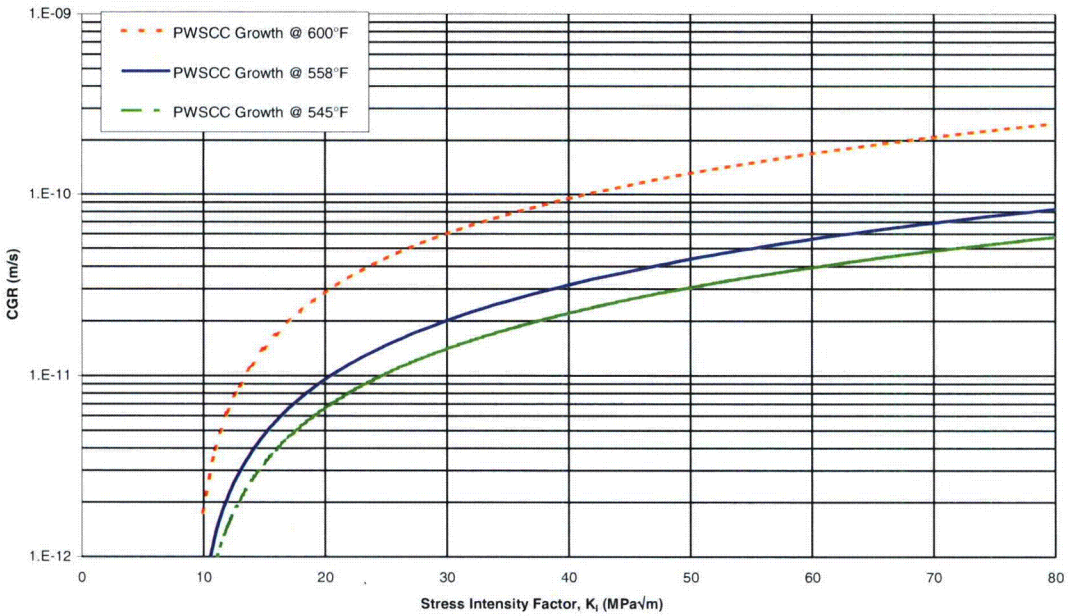


**Figure 5-2:** PWSCC Growth Rate Comparison for Cold vs. Hot RPV Head Temperatures

## 5.2 Byron Unit 2 PWSCC Growth Projections

### 5.2.1 Head Penetration Stresses

To perform the PWSCC crack growth projections, the stress fields from operating conditions and welding residual stress at the postulated flaw locations are needed. These stress fields were calculated using finite element analyses for the Byron Unit 2 head nozzles in Reference 13. Figure 5-3 displays the hoop direction stresses for the 47° head nozzle subjected to operating and weld residual stress loads. The maximum tensile stresses are located along the uphill and downhill locations around the circumference of the nozzle at the J-groove weld. At the uphill location, the largest tensile hoop stresses extend through the thickness of the nozzle and to the top of the J-groove weld and below the bottom of it. Above and below the J-groove weld, the hoop stresses reduce significantly and become negative along the outside surface. Although the extent of the large tensile hoop stresses is smaller in the downhill side of the nozzle, large hoop stresses similar to the uphill side are found here and this is the location of the flaw found in Nozzle 68. One of the contributors to the initiation and growth of the flaw in Nozzle 68 was the location of the lack of fusion being in this high tensile stress field.

Figure 5-4 displays the axial direction stresses for the 47° head nozzle subjected to operating loads and weld residual stress. Again the maximum tensile stresses are located along the uphill and downhill locations around the circumference of the nozzle at the J-groove weld. The amount of material with the highest axial tensile stress is much less than in the hoop direction and generally the magnitude of the axial tensile stresses is less than in the hoop direction, so axial flaws are significantly more likely than circumferential flaws. Figure 5-5 presents the axial stress through wall, along the plane formed by the top of the J-groove weld. This distribution shows a large part of the circumference is subjected to a compressive stress, which would prohibit further circumferential growth.

Details of the methods and material properties used to calculate these stress fields and the stress fields for the remaining head nozzles can be found in Reference 13.

The methodology used to estimate the weld residual stress in the head penetrations and combine it with the operating loads was independently assessed[40]. In this study, vessel head penetration weld residual stress was calculated using two different and independent methods and compared the results. The study concluded that the method used to calculate the stress used here, i.e. using a stress-strain curve for the Alloy 600 nozzle material based on cyclic stress-strain data, produced stresses that were similar or higher than the alternate method. The alternate method was developed Engineering Mechanics Corporation of Columbus for the U.S. NRC. This comparison provides additional confidence in the methodology used to calculate the stress distributions and the stress distributions used to predict the crack growth.

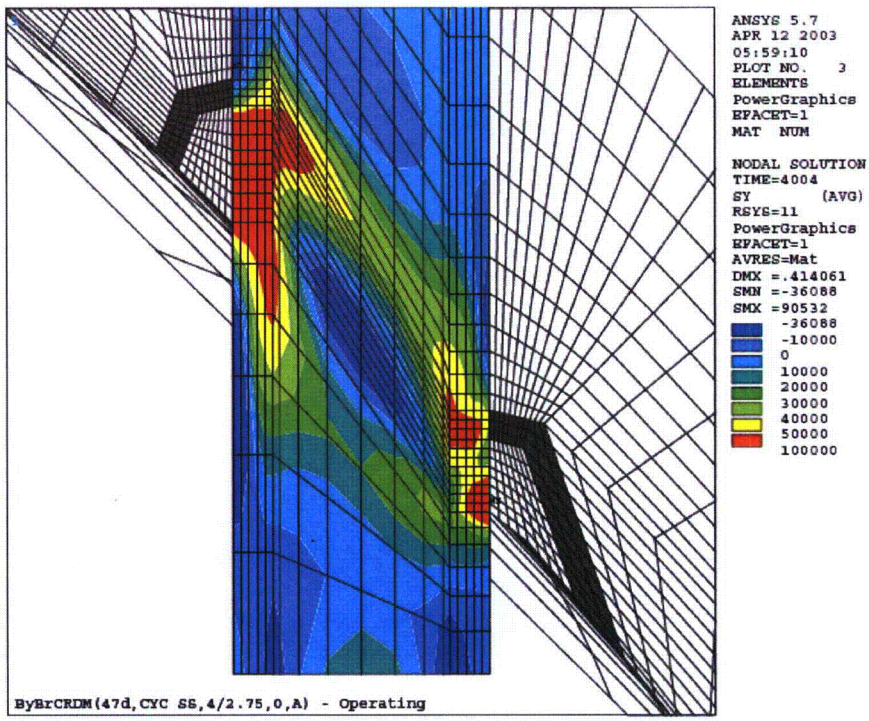


**Figure 5-3:** Typical Operating Plus Weld Residual Hoop Stress Field Used for Crack Growth – RPV Head 47° Nozzle (psi)

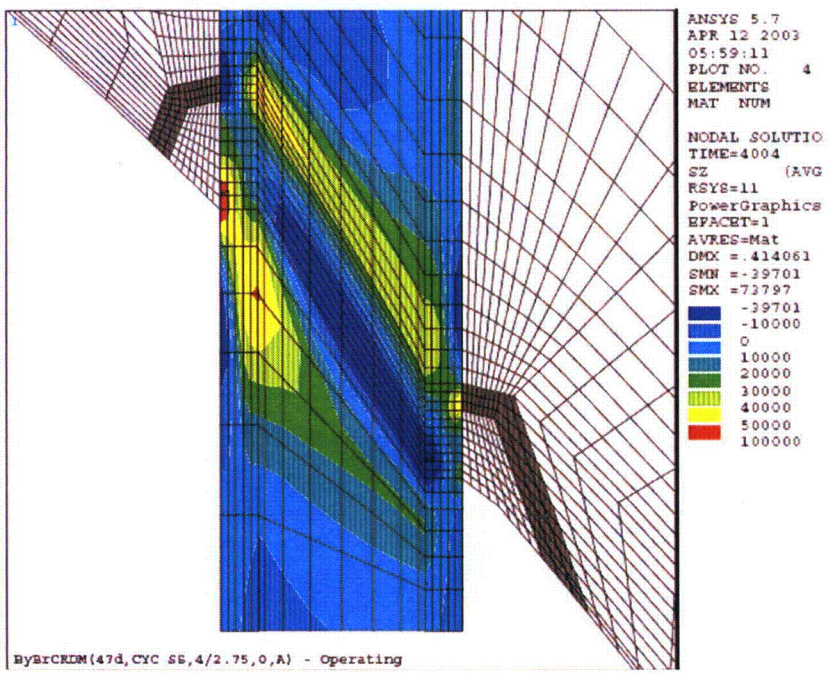


**Figure 5-4:** Typical Operating Plus Weld Residual Axial Stress Field Used for Crack Growth – RPV Head 47° Nozzle (psi)

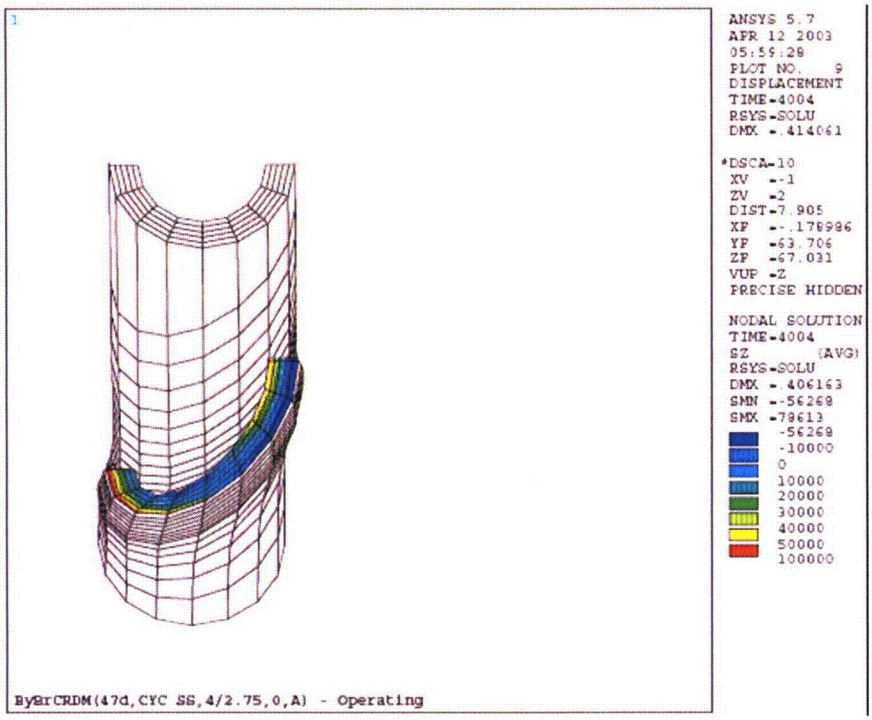


**Figure 5-5:** RPV Head 47° Nozzle Operating Plus Weld Residual Axial Stress Along the Top of the J-Grove Weld (psi)

### 5.2.2 Nozzle Outside Surface Axial Flaws

The inspection results of the Byron Unit 2 vessel head, as summarized in Section 2.2, and the conclusions drawn from the metallurgical examination of the flaw in Nozzle 68 have provided assurances that the probability of PWSCC degradation at this time is very small. Any PWSCC flaws that may exist would be smaller than the detectable limit of the examinations performed. Based on these inspection results, a flaw tolerance analysis is performed to determine the appropriate inspection interval for the next inspection. The initial size of the postulated flaw used in the evaluation was based on the threshold of detection for the nozzle volumetric examination technique. As justified in Section 2, the initial depth and length of the postulated flaw was defined as 0.075" and 0.15" respectively. This was the initial flaw size specified in the axial flaw growth projections documented in Reference 41[41], which performs flaw growth projections for the 0°, 25.4°, 42.8°, 43.8° and 47° nozzle groups, defined in Reference 13. Figure 5-6 shows the axially oriented flaw located on the uphill side of the nozzle at the highest hoop stress location on the outside diameter. Surface flaws were postulated on the outside diameter of the nozzle at both the uphill and the downhill sides. The initial flaw was centered at the highest stressed area in the nozzle material to be consistent with the flaw found in Nozzle 68; and with the higher hoop stresses at this location, it will grow faster than in other locations above or below the weld.

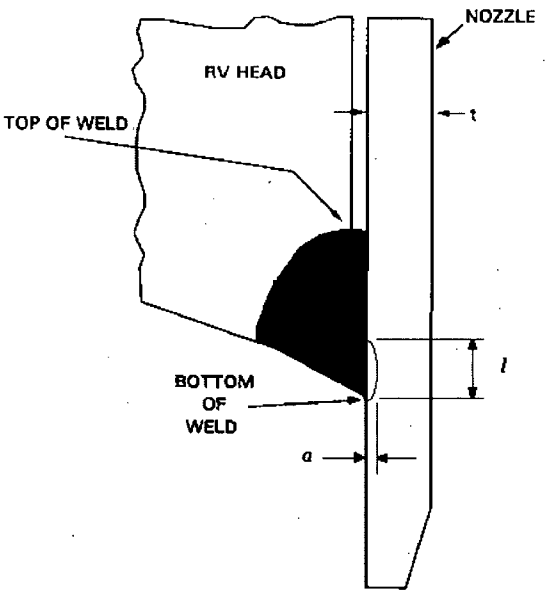


**Figure 5-6:** RPV Head Nozzle Schematic with Postulated Flaw Location

Flaws at these uphill and downhill positions were postulated to address other nozzle welds that may have weld defects similar to those found in Nozzle 68 and PWSCC initiated, but at less than the minimum detectable flaw size. Postulated flaws in these positions were grown in depth and length until the upper crack tip reached the top of the J-groove at which a leak path would be established. Stress intensity factors for semi-elliptical, part-through wall surface cracks in a cylinder were calculated at the deepest and the surface points along the crack front using Reference 42[42]. These stress intensity factors were used to calculate the change in crack depth and length of the postulated flaw. They would conservatively represent the crack driving force because the assumed surface flaw is restrained against crack opening by the J-groove weld. The leak path was chosen, as the crack size limit since the axial flaw size for the leak path is significantly smaller than the critical flaw size. Additional details of the evaluation methods used to calculate the projected crack growth are documented in Reference 41.

The results of these evaluations are summarized in Table 5-1. For each postulated flaw location, the operating time for the flaw to grow to its leakage limit is presented. The minimum time for a postulated axially oriented flaw located on the nozzle outside diameter at the highest hoop stress locations to grow in length and initiate a leak path is greater than 6 fuel cycles or 9.09 years of hot operation.

| Table 5-1<br>Operating Time for A Postulated Axial Flaw at the J-groove Weld to Grow Its Limit | |
|---|---|
| **Nozzle Group & Location** | **Available Operating Window (Fuel Cycles)[1]** |
| 0.0° Nozzle | 7.30 |
| 25.4° Nozzle; Downhill | 9.05 |
| 25.4° Nozzle; Uphill | 6.06 |
| 42.8° Nozzle; Downhill | 11.69 |
| 42.8° Nozzle; Uphill | 6.37 |
| 43.8° Nozzle; Downhill | 12.26 |
| 43.8° Nozzle; Uphill | 6.42 |
| 47.0° Nozzle; Downhill | 13.75 |
| 47.0° Nozzle; Uphill | 6.67 |

Note 1. A fuel cycle was assumed to be 18 months with a 98% capacity factor. Hot operating time conversion is 1.5 years/fuel cycle.

### 5.2.3 Nozzle Inside Surface Axial Flaws

Other postulated flaw locations in the nozzle were evaluated in Reference 43[43]. The crack growth projections in this evaluation used the same PWSCC growth rate as defined in Section 5.1 and the same operating and residual stress fields defined in Reference 13. In calculating the crack growth projections, the evaluation assumed a fixed aspect ratio of 6:1 for the flaw length and calculated the growth in the depth direction. For axially oriented flaws this is a very conservative assumption because the projected flaw lengths will extend well beyond the large tensile hoop stresses caused by the weld residual stress. Once the crack tip is beyond the weld residual stresses, growth in the length direction will be significantly slower than in the depth direction. Also, by assuming an initial flaw size with an aspect ratio of 6, the postulated flaw will be predicted to grow more rapidly in the depth direction then a flaw with a smaller aspect ratio because there would be less restraint on the crack tip. For an axially oriented surface flaw on the inside surface of the nozzle the most rapid growth is predicted to be on the uphill side of the J-groove weld for a flaw located at the weld. From Figure 5-7 and again using an initial flaw depth of 0.075" with a length of 0.45" the postulated flaw in the worst case, nozzle angle of 47° is predicted to grow to a depth ratio of less than 0.7 in 6 years of operation. Since the flaw is growing from the inside surface, a leak path is not possible, and the flaw depth of 0.431" is less than the ASME Section XI code[37] acceptance criteria of 75% through wall.

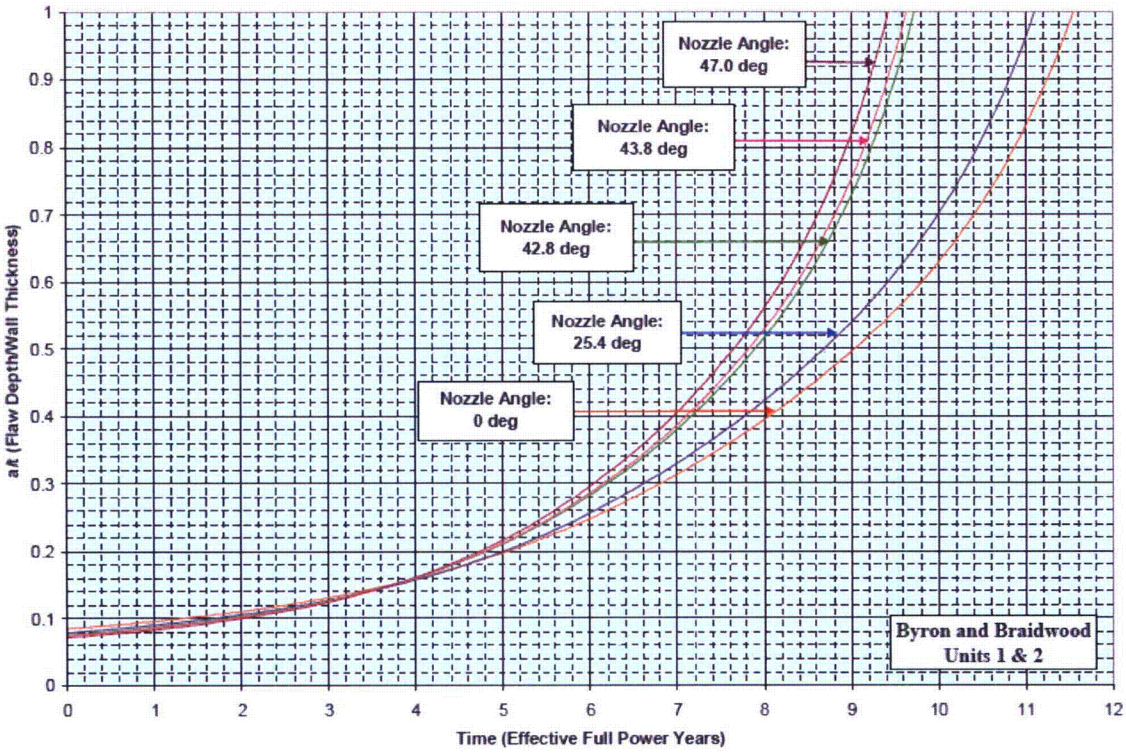


**Figure 5-7:** PWSCC Growth Projections for an Inside Surface, Axially Oriented Flaw on the Uphill Side at the J-groove Weld

### 5.2.4 Nozzle Circumferential Flaws

PWSCC growth of circumferentially oriented flaws in the nozzle was also evaluated in Reference 43. Based on the operating plus weld residual stress distributions in the axial direction, Figures 5-4 and 5-5, and field experience for circumferential cracks at Bugey 3, the most likely initiation point for a circumferential crack would be on the outside surface above the J-groove weld and propagate along the plane formed by the top of the weld. This would require a leak path to exist that would expose the outside surface of the nozzle the reactor water environment. The crack growth projections were based on a semi-elliptical surface flaw with an aspect ratio of 6:1. The stress intensity factor at the deepest point along the crack front was calculated using the correlations from Reference 42. The crack growth rate was based on the PWSCC rate defined in Section 5.1, however due to the creviced conditions required to expose the outside surface to the reactor water, a factor of 2 was applied to the rate to account for the uncertainty in the water chemistry, as recommended by Reference 36. The crack growth projections for this postulated flaw are shown in Figure 5-8.

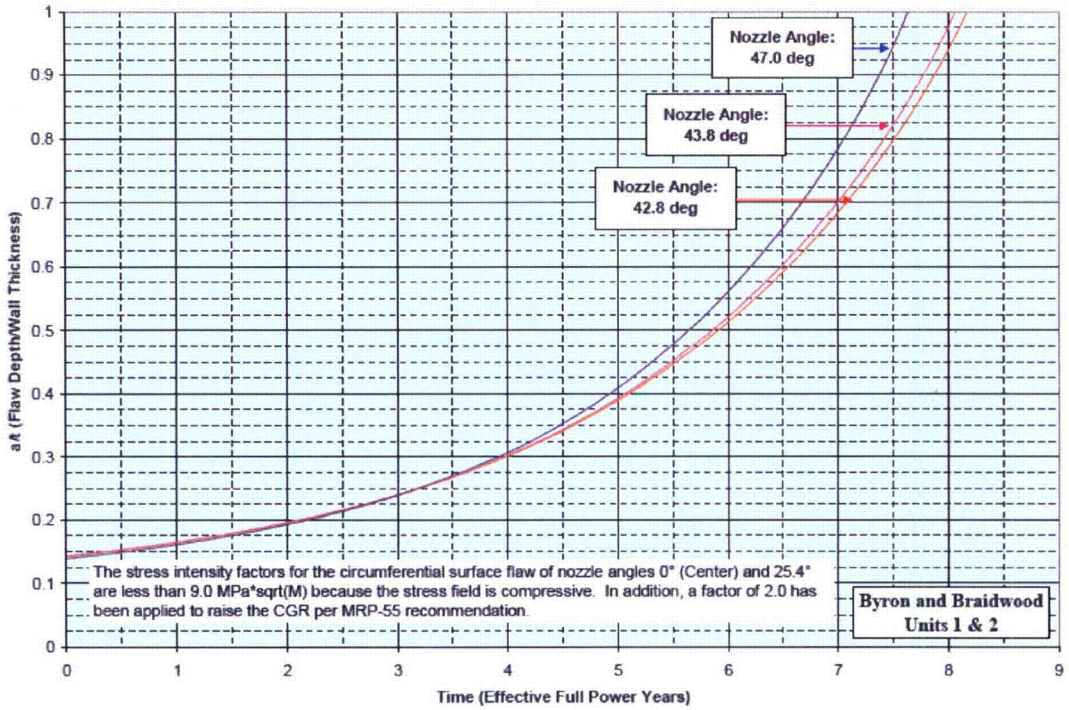


**Figure 5-8:** PWSCC Growth Projections for an Outside Surface, Circumferentially Oriented Flaw on the Downhill Side Above the J-groove Weld

For an initial flaw size of 0.075" in depth and 0.45" in length, the postulated flaw in the worst case, nozzle angle 47°, is predicted to grow to a depth ratio of 0.56 in 6 years of operation. For a nozzle thickness of 0.625", the predicted flaw depth is 0.35" with a length of 2.1", which is well within the structural integrity limits for the nozzle, i.e. through wall and greater than 300° (10.5") in length.

### 5.2.5 Head Penetration Weld Flaws

Radial or circumferential cracking in the J-groove welds will propagate much more rapidly than flaws in the nozzle material. This is due to the greater crack growth rates, which are several times faster than the rates for the base metal. However, these cracks will not lead directly to rupture of the pressure boundary. They can propagate through the weld and initiate a leak path, which can lead to cracking in the nozzle base metal or wastage of the vessel head low alloy steel. In both cases the time between inspection intervals would bound the intervals previously determined for the postulated flaws in the nozzle material.

### 5.3 Reactor Vessel Head Inspection Intervals

The postulated flaw PWSCC growth studies performed for an axial flaw on the outside surface of the nozzle at the location of the highest hoop stress, i.e. at the J-groove weld, has determined that it would take 9.09 years of operation to grow in length and initiate a leak path. The other postulated flaw locations and orientations in the nozzle have been evaluated and were shown to satisfy nozzle acceptance criteria after 6 years of hot operation. These evaluations were based on a postulated initial flaw depth of 0.075" and a 0.15" flaw length, which was determined to be the threshold of detection for the volumetric examinations being performed. The evaluations performed included margins in the crack growth rates to account for uncertainties and variations in the vessel head temperature. Conservative flaw shapes were assumed when calculating the crack growth times. The weld residual stress fields were determined using a methodology that was verified and determined to be similar or conservative to stress fields calculated by Engineering Mechanics Corporation of Columbus for the U.S. NRC. Based on these evaluations, a time interval of six years of operation between examinations of the head has been justified.

## 6 Summary and Conclusions

This report describes the inspections performed at Byron Unit 2 during B2R13 in accordance with NRC Order EA-03-009, and it discusses the indications that were detected during the inspections. The report highlights the outlier nature of this finding relative to the numerous inspections that have been performed in the industry according to the Order. The following conclusions can be drawn from the information presented:

- Byron Unit 2 CRDM Nozzle 68 is the only one of over 1400 cold head nozzles inspected to have found an indication. Statistically, the likelihood of Byron Unit 2 (or any low susceptibility head) finding PWSCC at their next outage is less than 1% and is independent of the indication found in Nozzle 68.

- The presence of PWSCC in Byron Unit 2 was discovered through required inspections, and the discovery was not made as the result of through-wall leakage.

- A crevice formed by a lack-of-fusion weld defect created during original fabrication was the initiator of PWSCC in Nozzle 68. Without the lack-of-fusion defect, the three necessary elements for SCC (i.e., susceptible material, tensile stress, and critical environment) would not have been simultaneously satisfied.

- The metallurgical failure analysis of the boat sample removed from Nozzle 68 illustrates that the direction of crack growth was from a subsurface location towards the wetted surface. None of the cracking of the tube material contained in the boat sample was connected to the wetted surface of the tube.

- Other examples of rounded surface indications in the industry concluded that the PWSCC associated with the indication had crack growth propagating from the wetted surface toward the interior.

- The results of the probabilistic assessments showed that the probability of having the observed 50% through-wall flaw in Nozzle 68 after 20 years of service was three orders of magnitude below that expected for flaw initiation and growth due to PWSCC in Byron Unit 2. Further, the assessments showed that the observed 50% through-wall flaw did not occur in the most likely nozzle location in Byron Unit 2.

- The conclusion of the probabilistic calculations is that the 50% through-wall flaw depth observed in vessel head penetration Nozzle 68 of Byron Unit 2 is not due to normal flaw initiation and growth by PWSCC in the Alloy 600 base metal. Additional conditions, such as those identified in the boat sample metallurgical analysis, are needed to initiate and grow a PWSCC flaw in Nozzle 68 in 20 years of operation.

- The effect of in-service inspection after 20 years of operation is to reduce the probability of a through-wall flaw due to initiation and growth by PWSCC after 60 years of operation by a factor of almost 40 for an inspection interval of six years.

- A statistical treatment of all the available inspection results for head penetrations estimated the probability that flaws would be found in the future as a function of inspection frequency. For the base case chosen, the results show there is approximately a one percent chance of cracking in the next cycle and about a five percent chance in the next six years.

- The PWSCC crack growth rate at a given $K_I$ for a typical hot reactor head at 600°F is three times greater than the crack growth rate at 558°F, which is the temperature that was used for the crack growth predictions. Further, the crack growth rate at 558°F is approximately 1.43 times greater than the rate at 545°F, the Byron Unit 2 measured head temperature.

- The minimum time for a postulated axially-oriented PWSCC flaw located on the nozzle outside diameter at the highest hoop stress locations to grow in length and initiate a leak path is greater than six fuel cycles, which is equivalent to approximately nine years of hot operation. The other postulated flaw locations and orientations in the nozzle were shown to satisfy nozzle inspection acceptance criteria after six years of hot operation or four fuel cycles.

- The use of conservative flaw shapes and head temperatures in the crack growth studies further justify a time interval of six years of operation between examinations of the head.

In summary, it was demonstrated that the flaw found in Byron Unit 2 Nozzle 68 did not originate from PWSCC. Two complementary approaches have shown that a six year inspection frequency results in a very low probability of the development of cracks in the future. Even if a flaw had been below the threshold of detection at B2R13, calculations show that it would remain acceptable according to the ASME Code criteria for at least six years. Based on these analyses, an inspection frequency for Byron Unit 2 that is consistent with a low susceptibility head would not significantly increase the probability of a through-wall crack and subsequent leakage on top of the RPV head; therefore, the low susceptibility inspection frequency is acceptable.

# 7 References

1. _____

1. NRC Order EA-03-009, "Issuance of First Revised NRC Order (EA-03-009) Establishing Interim Inspection Requirements for Reactor Pressure Vessel Heads at Pressurized Water Reactors," February 20, 2004.

2. NRC Bulletin 2002-02, "Reactor Pressure Vessel Head and Vessel Head Penetration Nozzle Inspection Programs," August 9, 2002.

3. Westinghouse Nuclear Services Field Service Procedure WDI-UT-013, "CRDM/ICI UT Analysis Guidelines, Revision 12," Westinghouse Electric Company LLC, January 2007.

4. Exelon Nuclear NDE Report 2007-276, April 13, 2007.

5. Exelon Nuclear NDE Report 2007-315, April 23, 2007.

6. PCI Energy Services, PCI Report 900866-001, April 27, 2007.

7. PCI Energy Services, PCI Report 900866-002, April 27, 2007.

8. "Materials Reliability Program: Demonstrations of Vendor Equipment and Procedures for the Inspection of Control Rod Drive Mechanism Head Penetrations (MRP-89), EPRI, 1007831, September 2003.

9. Chynoweth, J., Exelon PowerLabs Project BYR-48053, "Metallurgical Evaluations of A 'Boat' Sample from the #68 CRDM Penetration on Byron Unit 2," May 23, 2007

10. "2005 Interim Review of the Pressurized Water Reactor Primary Water Chemistry Guidelines – Revision 5," EPRI, 1009933, December 2005.

11. Davis, J. R., editor, *ASM Specialty Handbook: Nickel, Cobalt, and Their Alloys*, ASM International, Materials Park, OH, 2000.

12. "Grain Boundary Coverage Estimate for the Byron 2 Alloy 600 CRDM Penetration 68," electronic mail, G. V. Rao to B. A. Bishop, September 11, 2007.

13. Byron and Braidwood Units 1 and 2 CRDM Stress Analysis, Dominion Engineering, Inc. Task 77-70, Calculation C-7770-00-1, Rev. 0, April 25, 2003.

14. *Status Review of Initiation of Environmentally Assisted Cracking and Short Crack Growth.* EPRI, Palo Alto, CA: 2005. 1011788.

15. Bamford, Bishop, Duran and Boyle, "Background and Methodology for Evaluation of Reactor Vessel Closure Head Penetration Integrity for the Westinghouse Owners Group," WCAP-14901, Rev. 0, Westinghouse Electric Corporation, July 1997

16. Letter, J. A. Begley (APTECH) to B. A. Bishop (Westinghouse), "Review of the Westinghouse Structural Reliability Model for PWSCC of RV Head Penetrations," June 23, 1997.

17. Rao and Wright, "Evaluation and Resolution of the Primary Water Stress Corrosion Cracking (PWSCC) Incidents of Alloy 600 Primary System Pressure

1. ———————————————————————————

Boundary Penetrations in Pressurized Water Reactors," *Proceedings of Fontevraud II Symposium: Contribution of Materials Investigation to the Resolution of Problems Encountered in PWR Plants*, Royal Abbey of Fontevraud, France, September 10-14, 1990.

18. Hall, Magee, Woodman and Melton, "Evaluation of Leaking Alloy 600 Nozzles and Remaining Life Prediction for Similar Nozzles in PWR Primary System Application," *Service Experience and Reliability Improvement,* ASME PVP-Vol. 288, 1994.

19. Gold, Fletcher and Jacko, "The Status of Laboratory Evaluations in 400°C Steam of the Stress Corrosion of Alloy 600 Steam Generator Tubing," *Proceedings of 2nd International Topical Meeting on Nuclear Power Plant Thermal Hydraulics and Operations,* 1986.

20. Norring, Engstrom and Norberg, "Intergranular Stress Corrosion Cracking in Steam Generator Tubing, Testing of Alloy 690 and Alloy 600 Tubes," *Third International Symposium on Environmental Degradation of Materials in Nuclear Power Systems - Water Reactors - Proceedings,* The Metallurgical Society, 1988.

21. Ball et al., "RV Closure Head Penetration Alloy 600 PWSCC (Phase 2)," WCAP-13525, Rev. 1, Westinghouse Electric Corporation, December 1992 **(Proprietary Class 2)**.

22. Duran, Kim and Pezze, "Reactor Vessel Closure Head Penetration Key Parameters Comparison," WCAP-13493, Westinghouse Electric Corporation, September 1992 **(Proprietary Class 2)**.

23. Rao, "Microstructural and PWSCC Assessments of Alloy 600 R. V. Head Penetration at Beznau Unit 2 Station," WCAP-15388, Westinghouse Electric Company LLC, February 2000 **(Proprietary Class 2C)**.

24. Rao, "Microstructural Correlations with Material Certification Data in Several Commercial Heats of Alloy 600 Reactor Vessel Head Penetration Materials," WCAP-13876, Rev. 1, Westinghouse Electric Corporation, June 1997 **(Proprietary Class 2C)**.

25. Grambau and Fyfitch, "Vessel Head Penet. Nozzle Data for Byron 1 & 2, Braidwood 1 & 2," Engineering Information Record 51-5014160-00, FRAMATOME ANP, August 30, 2001

26. Bamford, Foster, and Rao, "Crack Growth and Microstructural Characterization of Alloy 600 Head Penetration Materials, WCAP 13929, Rev. 2, Westinghouse Electric Corporation, November 1996 **(Proprietary Class 2C).**

27. Newman and Raju, "Stress Intensity Factors for Internal Surface Cracks in Cylindrical Pressure Vessels" *Transactions ASME, Journal of Pressure Vessel Technology*, Volume 102, 1980, pp. 342-346.

1. ———————————————————————————————

28. Bishop, "Westinghouse Structural Reliability and Risk Assessment (SRRA) Model for Piping Risk-Informed In-service Inspection," WCAP-14572, Revision 1-NP-A, Supplement 1, Westinghouse Electric Corporation, February 1999.

29. "Risk-Based Inspection - Development of Guidelines, Volume 1, General Document," ASME Research Task Force on Risk-Based Inspection Guidelines Report CRTD-Vol. 20-1 (or NUREG/GR-005, Vol. 1), American Society of Mechanical Engineers, 1991.

30. Harris and Dedhia, "Theoretical and User's Manual for pc-PRAISE, A Probabilistic Fracture Mechanics Computer Code for Piping Reliability Analysis," NUREG/CR-5864, U.S. Nuclear Regulatory Commision, July 1992.

31. Bamford, Bishop, Duran and Boyle, "Probabilistic Evaluation of Reactor Vessel Closure Head Penetration Integrity for Beaver Valley Units 1 and 2," WCAP-14913, Rev. 1, Westinghouse Electric Corporation, October 1997 **(Proprietary Class 2C)**.

32. Bamford, Bishop, Duran and Boyle, "Probabilistic Evaluation of Reactor Vessel Closure Head Penetration Integrity for Farley Units 1 and 2," WCAP-14906, Rev. 1, Westinghouse Electric Corporation, October 1997 **(Proprietary Class 2C)**.

33. "Materials Reliability Program (MRP) Probabilistic Fracture Mechanics analysis of PWR Reactor Pressure Vessel Top Head Nozzle Cracking, (MRP-105), EPRI, April 2004.

34. Harris, John E., Turner, Arthur P., Gorman, Jeffery A., "Predicted Tube Degradation for Westinghouse Models D5 and F Type Steam Generators," EPRI, TR-108501, September 1997.

35. Nelson, Wayne, "Weibull Prediction of a Future Number of Failures," Quality and Reliability Engineering International, 16: 23-26, 2000.

36. "Materials Reliability Program (MRP) Crack Growth Rates for Evaluating Primary Water Stress Corrosion Cracking (PWSCC) of Thick-Wall Alloy 600 Materials," (MRP-55) Revision 1, EPRI, 1006695, November 2002.

37. ASME B&PV Code, Section XI, 2004 Edition.

38. Byron/Braidwood UFSAR, Figure E.31-5, Probe Holder Assembly and Sensor Location.

39. Byron/Braidwood UFSAR, Figure E.31-8, Normal Operating Flow Pattern with Reactor Coolant Pumps On.

40. Rudland, D., Chen, Y., Zhang, T., Wilkowski, G., Broussard, J., and White, G., "Comparison of Welding Residual Stress Solutions for Control Rod Drive Mechanism Nozzles," 2007 ASME Pressure Vessels and Piping Division Conference, PVP2007-26045, July 2007.

1. _____

41. "Evaluation of Crack Growth of a Postulated Flaw in Byron Unit 2 CRDM Nozzles by Primary Water Stress Corrosion Cracking," Exelon Report AM-2007-006, Revision 0.

42. Mettu, S.R., Raju, I. S., and Forman, R. G., NASA Lyndon B. Johnson Space Center report number NASA-TM-111707, "Stress Intensity Factors for Part-Through Surface Cracks in Hollow Cylinders," Structures and Mechanics Division, July 1992.

43. Westinghouse Report WCAP-16394-P, "Structural Integrity Evaluation of Reactor Vessel Upper Head Penetrations to Support Continued Operation: Byron and Braidwood Units 1 and 2," February 2005.

**Exelon PowerLabs®, LLC.**
Technical Services West
36400 S. Essex Road
Wilmington, IL 60481-9500

www.exelonpowerlabs.com
815-458-7640
815-458-7851 fax

# EXELON POWERLABS PROJECT BYR-48053

# METALLURGICAL EVALUATIONS OF A 'BOAT' SAMPLE FROM THE #68 CRDM PENETRATION ON BYRON UNIT 2

## REPORT DATE: MAY 23, 2007

Reported by: Jim Chynoweth
Senior Metallurgical Engineer
Exelon PowerLabs West

Approved by: Jean Smith
Corporate Engineering-Asset Management
Exelon Nuclear

Concurrence: Jai Brihmadesam
Technical Consultant to Exelon

## Executive Summary

In accordance with NRC Order EA-03-009 requirements, internal ultrasonic inspections were performed on the Byron Unit 2 reactor vessel head penetrations during the B2R13 outage. The inspections identified a 0.52" long x 0.326" deep axial indication near the J-groove weld in one of the 79 penetrations (i.e., #68 CRDM tube). A subsequent dye penetrant examination identified one axial and one rounded indication on the surface of #68 penetration J-groove weld approximately 16.5 degrees from the downhill azimuth.

A 'boat' sample was removed from the #68 penetration to determine the cause of the indications. The sample contained a portion of the axial indication but did not capture the rounded surface indication. The boat sample excavation also uncovered a sub-surface linear defect that intersected the axial indication. The sub-surface defect was partially captured by the boat sample.

The laboratory evaluations identified the axial indication as a combination of primary water stress corrosion cracking (PWSCC) and welding defects (i.e., lack of fusion and hot cracking). The sub-surface defect was identified as lack of fusion between the outer diameter (OD) of the tube and the J-groove weld. Within the boat sample, the cracking characteristics indicated the PWSCC initiated at a sub-surface location on the tube OD, propagated in an axial/radial direction into the tube, and propagated toward the wetted surface of the J-groove weld fillet leg.

The presence of PWSCC at this time is unexpected, since Byron Unit 2 is categorized as a low susceptibility plant per the methodology of NRC Order EA-03-009. The premature initiation is attributed to wetting of the tube OD surface at the sub-surface lack of fusion defect, which created a conducive crevice corrosion environment that allowed for PWSCC to initiate in the high stress region of the J-groove weld. The surface connected path for the lack of fusion defect was not contained in the boat sample but is attributed to the rounded surface indication that was not captured by the boat sample.

## 1.0 Background

In accordance with Nuclear Regulatory Commission (NRC) Order EA-03-009, ultrasonic inspections were performed on the inside of the Byron Unit 2 reactor head control rod drive mechanism (CRDM) tube penetrations during the B2R13 refueling outage. The inspections identified a 0.52" long x 0.326" deep axial indication in the #68 CRDM tube, near the J-groove weld (Figure 1). No indications were detected in the other 78 penetrations. The #68 penetration is a periphery tube and the maximum ultrasonic reflector was located 16.5° counter clockwise from the zero reference.

A dye penetrant (PT) examination was performed on the surface of the #68 penetration weld zone and the result is shown in Figure 2. The PT exam identified a 0.150" axial linear indication at the approximate orientation of the maximum ultrasonic reflector. In addition, a 0.050" diameter rounded indication was detected on the J-groove weld.

To evaluate the indications, a 'boat' sample was removed from the #68 tube and the J-groove weld by electrode discharge machining (EDM). However, the removed sample did not capture the rounded surface indication or the deepest portion of the axial indication (Figure 3). In addition, the excavation uncovered an angled, sub-surface defect that was connected to the axial indication. The remaining indications were left in the excavation and repaired in accordance with the Westinghouse embedded flaw weld overlay process.

This report documents the laboratory metallurgical evaluations that were performed on the removed boat sample. The primary objective was to determine the nature and cause of the indications in the boat sample.

## 2.0 Results and Conclusions

The boat sample contained a 0.032" long portion of the angled, sub-surface defect that was uncovered by the boat sample excavation. The defect was caused by lack of fusion between the next to last weld pass and the tube surface. The metallurgical sections identified several incipient cracks that had initiated from the sides of the lack of fusion crevice. Based on the field dye penetrant results, the lack of fusion defect was connected to the axial indication; although, this connection was not observed within the boat sample material.

The surface connected portion of the axial indication measured 0.18" long and was located in the fillet leg of the J-groove weld that was adjacent to the wrought tube. Within the weld, the axial indication exhibited multiple defect/crack morphologies that were characterized as lack of fusion between weld passes, welding hot cracks, primary water stress corrosion cracking (PWSCC), and local regions of ductile tearing between crack ligaments. The general direction of crack propagation was toward the wetted surface of the weld, which indicates the PWSCC cracking did not initiate from the wetted surface of the boat sample.

In the wrought tube material, the axial indication exhibited branched, intergranular features that were typical of PWSCC.

The tube/weld microstructures and chemistries were consistent with the specified materials (i.e., mill annealed Inconel 600 tube and Inconel 182 weld). Based on the presence of random intragranular carbides and partially decorated grain boundaries, the tube material had a relatively high susceptibility to PWSCC which is typical for mill annealed tubing produced during the 1970's.

The tube microhardness measurements ranged from equivalent values of 82.0 to 88.1 Rockwell B scale, which indicates there was not a high degree of cold working.

The weld surface exhibited heavy grinding that resulted in a 0.0007" thick cold worked layer and grinding laps. The microhardness measurements for the cold worked layer measured up to 25.3 Rockwell C scale. There was no evidence of crack initiation from the cold worked layer or the grinding laps.

Since Byron Unit 2 is categorized as a low susceptibility plant per NRC Order EA-03-009, the detection of PWSCC at this time is unexpected. The premature cracking and the detection of cracking in only one of 79 Byron Unit 2 nozzles suggests that an atypical condition was present with the #68 CRDM penetration. This conclusion is supported by the lack of detected cracking by the ultrasonic inspections of other Heat 80054 tube penetrations at Exelon plants (i.e., 28 additional tubes).

Based on the laboratory evaluations, the PWSCC cracking is attributed to the detected welding defects, a susceptible tube material microstructure, the existence of a tight crevice condition created by the welding defects, and the presence of high hoop stresses on the outer diameter of the tube at this location. The following is considered the most probable scenario for the PWSCC cracking.

- The original four layer welding process generated a sub-surface lack of fusion defect that was not detected by the fabrication surface non-destructive examination (NDE). The lack of fusion defect corresponds to the angled, sub-surface defect that was uncovered by the boat sample excavation and was partially captured in the boat sample.

- The fabrication welding process also generated a non-detected defect or a non-relevant indication that was connected to the lack of fusion defect and the weld surface. This defect corresponds to the rounded dye penetrant surface indication that was not captured by the boat sample. The imperfection may not have been detected by the fabrication surface exams due to the heavy surface grinding, a defect location that was slightly below the weld surface, or a rounded indication size that was acceptable per the code of construction (i.e., < 3/16" diameter). A review of the original fabrication records indicated grinding was performed on all four weld passes for the #68 CRDM, which suggests there were some difficulties in fabricating the periphery tube weld.

- During service, the rounded surface connected defect allowed primary water to enter the tight crevice formed by the sub-surface lack of fusion defect. The combination of the wetted crevice environment, a susceptible tube microstructure, and a high hoop stress from the welding process allowed PWSCC to initiate. Without a surface connected flaw that allowed for wetting of the lack of fusion crevice, the PWSCC would not have initiated at this time.

## 3.0 Laboratory Test Plan

A laboratory test plan was developed with the assistance of industry materials experts from Exelon Nuclear, EPRI, Westinghouse, Framatome, and several nuclear utilities. The test plan is provided in Appendix A to this report. Due to radioactive contamination, the laboratory evaluations were performed at the BWXT, Inc. facility in Lynchburg, Virginia. The work was performed under Exelon PowerLabs–BWXT Purchase Order 00059971-0001-2007040335. The laboratory testing was observed by Exelon PowerLabs, Exelon Nuclear Corporate Engineering, and Mr. Jai Brihmadesam who is a technical consultant for Exelon Nuclear.

## 4.0 Laboratory Pre-Sectioning Evaluations

### 4.1 Visual Inspections

The as-received boat sample is shown in Figures 4 and 5. The sample measured approximately 1.5" long x 0.75" wide and had a maximum thickness of 0.375". In this report, the sample directional descriptions (e.g., up, down, left, right) will be referenced as viewing the non-cut (i.e., wetted) surface that is shown in Figure 4.

The visual inspections did not identify cracking or other linear indications that corresponded to the field dye penetrant indications. The most significant observation was the presence of heavy surface grinding toward the upper half (i.e., weld side) of the sample. Due to the surface grinding, the weld toe could not be identified by the visual inspection. The EDM surface exhibited smooth, rounded features that were typical of the EDM cutting process.

### 4.2 Fluorescent Dye Penetrant Results

The fluorescent dye penetrant results are shown in Figures 6 and 7. The upper left portion of the sample contained a linear indication that bled heavily on both the wetted and EDM cut surfaces. The indication measured approximately 0.18" long on the non-cut surface and 0.375" long on the EDM surface. Although the indication was not continuous around the upper edge of the EDM cut, a subsequent dye penetrant exam confirmed the two linear indications were connected. Both linear indications were visible in the second exam, even though the fluorescent dye was only applied to the EDM surface. The location and orientation of the linear indications corresponded to the axial indication that was identified by the field NDE inspections (i.e., the axial indication in Figure 2 and Indication #2 in Figure 3).

The fluorescent dye penetrant examination also detected a single rounded indication on the EDM surface. The rounded indication was located approximately 0.090" from the axial indication.

### 4.3 Laboratory Microfocus Radiography

The boat sample was examined using BWXT's real-time Microfocus X-ray system. The examination detected the axial indication that was identified by the fluorescent dye penetrant testing; although, no other indications were detected. Figure 8 contains a montage of the boat sample X-ray results.

4.4 Stereoscope Examinations

The boat sample surfaces were examined using a stereoscope, with particular emphasis on the dye penetrant indications. Due to surface grinding marks, the axial indication could not be identified by the stereoscope inspection of the non-cut surface (Figure 9). The axial indication was detected on the EDM surface (Figure 10).

A stereoscope inspection was also performed at the rounded indication on the EDM surface. However, the defect characteristics were obscured by globular debris from the EDM cutting process.

4.5 Surface Scanning Electron Microscope (SEM) Examinations

A low magnification SEM view of the non-cut surface is shown in Figure 11. On the non-cut surface, the axial indication was relatively tight and could only be detected at high magnifications. The indication followed a non-branching irregular path that did not necessarily coincide with the local grinding marks (Figures 12 & 13). In one region, the indication coincided with a local patch of ductile features, which appeared to be related to smeared metal from the surface grinding (Figure 14). No crack branching was observed on the non-cut surface.

During the SEM inspections of the non-cut surface, several angled fissures were also detected (Figures 15). The fissures tended to follow to the local grinding direction.

The axial indication was easily detected by the SEM examination of the EDM surface (Figure 16). Figures 17 and 18 provide typical views of the crack. There was little crack branching, except near the ends of the indication.

The Figure 17 photo also provides a view of the rounded dye penetrant indication on EDM surface. As was reported during the stereoscope inspection, the indication features were obscured by globular debris from the EDM cutting process.

**5.0 Laboratory Sectioning Plan and Sample Identifications**

The laboratory NDE results indicated the upper left portion of the boat sample in Figure 4 contained the axial indication that was detected by the field NDE inspections. The boat sample also contained a rounded indication on the EDM cut, which corresponded to a portion of the angled, sub-surface indication that was uncovered by the boat sample removal (Indication #3 in Figure 3).

A boat sample sectioning plan was developed to allow for metallurgical characterization of the two indications and to perform the remaining evaluations that were identified in the test plan. The boat sample sectioning details, sample identifications, and planned examinations are summarized in Figures 19 and 20.

**6.0 Sample C Macro-Etch Results**

The Section C cut face was lightly ground and macro-etched as shown in Figures 21 and 22. The etching revealed the boat sample contained portions of the last two weld passes. Based on the profile

of the wetted surface of the tube, there was minor surface grinding of the tube near the toe of the weld.

## 7.0 Sample B Metallography

The horizontal cut that separated Samples A and B was approximately 0.23" from the upper EDM edge. The cut location was below the axial indication on the wetted surface of the boat sample, but intersected the axial indication on the EDM surface.

The horizontal cut face on Sample B was prepared in a metallurgical mount. The tube base metal contained branched, intergranular cracking (Figures 23-25) that was typical of PWSCC. The crack branches had sharp tips and contained little oxidation. No crack blunting was observed. There was limited interdendritic cracking into the weld (Figure 26). Within the Sample B mount, none of the cracking extended to the wetted surface of the boat sample.

The surface of the weld exhibited an irregular contour and several linear indications were observed (Figure 27 – 29). Based on the heavily deformed surface microstructure, the linear indications appeared to be laps that were formed by metal deformation during grinding. In the examined section, the deformed layer measured up to 0.0007" thick. There was no evidence of service related crack initiation from the indications. The deformed metal and local crevices are believed to be the source of the fissures that were detected by the SEM examination of the wetted surface.

The tube material had a relatively fine duplex grain structure with the smallest grains measuring ASTM Size 7 and the largest grains ASTM Size 5. The microstructure contained large quantities of random intragranular carbides and the grain boundaries were partially decorated with carbides (Figure 30). Nuclear industry literature indicates this microstructure will have a relatively high susceptibility to PWSCC (Ref. 4, 5). The microstructure is considered typical for mill annealed Alloy 600 tubing that was fabricated during the 1970's.

## 8.0 Sample A1, Crack Surface Examinations

The axial indication was exposed by bending and the Sample A1 side of the crack is shown in Figure 31. The crack surface was reflective and appeared intergranular. There were no clear indications of crack age; although, a thumbnail-shaped region on the tube appeared to be more oxidized than the remainder of the sample.

A low magnification SEM view of the A1 crack surface is shown in Figure 32. The general shape of the thumbnail region in the vicinity of the fusion line suggested the direction of crack propagation was from the tube material into the weld (i.e., toward the wetted surface of the J-groove weld along the tube side fillet leg). The tube portion of the sample exhibited an intergranular morphology in all examined regions (Figures 33-35). A close examination of the 'thumbnail' region revealed fine globular particles on the surface. Several of the particles were evaluated by energy dispersive X-ray spectrometry (EDS) techniques and found to contain tungsten, oxygen and the base metal elements (i.e., nickel, chromium, iron). As a result, it was concluded that the thumbnail region was contaminated during the EDM cutting process.

The exposed surface of the weld exhibited several characteristics. At low magnification, the weld

cracking appeared to follow the columnar interdendritic features of the solidification pattern (Figure 36), which is typical of stress corrosion cracking. However, at higher magnifications, some of the features were smoother than is typical for PWSCC (Figure 37 & 38). Industry literature indicates the smooth interdendritic features are more indicative hot cracking than PWSCC (Ref. 6). Several of the smooth regions were evaluated by EDS techniques; however, the areas did not exhibit manganese segregation that can be associated with hot cracks. Based on the crack surface features, it was concluded that there was evidence of both PWSCC and hot cracking in the weld.

The exposed weld surface also contained a planar defect that was parallel to the fusion line (Figures 39 & 40). Based on defect location and orientation, the defect was caused by lack of fusion between weld passes. Within the weld, there were several cracks that were connected to the defect.

Various portions of the weld contained local patches of dimpled voids, which are indicative of ductile tearing (Figure 41). The tearing may have occurred during service PWSCC propagation due to residual stresses from the welding process, but it is also possible the regions were small intact ligaments that failed when the crack surface was broken open in the lab. In general, there were more ductile tearing regions toward the wetted surface of the sample.

Based on the general characteristics of the weld defects, interdendritic weld separations, direction of crack branching, and local ductile tearing, it was concluded that the primary direction of cracking within the weld was toward the wetted surface of the boat sample. This suggests the PWSCC did not initiate from the wetted surface of the boat sample.

**9.0 Sample A2A Evaluations**

The Section A2A axial cut was located approximately 0.040" from the rounded dye penetrant indication on the EDM surface. The cut face was placed in a metallurgical mount and multiple grind-polish-examine steps were performed until the indication was uncovered. The indication was identified as a weld lack of fusion defect between the surface of the tube and the weld (Figures 42-44).

The metallurgical sample was re-polished in preparation for an SEM exam. The polishing step uncovered a porous inclusion near the edge of the lack of fusion crevice (Figure 45). Several incipient interdendritic cracks had initiated from the edge of the inclusion and the lack of fusion crevice (Figures 46 & 47). Most of the cracks appeared to be hot cracks; however, the angular appearance of two indications appeared similar to incipient PWSCC.

Qualitative EDS evaluations were performed on the large inclusion, the material in the lack of fusion crevice, several small inclusions that were adjacent to the crevice, and the oxide within several cracks. A general dot map scan of the elements was also performed. The results are summarized below.

- The large inclusion and most of the smaller inclusions contained titanium, nitrogen, and oxygen, which suggests they were titanium nitrides or oxides. One very small weld metal inclusion contained calcium and fluorine, which was likely related to the welding flux.
- The lack of fusion crevice contained oxidized metallic particles from the EDM wire and base metal cutting debris (i.e., tungsten, oxygen, iron, nickel, chromium and niobium).

- The material within the incipient cracks was consistent with Inconel 182 weld metal oxidation products.
- No measurable fluorine or other potentially corrosive elements were identified in the incipient cracks or the lack of fusion crevice.

After the SEM evaluations, additional grinding was performed to determine if the lack of fusion crevice continued toward the axial crack. However, the lack of fusion defect rapidly disappeared after another grinding sequence. Within the boat sample, the lack of fusion defect measured approximately 0.032" long, which indicates that only a small portion of the angled, sub-surface defect was captured by the boat sample.

The remaining Sample A2A metal was removed from the mount and re-oriented in a new metallurgical mount. The sample was positioned so the axial crack was perpendicular to the mount face, with the upper portion of the EDM cut parallel to the mount face. The primary objective for the mount was to determine if the lack of fusion defect continued toward the axial crack within the mount. The re-oriented mount was evaluated at three locations within 0.013" of the EDM surface. No lack of fusion or other anomalies were identified.

The grinding continued for another 0.094" on the re-oriented sample and the weld edge is shown in Figures 48 and 49. There was limited crack branching within the weld. The tube cracking exhibited intergranular features (Figure 50).

## 10.0 Chemistry Results

The boat sample size did not allow for a full chemical analysis of the weld metal. As a result, the weld chemistry was measured by energy dispersive X-ray spectroscopy (EDS), which is not capable of accurately measuring small quantities of elements that may be specified (e.g., carbon, sulfur). The weld chemistry was evaluated near the middle of the weld on the sample A2A metallurgical mount and the results are summarized in Table 1. Based on the EDS results, the weld chemistry was consistent with Inconel 182 filler metal.

Table 1 – Weld Chemistry Measured by EDS Techniques (Wt.%)

| Element | Weld |
|---|---|
| Nickel | 67.18 |
| Manganese | 6.67 |
| Iron | 8.56 |
| Silicon | 0.64 |
| Chromium | 14.80 |
| Titanium | 0.49 |
| Niobium | 1.66 |

The tube chemistry was analyzed by inductively-coupled-plasma spectroscopy (ICP) and Leco combustion techniques. The results are provided in Table 2 along with the fabrication test report for

Heat 80054 tubing. The tube chemistry was consistent with the fabrication records.

Table 2 – Tube Chemistry Results and Babcock & Wilcox Test Report for Heat 80054 (Wt.%)

| Element | Tube | Heat 80054 |
|---|---|---|
| Carbon* | 0.023 | 0.029 |
| Manganese | 0.14 | 0.27 |
| Sulfur* | 0.002 | 0.002 |
| Phosphorus | < 0.005 | -- |
| Silicon | 0.35 | 0.29 |
| Chromium | 16.24 | 16.30 |
| Nickel | 76.0 | 76.32 |
| Copper | 0.009 | 0.02 |
| Cobalt | 0.046 | 0.007 |
| Iron | 6.68 | 6.30 |
| Aluminum | 0.17 | -- |

*Carbon and sulfur were measured by Leco combustion techniques. The remaining elements were measured by ICP.

## 11.0 Microhardness Testing

Microhardness measurements were performed at several areas of interest in the sample B metallurgical mount and the results are reported in Table 3. The results can be summarized as follows:

- The equivalent weld hardness values ranged from 89.7 Rockwell B (HRB) to 98.6 HRB in areas away from the ground (cold worked) surface. The weld hardness in the cold worked surface layer was between 21.2 Rockwell C to 25.3 HRC.
- The equivalent tube hardness measurements were between 82:0 HRB and 88.1 HRB. In general, the higher measurements were located toward the outer diameter of the tube.

Other than the relatively high hardness on the cold worked surface layer of the weld, the measurements are considered typical for the fabrication materials (i.e., mill annealed Alloy 600 tubing and Inconel 182 weld metal).

Table 3 – Knoop Microhardness Results and Equivalent Rockwell Scale Hardness*

| Location | Knoop Measurements | Equivalent Rockwell Hardness Range |
|---|---|---|
| Weld Metal (Area 1) | | |
| - Away from Deformed Surface Layer | HK = 259.1, 271.7, 226.6, 224.3, 234.2 | 91.7 HRB to 98.6 HRB |
| - In Deformed Surface Layer | HK = 286.4, 274,8, 290.8 | 21.2 HRC to 23.6 HRC |

| | | |
|---|---|---|
| Weld Metal (Area 2)<br>- Away from Deformed Surface Layer | HK = 213.4, 224.3, 225.0, 245.9, 251.2 | 89.7 HRB to 96.0 HRB |
| - In Deformed Surface Layer | HK = 303.1 | 25.3 HRC |
| Weld Metal (Area 3)<br>- Surrounding weld cracking near fusion line | HK = 223.5, 227.1, 243.3 | 91.5 HRB to 94.7 HRB |
| Tube, Near Surface | HK = 195.8, 204.5, 204.5, 203.2, 201.9 | 86.2 HRB to 88.1 HRB |
| Tube, Away from Surface | HK = 201.9, 181.3, 195.2, 185.2, 180.2 | 82.0 HRB to 87.6 HRB |

*The microhardness measurements were performed at approximately 0.010" increments in the areas of interest with a 500 gram load. The equivalent Rockwell hardness values were obtained from ASTM E140, Conversion Table 3 for nickel alloys.

**12.0 Fabrication Records**

The Byron Unit 2 reactor head was fabricated at the Babcock & Wilcox, Mt. Vernon, Indiana shop in 1977. The applicable code was the 1971 Edition of the ASME Section III, Summer 1973 Addenda. The fabrication summary that is documented in Reference 7 indicates the #68 CRDM nozzle for Byron Unit 2 came from material Heat 80054. The nozzle tube was supplied by the Babcock & Wilcox Tubular Division in accordance with ASME Section II, Part B, SB-167. The reported mechanical properties for Heat 80054 were 94.6 ksi tensile, 36.5 ksi yield strength, and 48% elongation. The Heat 80054 material was used in 26 penetrations on Byron Unit 2 and three penetrations on Braidwood Unit 2.

The Reference 7 summary reported that the CRDM J-groove welds were fabricated with four passes. The #68 penetration was a periphery tube and the axial indication was located 16.5 degrees from the downhill side of the weld. For the #68 penetration, grinding was performed on all four weld passes to remove indications, which suggests there were some difficulties in fabricating the #68 penetration weld. No weld repairs were reported for the #68 penetration. There were no available fabrication records that mapped out the grinding excavations or the dye penetrant results for the individual weld layers. Per the 1971 edition of ASME Section III, NB-5000, an isolated 3/16" long rounded dye penetrant indication would be acceptable.

**13.0 Discussion of Results**

Based on the information provided by the site in Reference 8, Byron Unit 2 had accumulated 2.219 effective degradation years (EDY) at the end of cycle 13. Since the accumulated EDY categorizes Byron Unit 2 as low susceptibility PWSCC plant per NRC Order EA-03-009, it is unexpected to have identified PWSCC at this time.

The three factors that control PWSCC are material susceptibility, stress and corrosion environment. Based on the microstructure in the boat sample materials (i.e., random intragranular carbides and partially decorated grain boundaries), the tube material had a relatively high susceptibility to PWSCC. However, the observed microstructure and material susceptibility were not considered unusual for mill annealed Alloy 600 tubing produced during the 1970's. As a result, the tube microstructure and material susceptibility were not considered the cause for early PWSCC initiation. This conclusion is supported by the fact that no other cracking was detected by the ultrasonic inspections of the other 28 penetrations in Exelon plants that were fabricated from Heat 80054 tubing.

The Reference 9 document contains multiple stress analyses for the Byron Unit 2 CRDM penetrations. A hoop stress plot for the configuration of the #68 penetration is shown in Figure 51. The plot combines the residual welding and operating pressure stresses. There are three high stress regions on the tube, where the calculated hoop stress is between 50 to 100 ksi. One high stress region is located on the outer diameter of the tube near the downhill side of the J-groove weld, which is the approximate location of the axial cracking. No cracking was detected at the other two high stress locations, which suggests that an atypical environment may have existed at the axial crack location.

The lab evaluations identified welding defects in the form of lack of fusion between weld passes, lack of fusion to the tube, and hot cracks within the weld. The presence of the sub-surface lack of fusion defect is considered the cause of the atypical environment that promoted PWSCC. When wetted, the lack of fusion defect would have generated an atypical crevice corrosion environment that is conducive to PWSCC. Without the lack of fusion defect, the crevice environment would not been present and PWSCC would not have initiated at this time.

For PWSCC to occur, the Alloy 600 material must be wetted at the crack initiation site. Since the boat sample lab evaluations indicated the general direction of axial cracking within the weld was toward the wetted surface, there must have been another surface connected path for the lack of fusion defect. The field dye penetrant exams detected one other indication on the J-groove weld surface (i.e., the rounded indication that was not captured by the boat sample). As a result, it is likely the rounded surface indication was connected to the angled lack of fusion defect, which intersected the axial indication.

Since the rounded indication was not captured by the boat sample, it was not possible to determine the cause of the defect. However, based on the presence of welding defects in the boat sample, the most probable cause is considered a welding imperfection that was not detectable or an indication that was considered acceptable per the fabrication inspection requirements. This conclusion is supported by the fabrication records, which indicated grinding was required for all four weld passes. Since a final fabrication dye penetrant examination was performed, it is possible the defect was covered by smeared metal from the surface grinding, situated at a non-detectable location slightly below the weld surface, or the dye penetrant indication size was less than the minimum relevant size for a rounded indication. The code of construction would have accepted an isolated rounded dye penetrant indication that was less than 3/16" long.

## 14.0 Statement of Quality

Testing was performed with standard equipment that have accuracies traceable to nationally recognized standards, or to physical constants, by qualified personnel, and in accordance with the Exelon PowerLabs Quality Assurance Program revision 18 dated 01/11/2007.

*The internal PowerLabs Project review and approval is electronically authenticated in Exelon PowerLabs project record.*

## 15.0 - References


1. Westinghouse Ultrasonic Report Sheet for Byron Unit 2, Penetration 68, File CBE-R13-BP01-68-01, Dated 4/9/2007.
2. Exelon Nuclear Liquid Penetrant Examination Data Sheet Report 2007-276, Dated 4/10/07.
3. Exelon Nuclear Liquid Penetrant Examination Data Sheet Report 2007-315, Dated 4/23/07.
4. EPRI Report 1002792, Materials Handbook for Nuclear Plant Pressure Boundary Applications, December 2002.
5. Microstructural and Mechanical Property Evaluation of Alloy 600 CRDM Nozzles from B&W Design Reactor Vessel Heads, S. Fyfitch, et. al., AREVA NP Inc.
6. Differentiation Between Hot Cracking and Stress Corrosion Cracking in PWR Primary Water of Alloy 182 Weld Material, J.M. Boursier, et. al., Electricite De France.
7. AREVA Engineering Information Record 51-5014160-001, Vessel Head Penet. Nozzle Data For Byron 1 & 2, Braidwood 1& 2, Dated 5/11/07.
8. Exelon Nuclear EC 364572, Rev. 00, Titled B2R13 End of Cycle 13 Effective Degradation Years (EDY) In Accordance With NRC Order EA-03-009.
9. Byron and Braidwood Units 1 and 2 CRDM Stress Analysis, Dominion Engineering, Inc. Task 77-70, Calculation C-7770-00-1, Rev. 0, Dated 4/25/03.

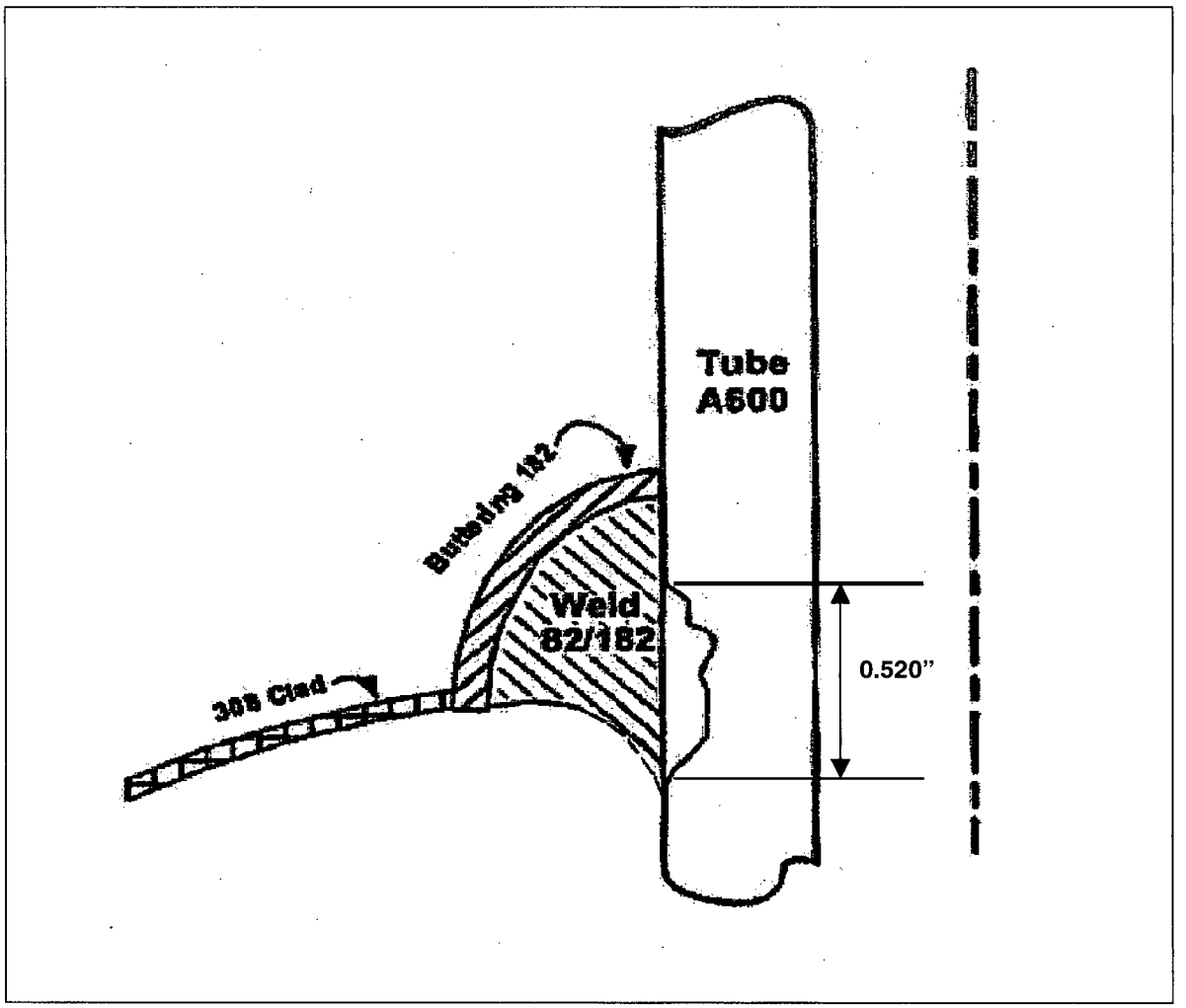


Figure 1 – A non-scale sketch of the ultrasonic indication identified in the Reference 1 report. The inspection identified a 0.520" long x 0.326" deep axial, external indication in the #68 CRDM penetration tube near the J-groove elevation. The 0.326" depth corresponds to approximately 52% of the 0.625" tube thickness. The maximum ultrasonic reflector was approximately 16.5 degrees counter clockwise from the zero reference (as looking upward). The zero reference was the downhill side of the periphery tube. A follow-up eddy current exam detected no relevant indications on the inner surface of the tube.

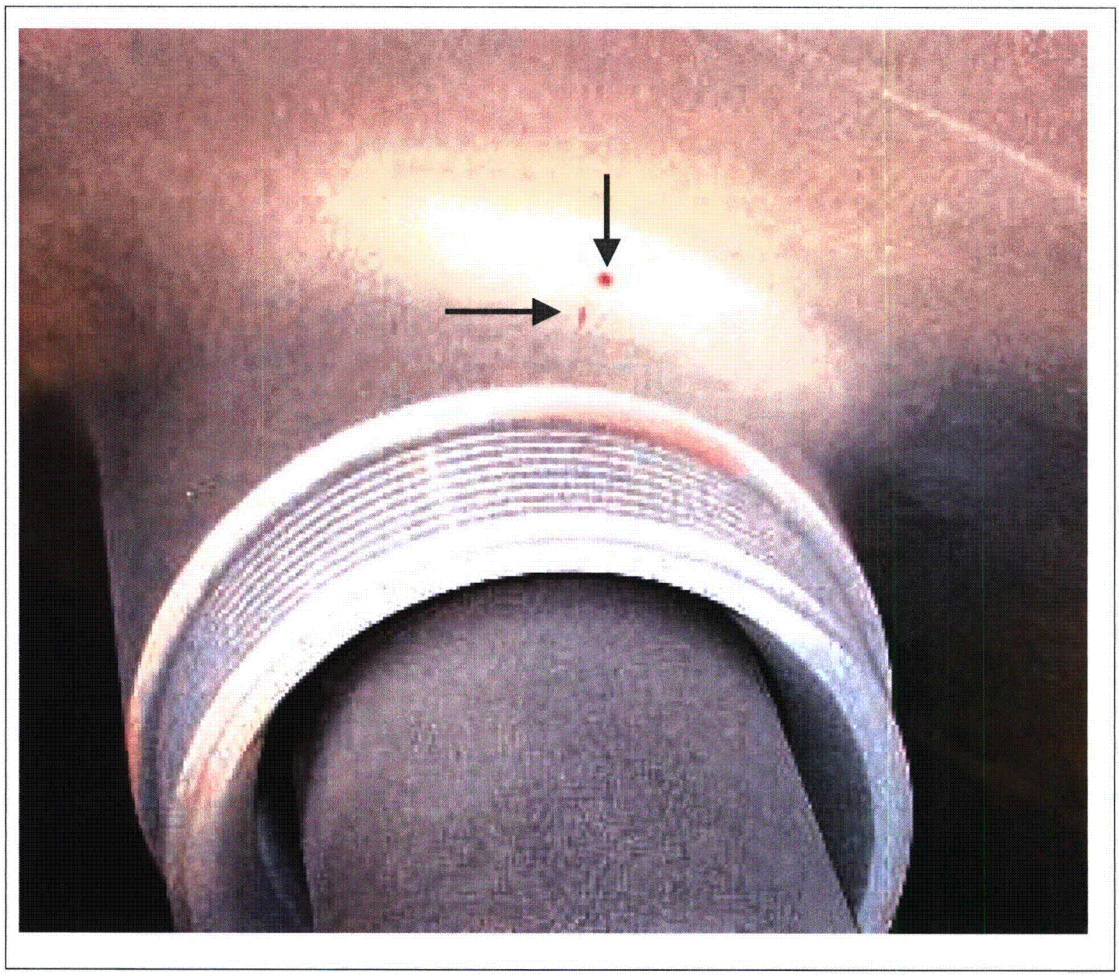

Figure 2 – A photo showing two dye penetrant indications on the surface of the J-groove weld zone for the #68 CRDM penetration (Ref. 2). The axial indication (left arrow) measured 0.150" long and corresponded to the approximate location of the axial ultrasonic reflector. A rounded 0.050" diameter indication was also detected (upper arrow). The lab evaluations indicated the J-groove weld toe was below the axial indication.

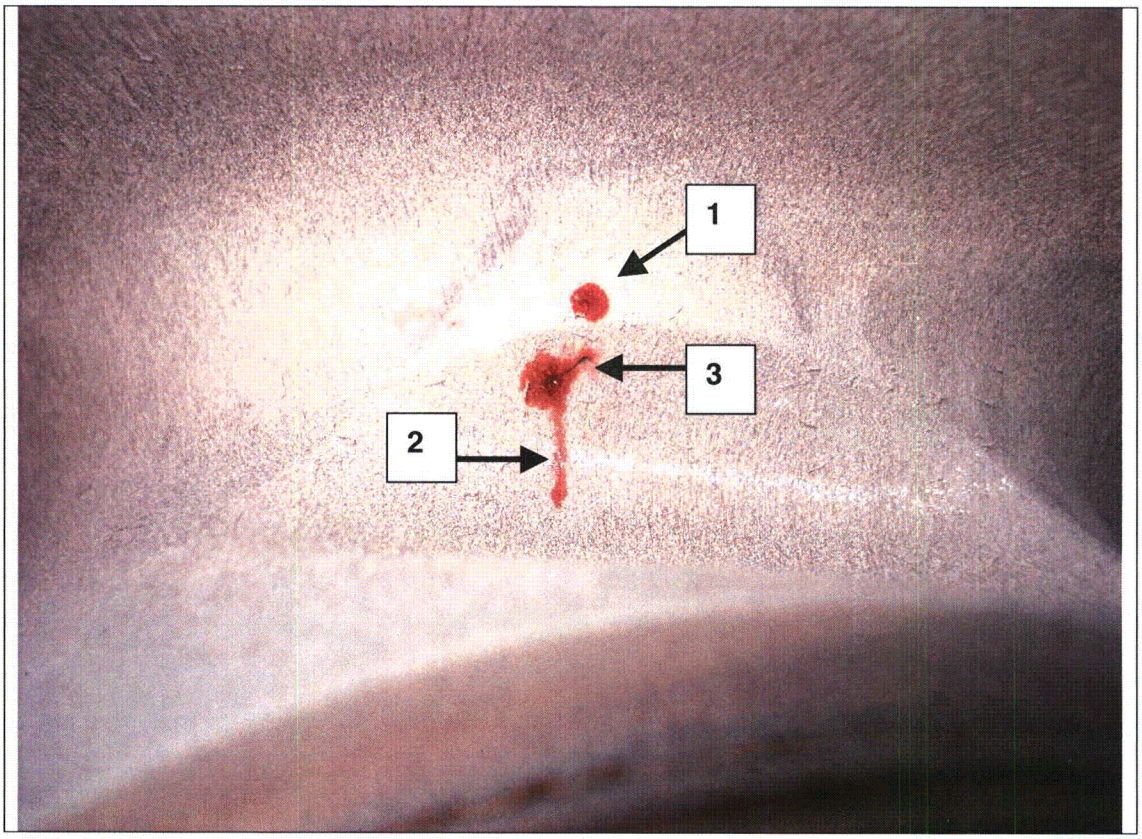


Figure 3 – A photo showing the field dye penetrant results for the excavation site after the boat sample was removed (Ref. 3). The boat sample did not capture the rounded indication (#1) or the deepest portion of the axial indication (#2). In addition, the excavation uncovered an angled, sub-surface linear defect (#3) that intersected the axial indication.

Figure 4 – The non-cut (i.e. wetted) surface of the boat sample. Note the relatively heavy grinding toward the upper half (weld side) of the sample. The sample measured 1.5" long x 0.75" wide. No crack-like indications were visible. (4x Magnification)

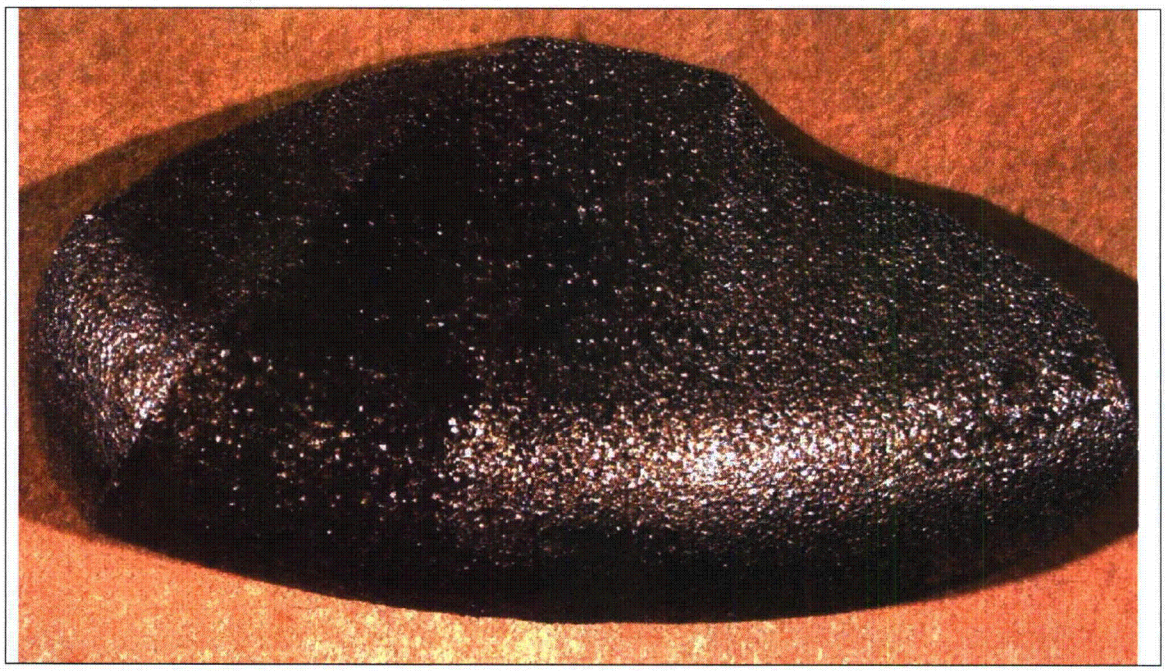

Figure 5 – The EDM cut surface. No cracking was visible. (4x Magnification)

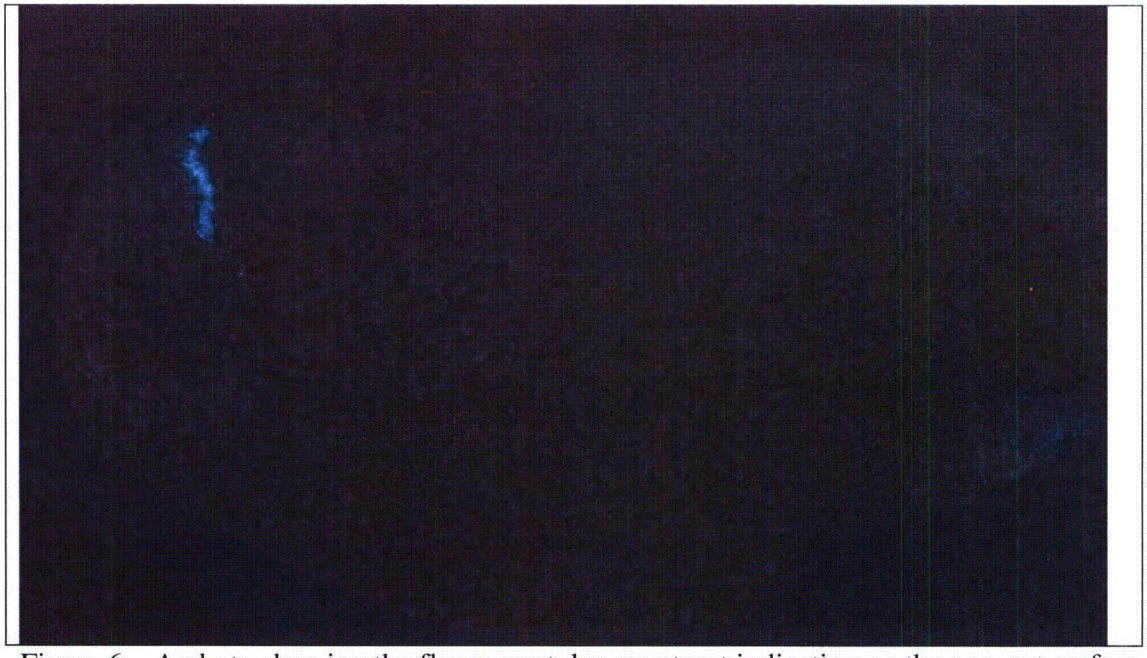

Figure 6 – A photo showing the fluorescent dye penetrant indication on the non-cut surface of the boat sample. The indication measured 0.18" long and followed an irregular path.

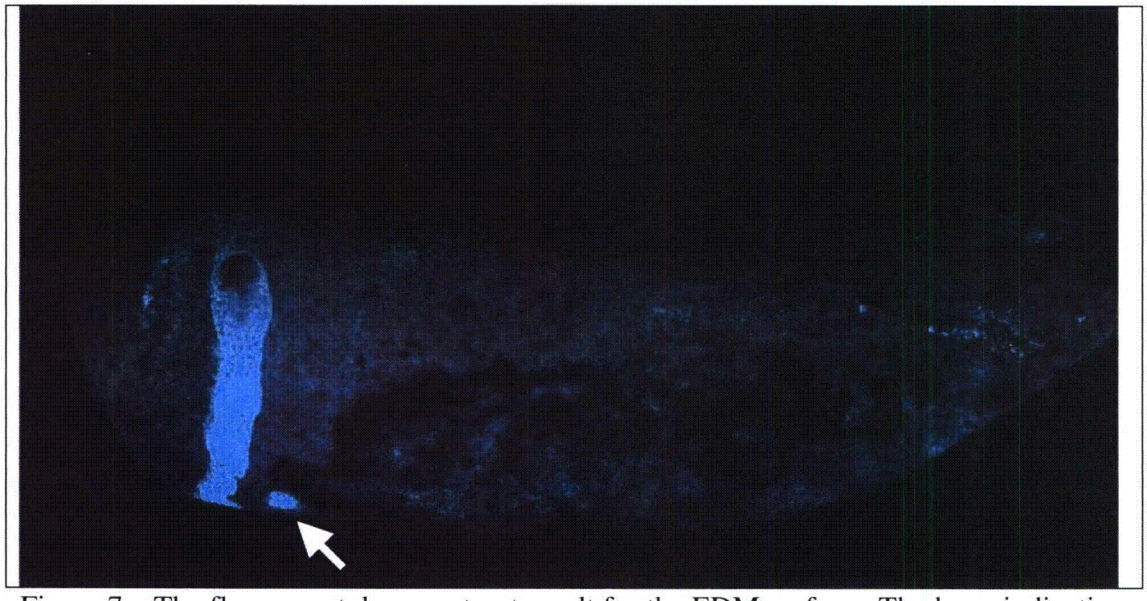

Figure 7 – The fluorescent dye penetrant result for the EDM surface. The large indication measured 0.375" long. Also note the smaller rounded indication (arrow).

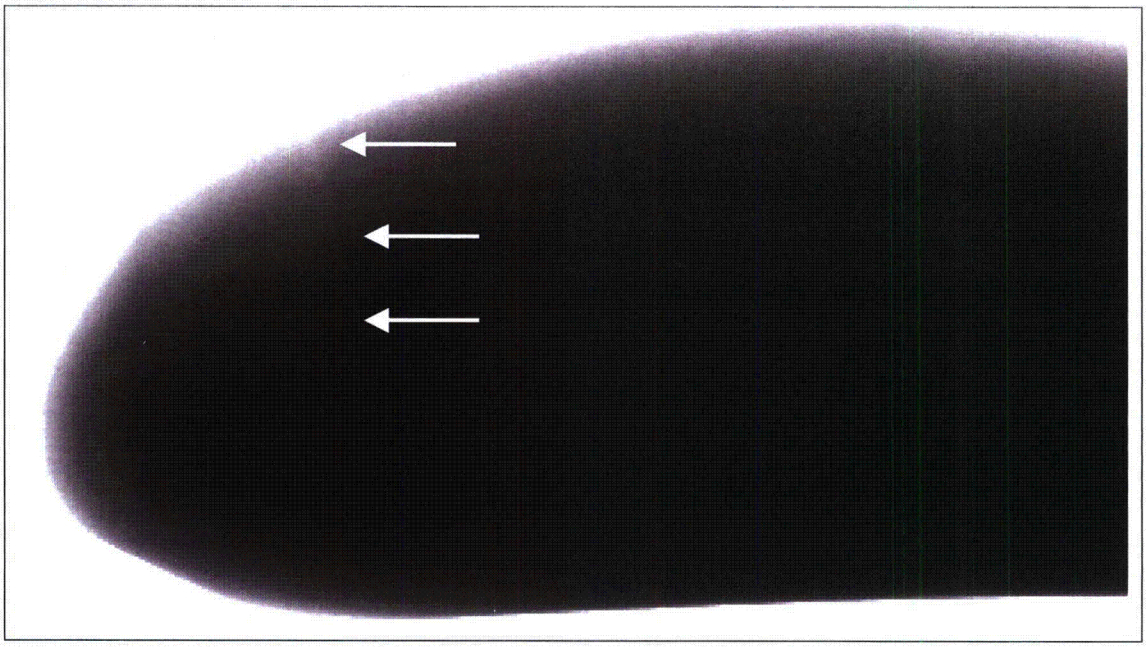

Figure 8 – An X-ray photo with the axial indication highlighted by arrows.

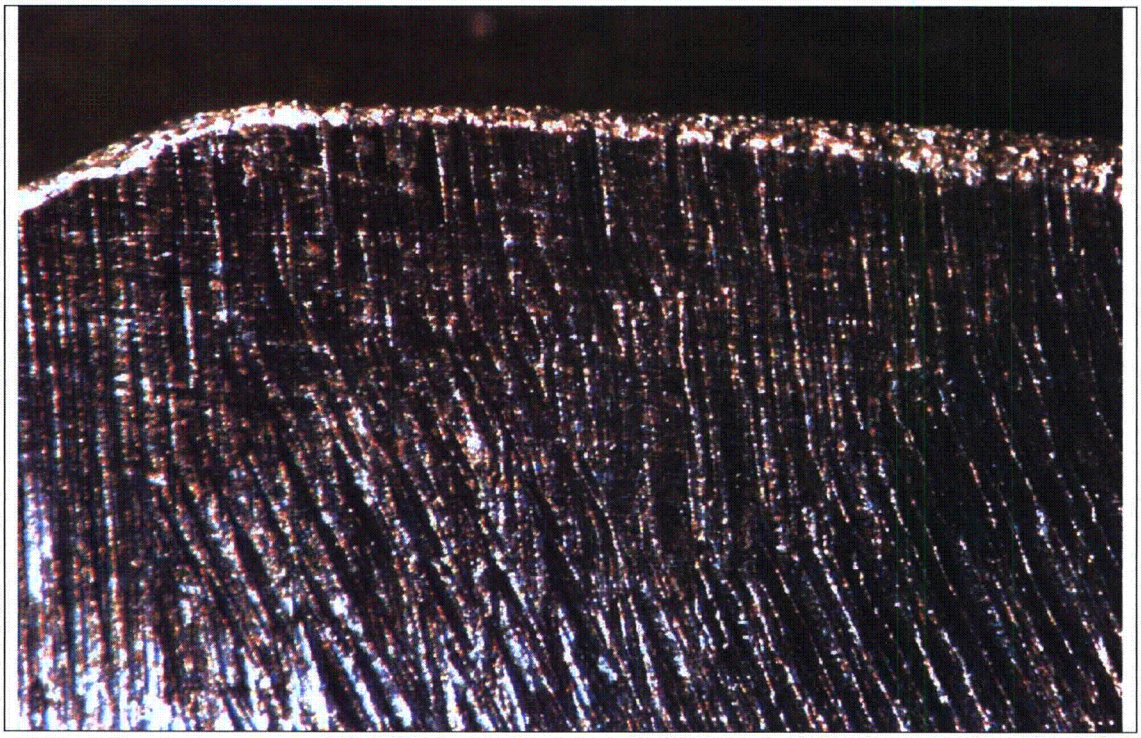

Figure 9 – A stereoscope view in the area of the axial indication region on the non-cut surface. Due to the grinding marks, the indication is not visible. (27x Magnification)

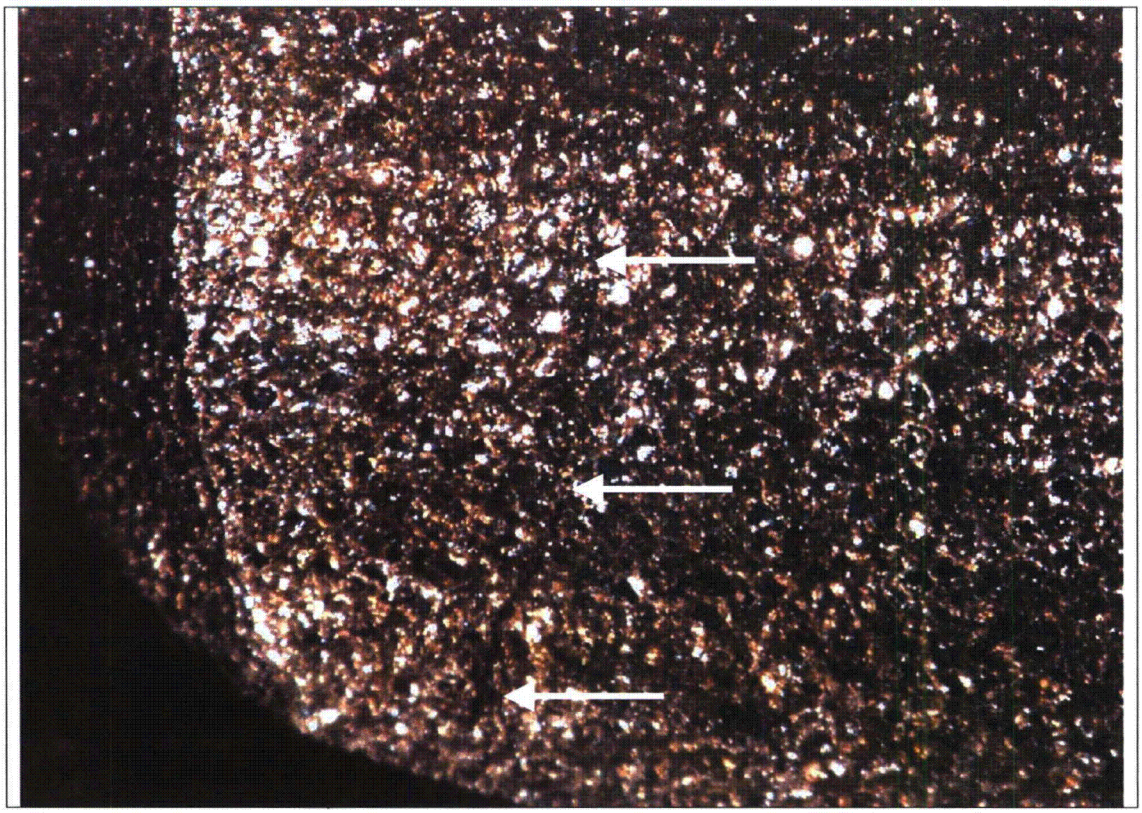

Figure 10 – A stereoscope photo showing the axial crack on the EDM cut surface. (17x Magnification)

Figure 11 – A low magnification SEM photo of the non-cut surface. (4x Magnification)

Figure 12 – An SEM photo near the upper end of the axial indication on the non-cut surface. There is evidence of smearing from the surface grinding. (500x Magnification)

Figure 13 – An SEM photo of the axial crack on the non-cut surface. The crack followed an irregular path and was non-branching. In this area, the crack did not follow the local grinding marks. (500x Magnification)

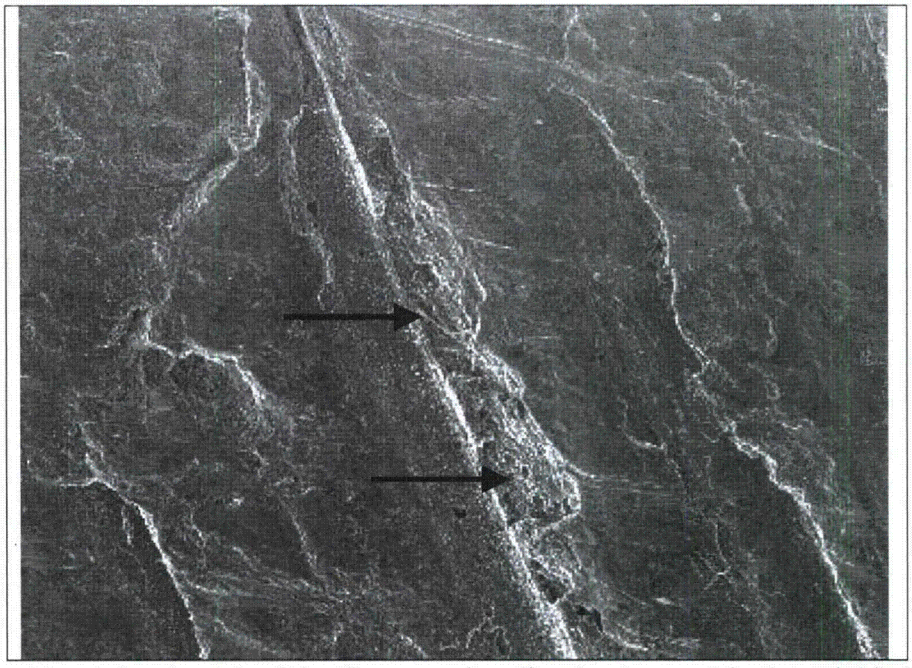

Figure 14 – A local patch of ductile appearing dimples (arrows) in the axial indication on the non-cut surface. The dimples were likely related to the surface grinding. In this area the indication followed the grinding direction. (500x Magnification)

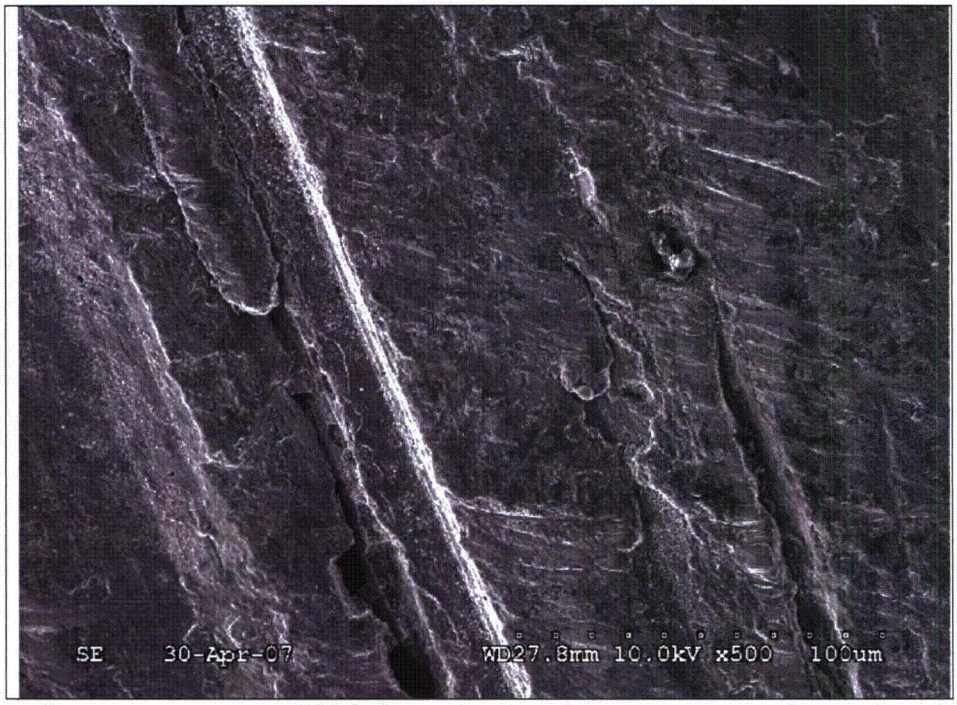


Figure 15 – A representative SEM photo showing fissures that were detected on the non-cut surface. The fissures tended to follow the local grinding marks. None of the fissures were detected by the dye penetrant examination. (500x Magnification)

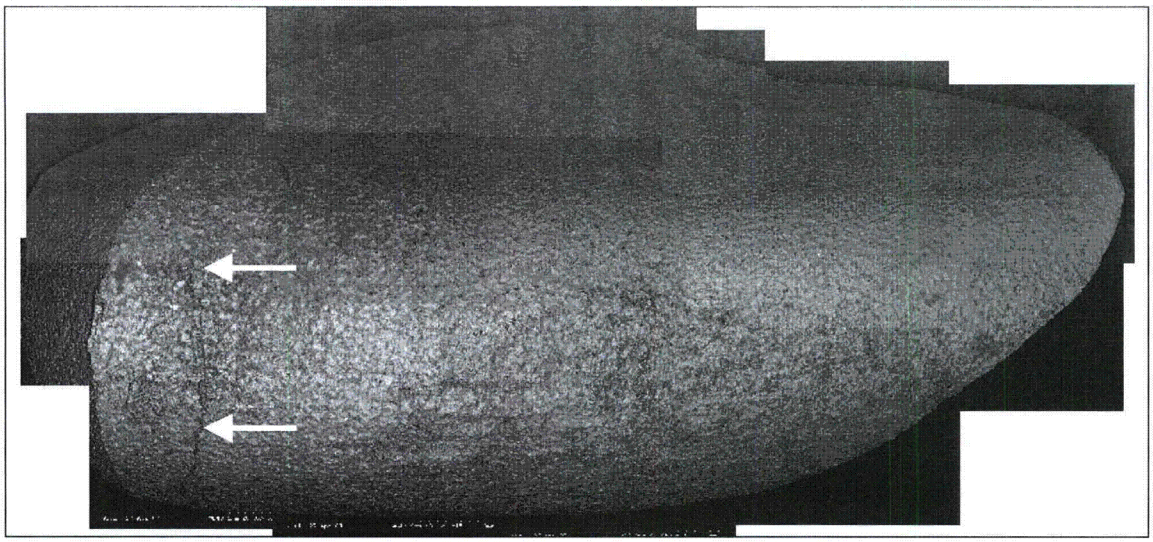

Figure 16 – A backscatter SEM montage of the EDM cut surface. The arrows point to the crack. (4x Magnification)

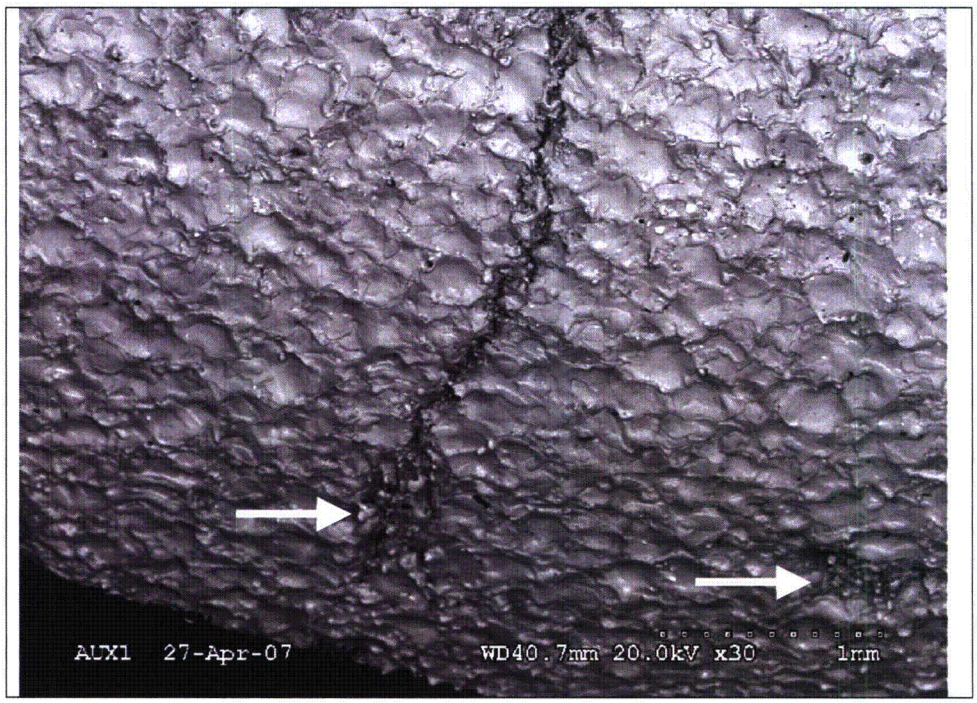


Figure 17 – An SEM photo near the upper end of the axial indication on the EDM surface. The left arrow points to crack branching near the non-cut surface edge. The right arrow points to the globular particles that covered the rounded dye penetrant indication. (30x Magnification)

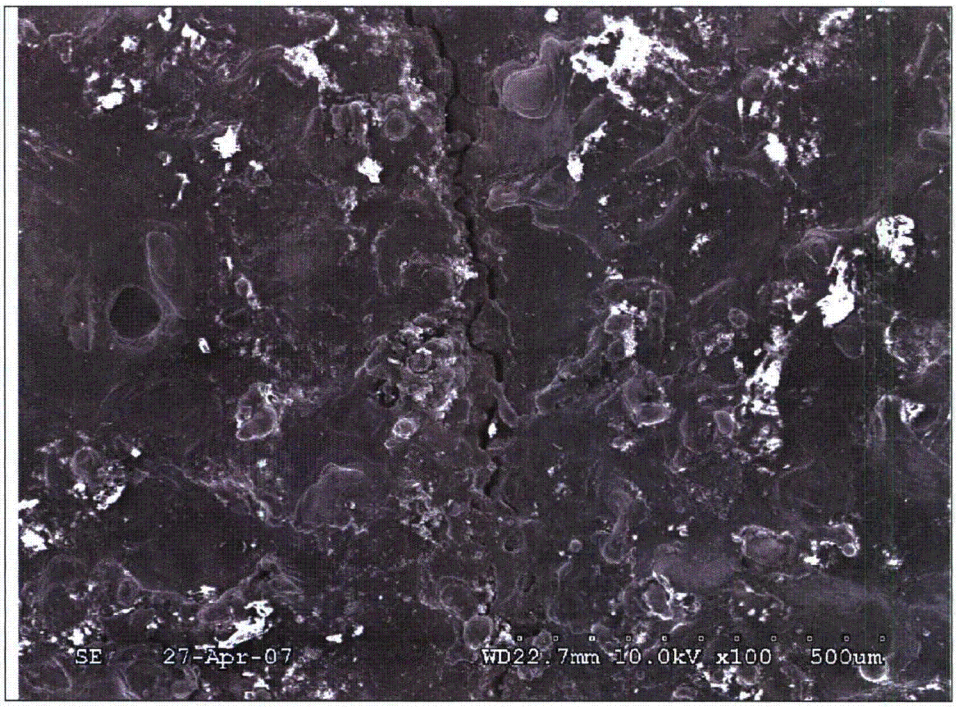

Figure 18 – A typical SEM view of the axial indication on the EDM surface. The crack generally appeared to have intergranular features, although interpretation was difficult due to the EDM process. (100x Magnification)

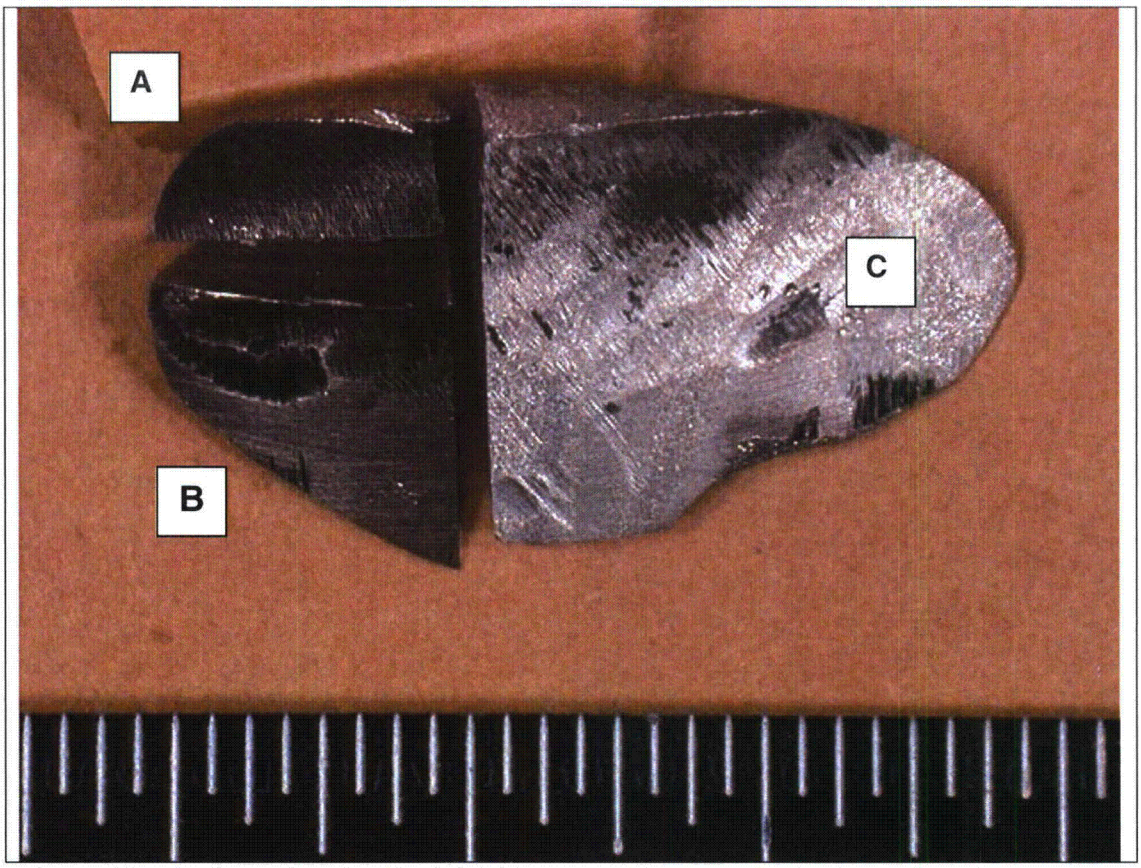


Figure 19 – A photo showing the initial boat sample cuts. The horizontal cut between samples A and B was located approximately 0.050" below the tip of the axial indication. Planned work includes:
Sample A: Additional sectioning as shown in Figure 20.
Sample B: Metallography of horizontal cut face. Microhardness testing
Sample C: Macro-etch cut face to ID weld location. Chemical analysis of tube.

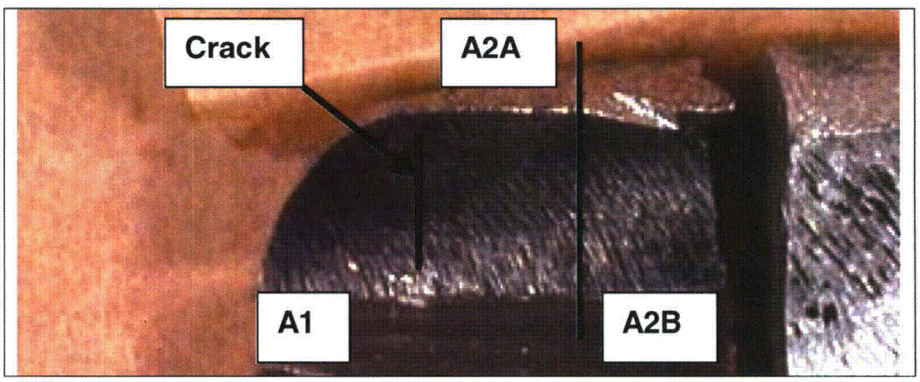


Figure 20 – The sub-sectioning and work plan for Sample A.
Sample A1: Expose crack surface and examine with stereoscope and SEM
Sample A2: Metallurgy mounts on lab A2A/A2B cut face and EDM cut surface
Sample A2B: No work planned

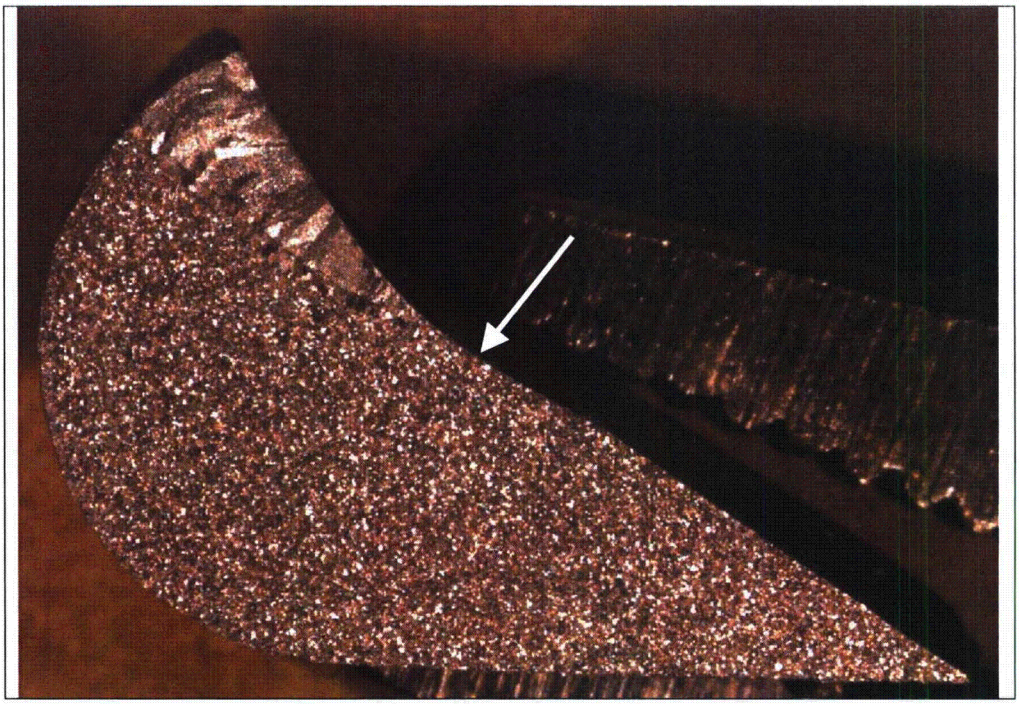

Figure 21 – A macro-etched view of the Sample C cut face. The arrow points to the location of the weld toe on the wetted surface of the boat sample. The tube profile indicates there was minor grinding past the weld toe. (7x Magnification)

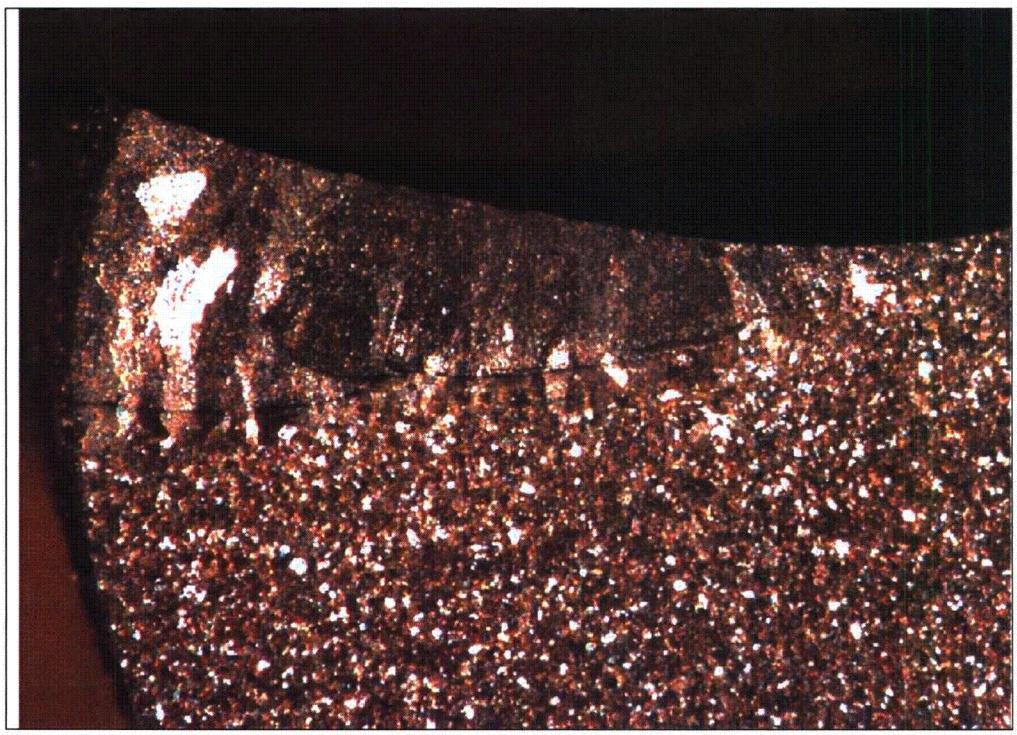

Figure 22 – A closer look at the macro-etched weld. The boat sample contained portions of the last two weld passes. (15.2x Magnification)

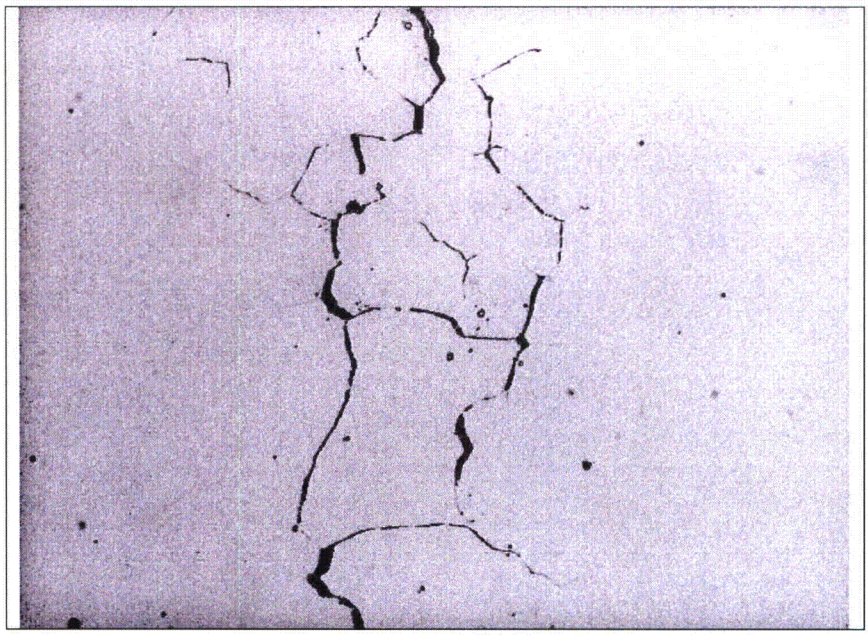

Figure 23 – An un-etched view showing branched, intergranular cracking in the tube portion of the Sample B metallurgical mount. (375x Magnification)

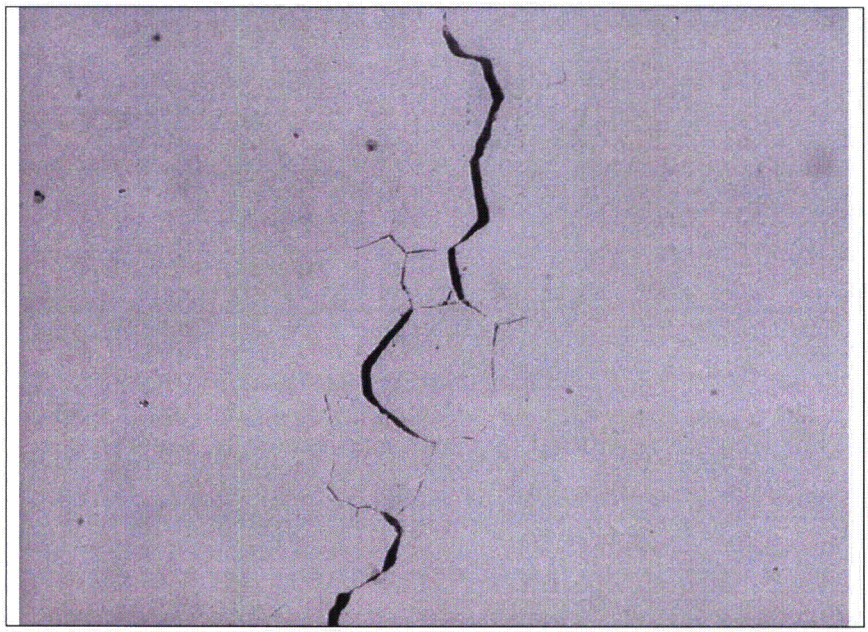

Figure 24 – Additional branched, intergranular cracking in the Sample B tube material. (375x Magnification, Un-etched)

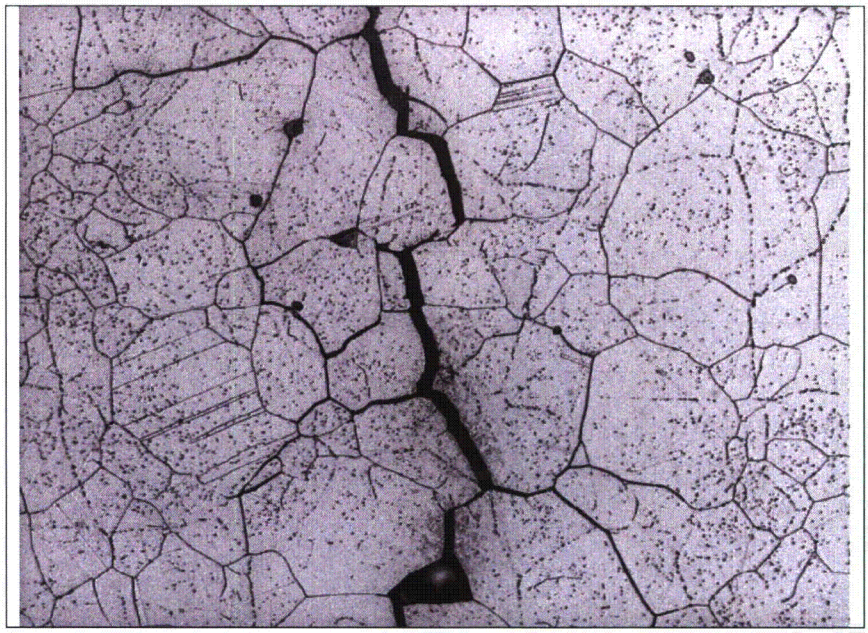

Figure 25 – An etched view of the branched, intergranular cracking in the Sample B tube material. (375x Magnification, Electrolytic Phosphoric-Nital Dual Etch)

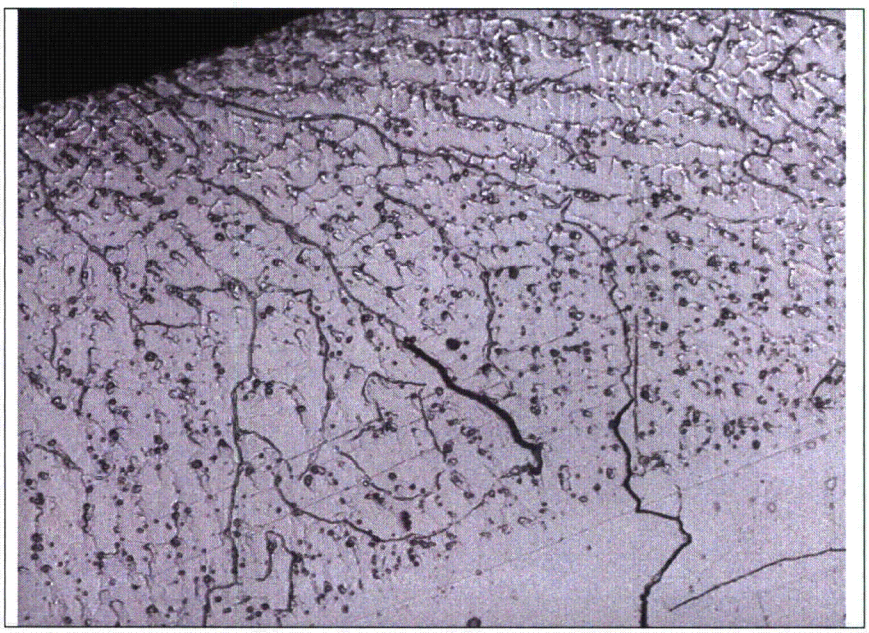

Figure 26 – An etched view near the weld metal crack end in Sample B. The two cracks have an interdendritic appearance. Within Sample B, the cracking did not extend to the wetted surface of the mount. (375x Mag., Electrolytic Phosphoric-Nital Dual Etch)

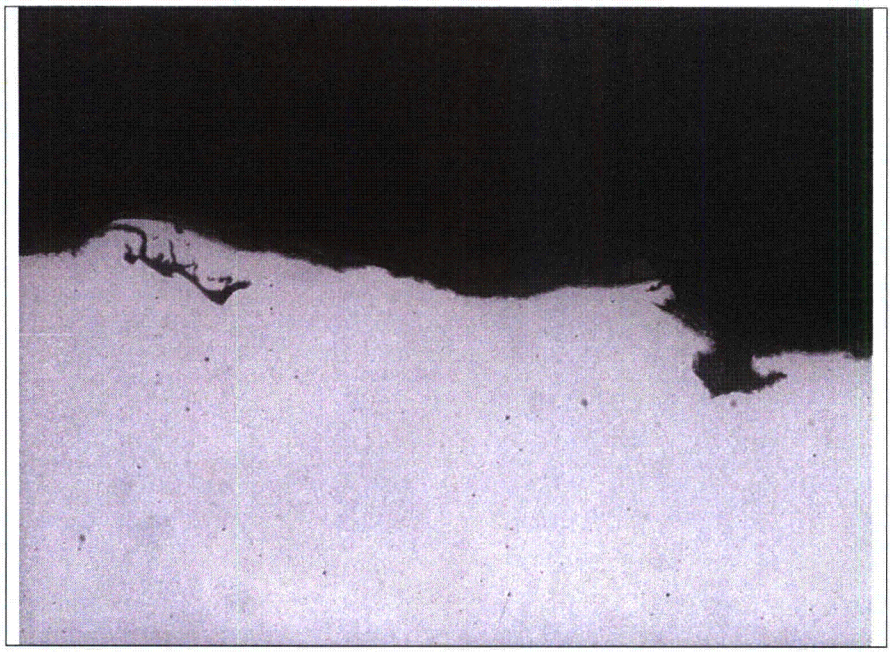

Figure 27 – An un-etched view of two linear irregularities on the weld surface in the Sample B mount. (375x Magnification)

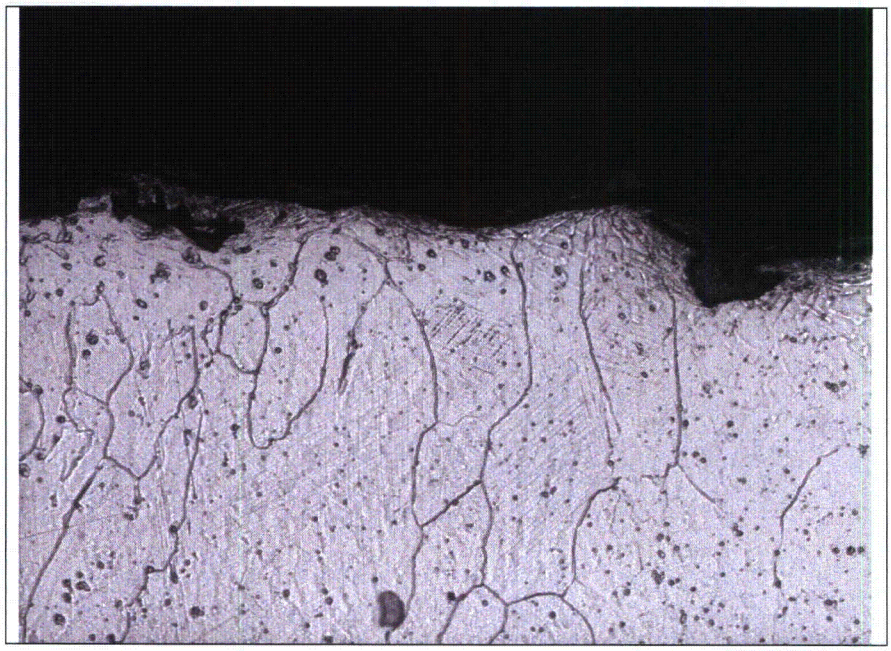

Figure 28 – An etched view of the Figure 27. The locally deformed microstructure suggests the indications were laps from surface grinding. (375x Mag., Electrolytic Phosphoric-Nital Dual Etch)

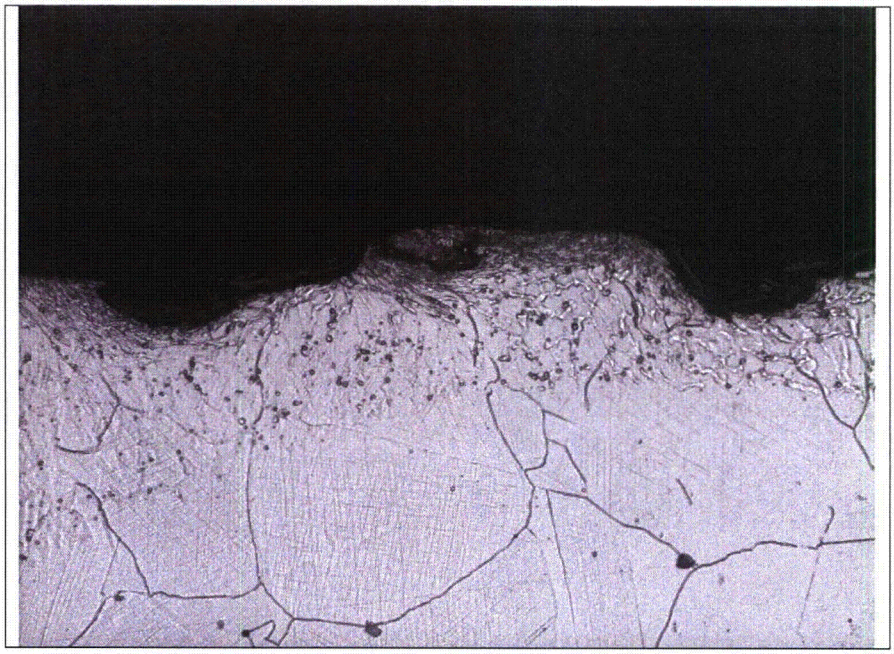

Figure 29 – Another surface indication in the Sample B mount. There was no evidence of crack extension from any of the surface indications. (375x Mag., Electrolytic Phosphoric-Nital Dual Etch)

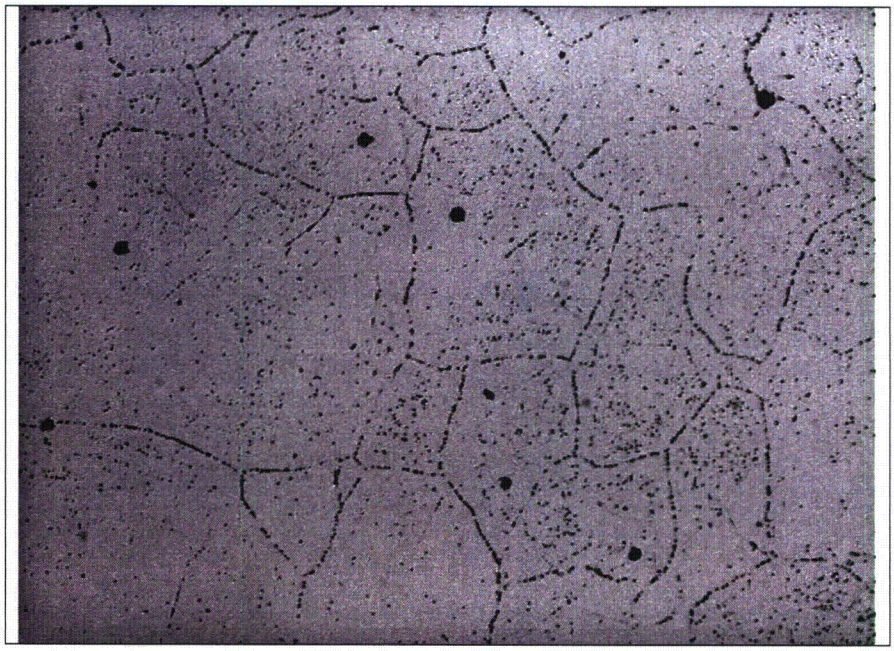

Figure 30 – The Sample B tube material with an electrolytic phosphoric acid etch to reveal the carbide structure. The tube microstructure contained significant intragranular carbides and partially decorated grain boundaries. (375x Magnification)

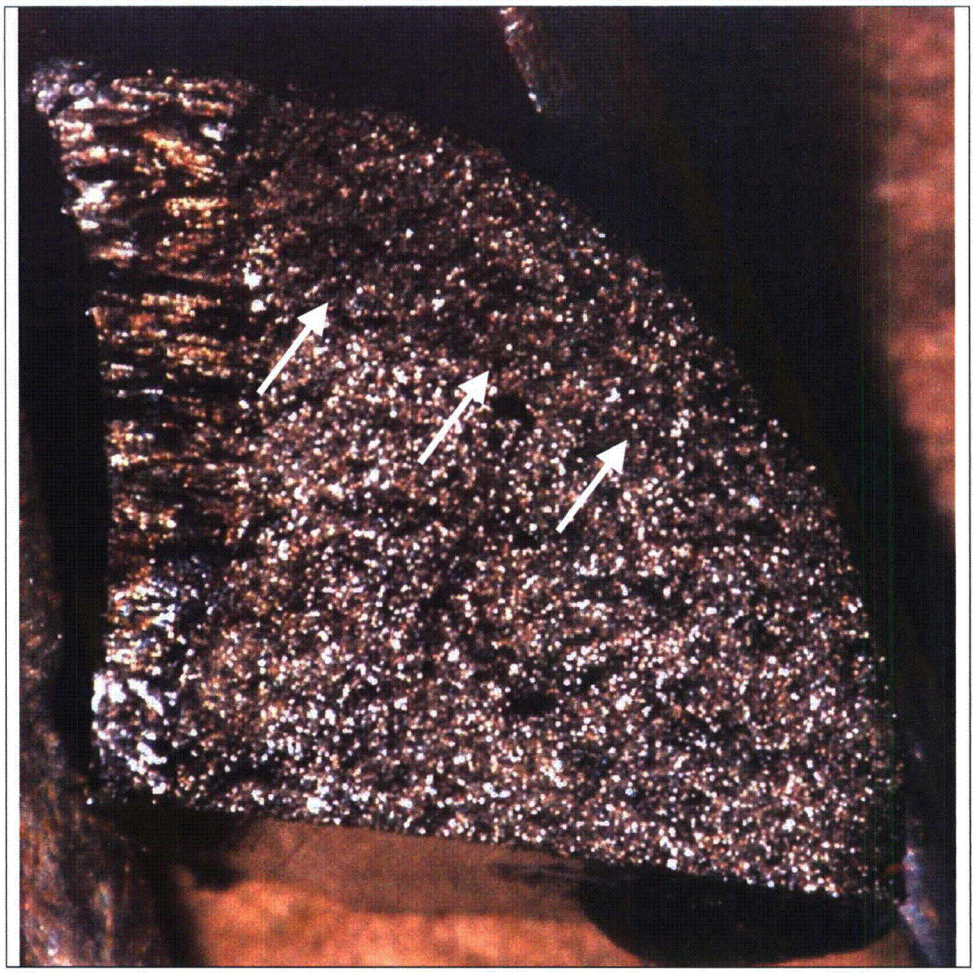

Figure 31 – A stereoscope view of the exposed surface of the axial crack in Sample A1. The weld is toward the left side of the sample. The crack surface was reflective and had an interganular/interdendritic appearance. The arrows point to the edge of a thumbnail-shaped region that appeared to be more oxidized than the remainder of the surface.


Figure 32 – A low magnification backscatter SEM view of the Sample A1 crack surface with the weld along the left edge of the sample. The 'thumbnail' region is also visible. (15x Mag.)

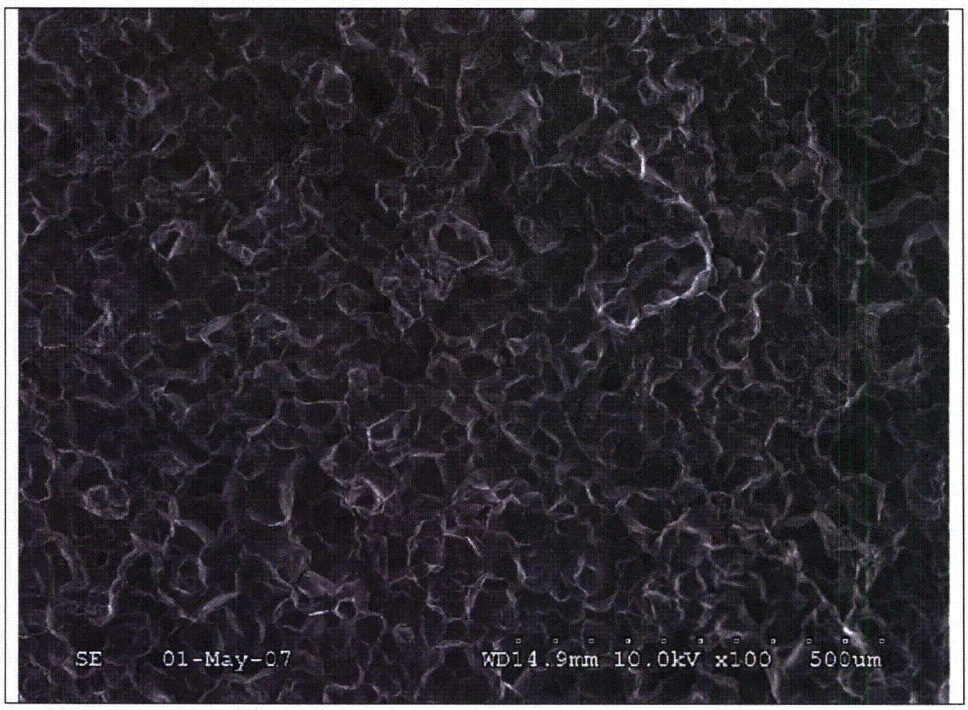


Figure 33 – A typical SEM view of the tube crack surface in the Sample A1. The tube material exhibited intergranular features throughout the sample. (100x Magnification)


Figure 34 – A backscatter SEM image of the intergranular cracking in the dark 'oxidized' region in the Figure 31 stereoscope photo. An EDS evaluation indicated the fine globular particles contained tungsten, which suggests the surface was contaminated with debris from EDM cutting process. (300x Magnification)

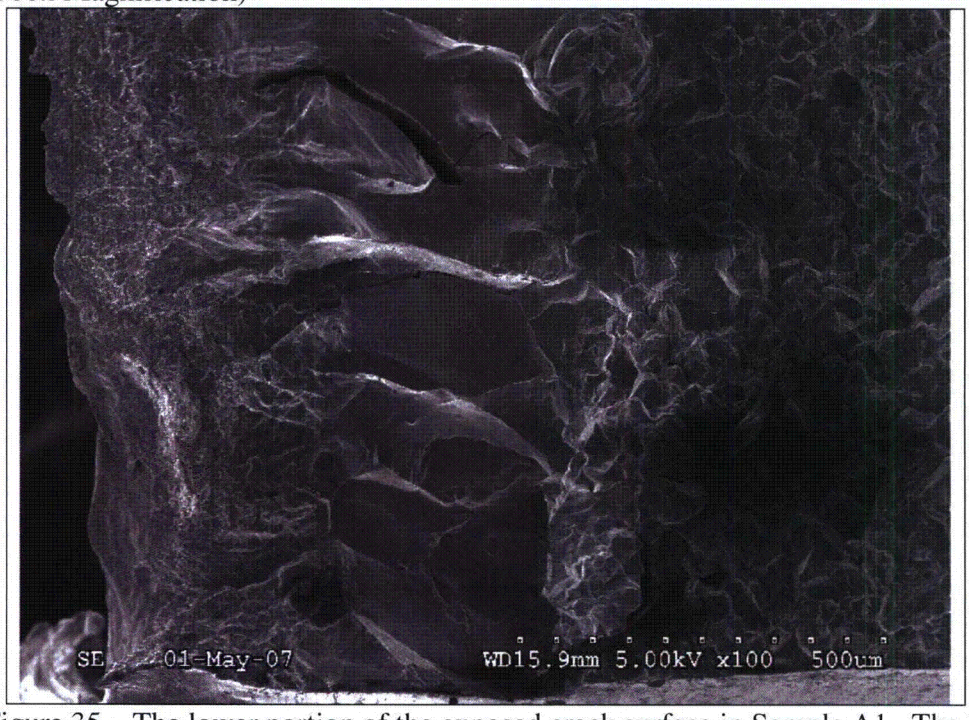


Figure 35 – The lower portion of the exposed crack surface in Sample A1. The left side of the sample is intact weld metal that was broken open in the lab. The large grained area near the center of the photo was located in the base metal heat affected zone. (100x Magnification)


Figure 36 – An SEM photo near the center of the exposed crack in the sample A1 weld. At low magnification, the weld cracking appeared to follow the columnar, interdendritic features of the weld solidification pattern. (50x Magnification)

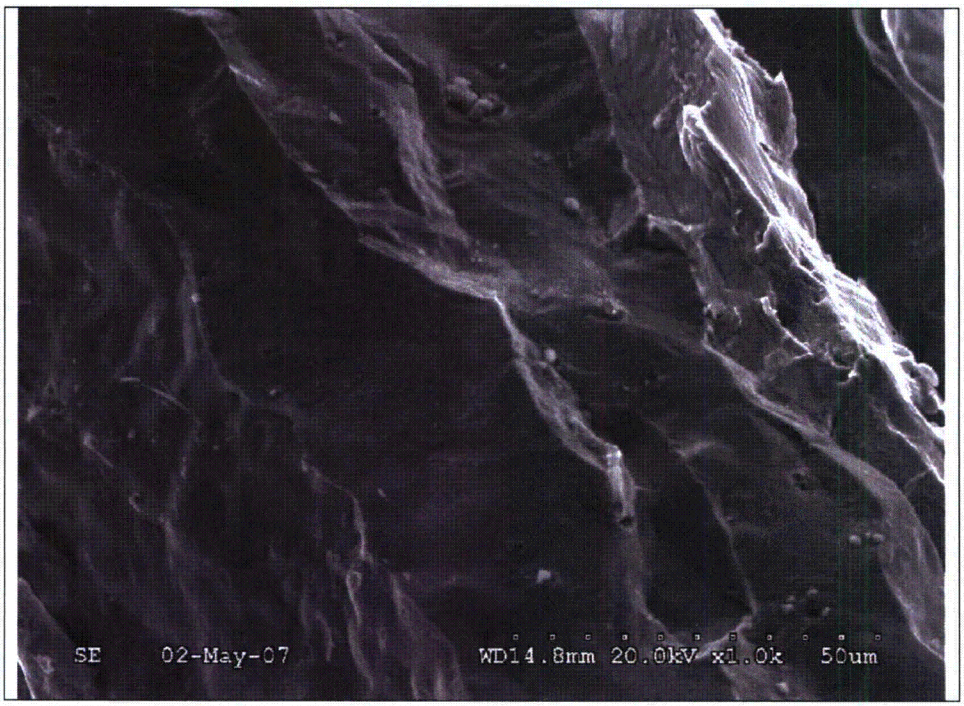


Figure 37 – An SEM photo showing a relatively smooth region of the exposed crack surface of the Sample A1 weld. (1000x Magnification)

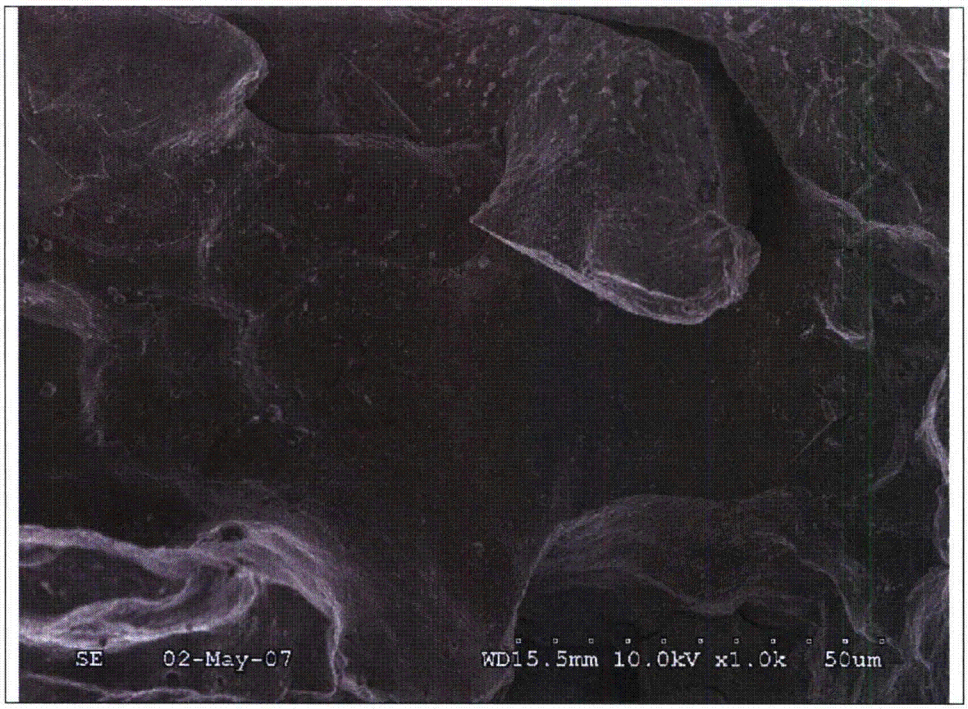


Figure 38 – Another smooth crack surface region in the Sample A1 weld. The smooth appearance is considered more typical of a hot crack than stress corrosion cracking. (1000x Magnification.)

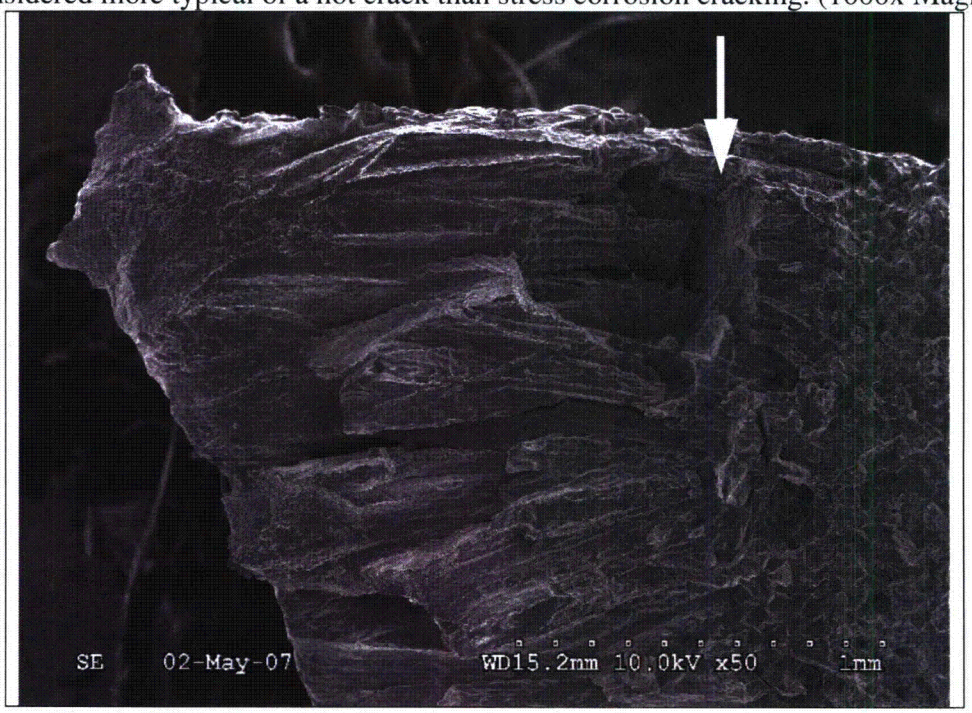


Figure 39 – A SEM view of the Sample A1 crack surface near the upper end of the weld. The arrow points to a planar defect in the weld. There are several cracks within the weld that are connected to the defect. The ductile region toward the upper left corner of the sample was broken open in the lab. (50x Magnification)

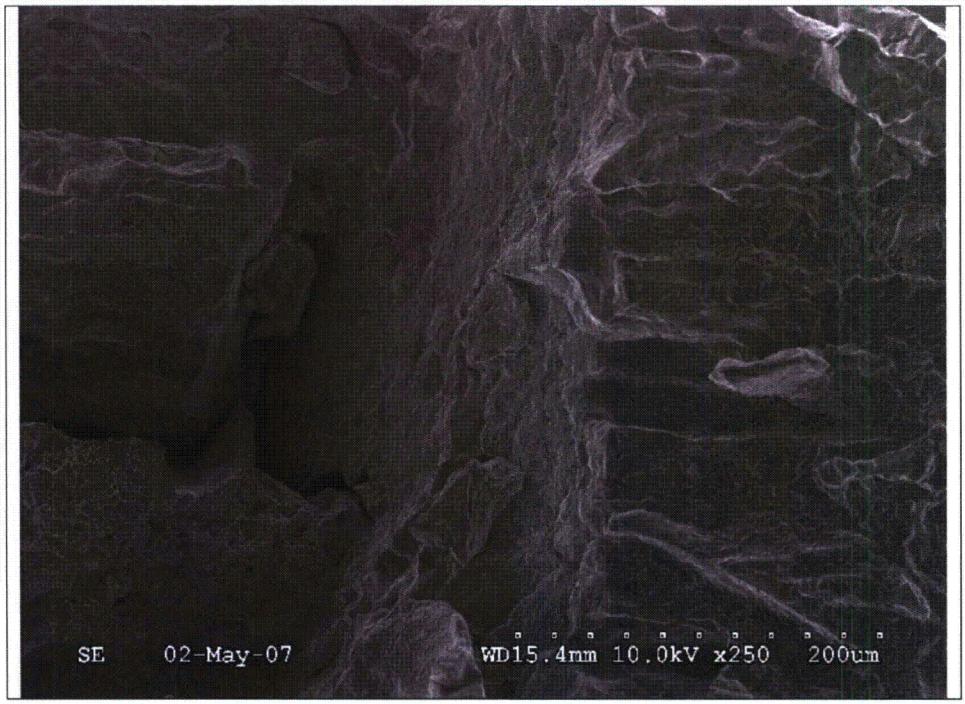


Figure 40 – A higher magnification view of the Figure 39 defect. The defect location and orientation is consistent with lack of fusion between weld passes. (250x Magnification)

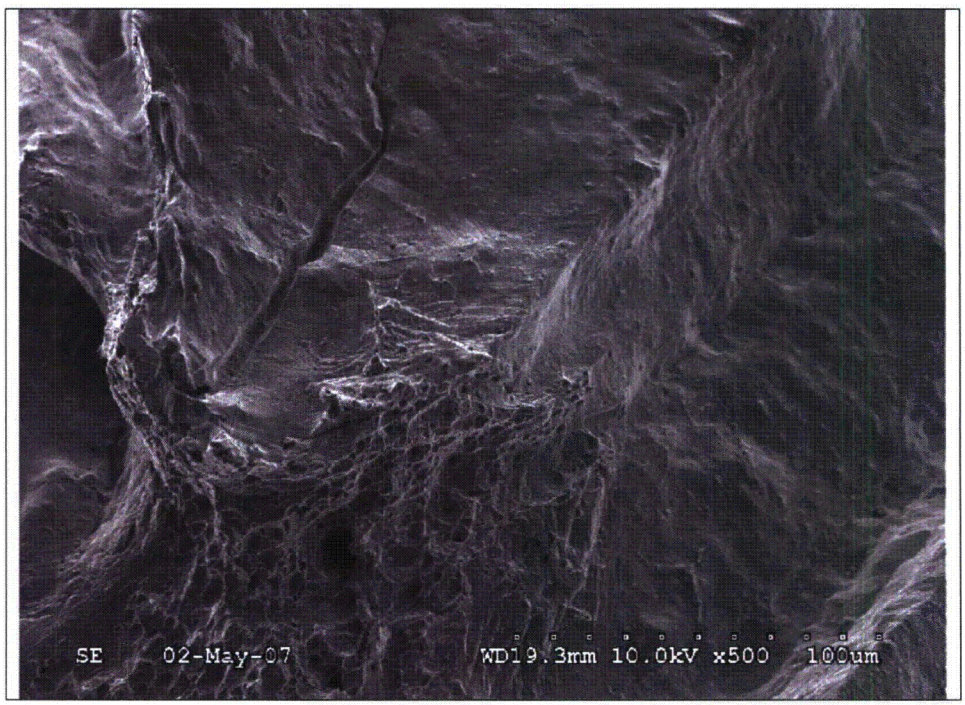


Figure 41 – A local patch of ductile dimples on the exposed crack surface in Sample A1. In general, most of the ductile patches were located toward the wetted surface of the weld. (500x Magnification)

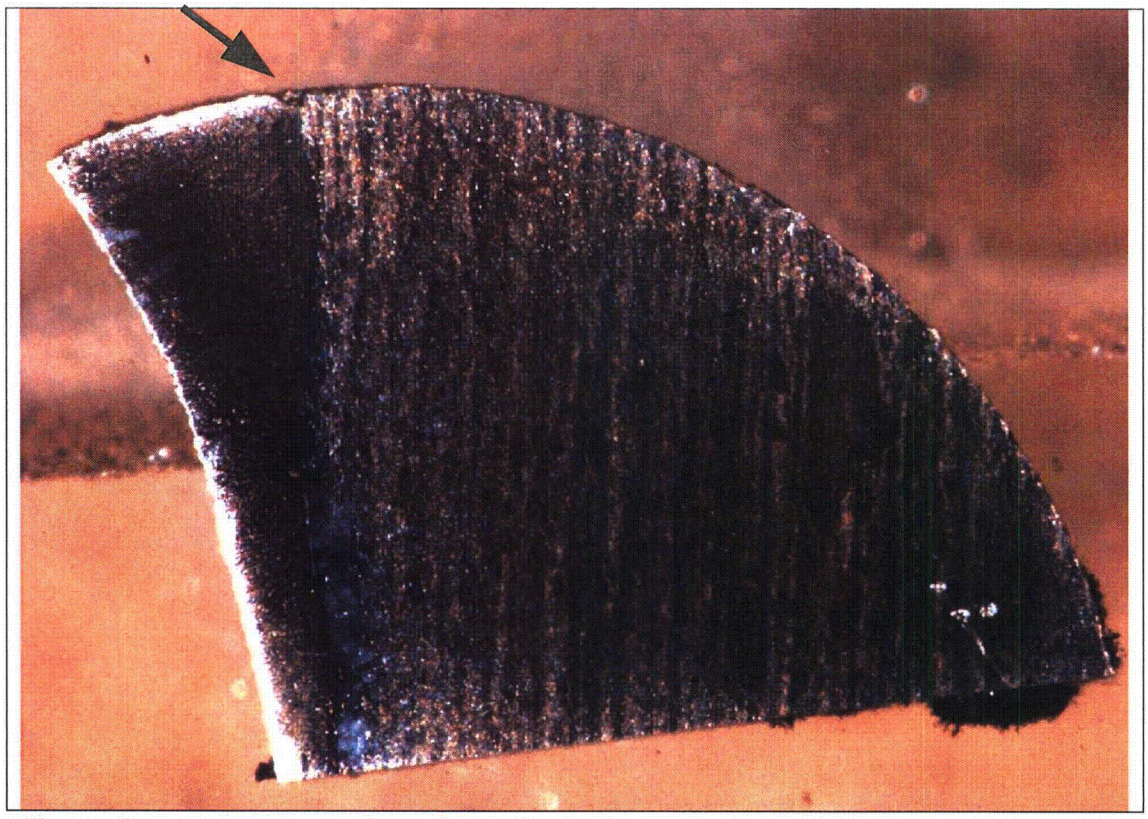

Figure 42 – A stereoscope view of metallurgical Sample A2A. The arrow points to the lack of fusion defect. (17x Magnification)

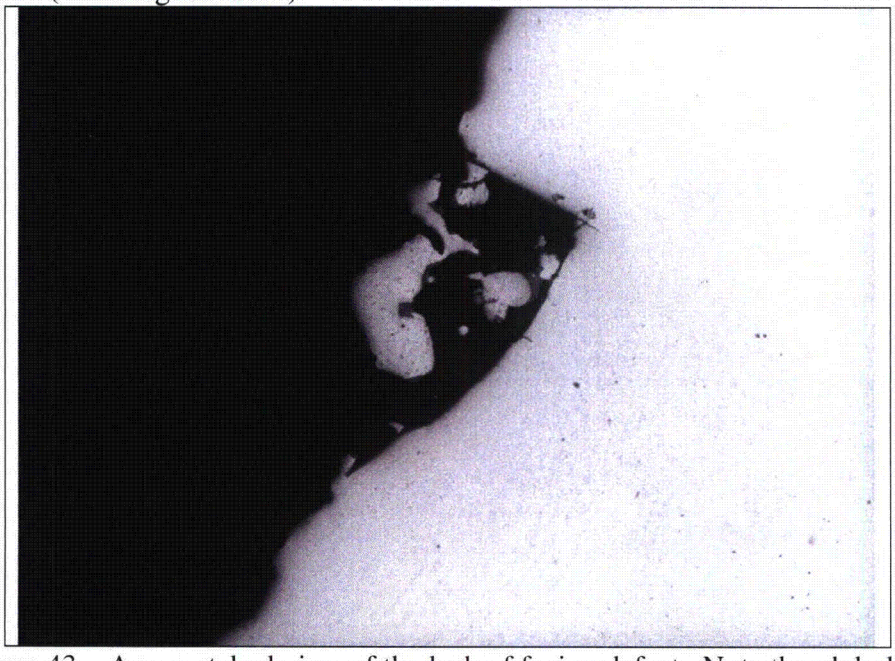

Figure 43 – An un-etched view of the lack of fusion defect. Note the globular debris from the EDM cutting process. The flat region is the tube side of the defect (190x Magnification)

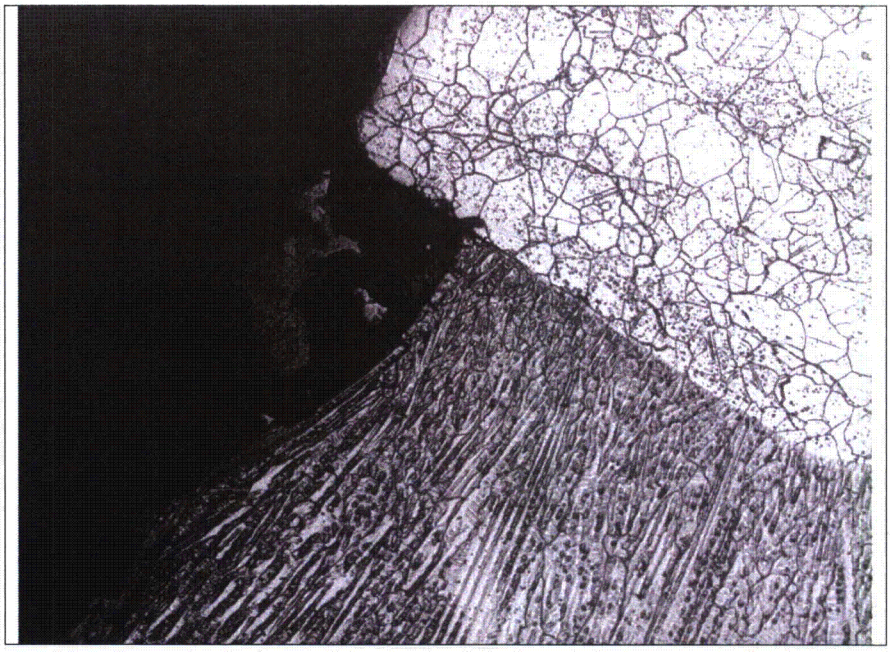

Figure 44 – An etched view of the lack of fusion defect in Sample A2A. Also note the flat interface at the fusion line, which indicates there was little penetration at this location. (190x Magnification, Electrolytic Phosphoric-Nital Dual Etch)

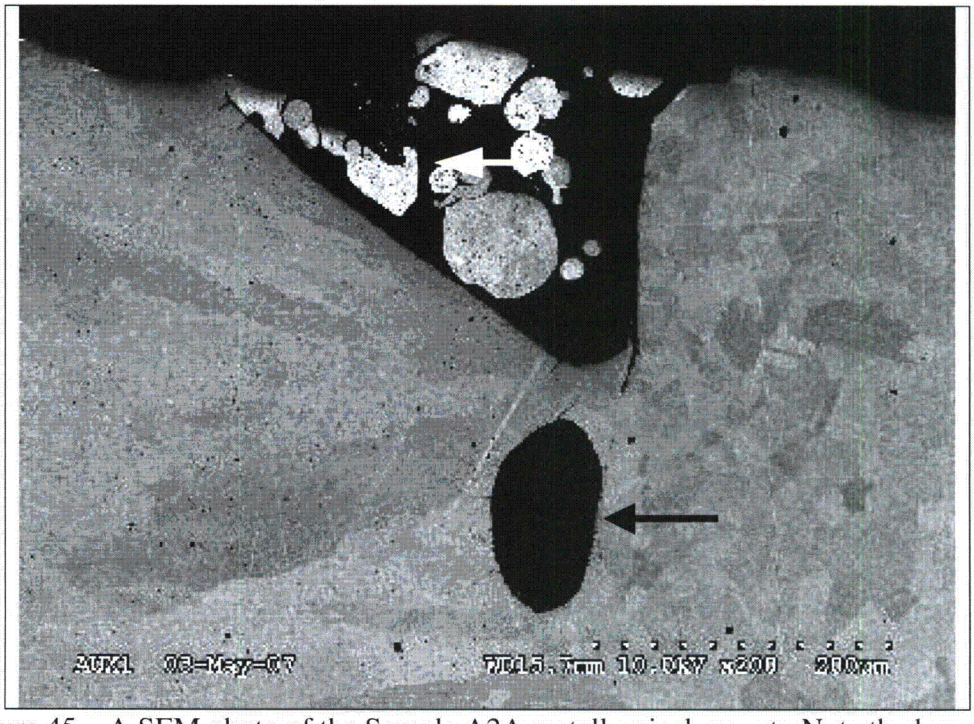


Figure 45 – A SEM photo of the Sample A2A metallurgical mount. Note the large inclusion (arrow) that is adjacent to the lack of fusion defect (200x Magnification).


Figure 46 – A SEM photo of the Sample A2A mount. The arrows point to several incipient cracks that initiated from the inclusion and the lack of fusion defects. The defects are typical of hot cracking. (600x Magnification)

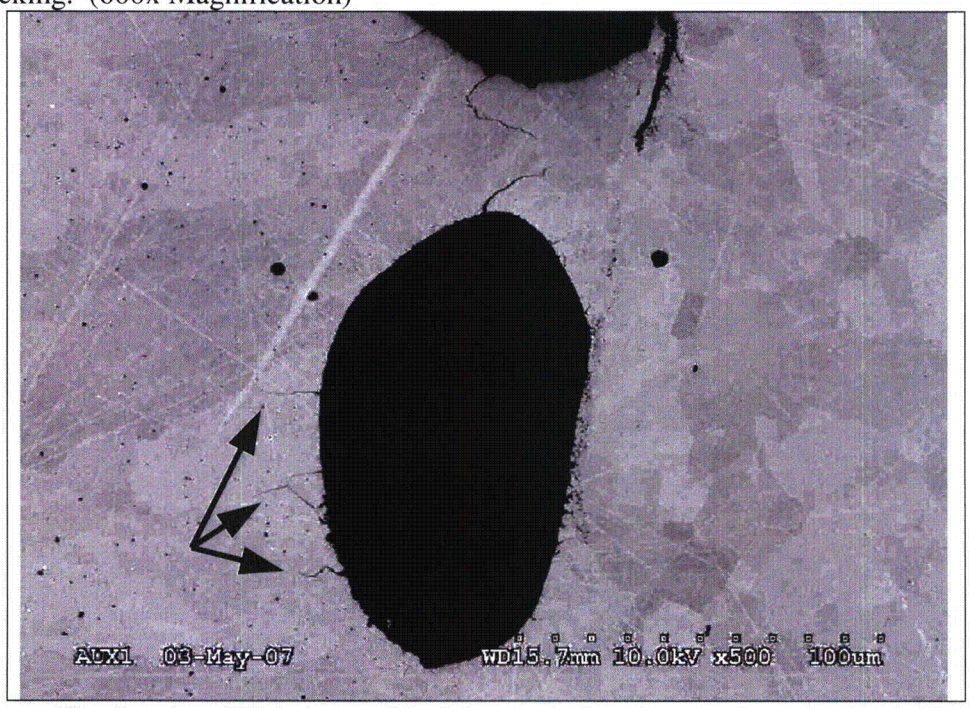


Figure 47 – Another SEM photo with arrows pointing to several cracks that initiated from the edge of the inclusion. The angled appearance of the lower two cracks appears similar to incipient PWSCC. Also note the incipient penetrations along the tube (right) side of the inclusion. (500x Magnification)

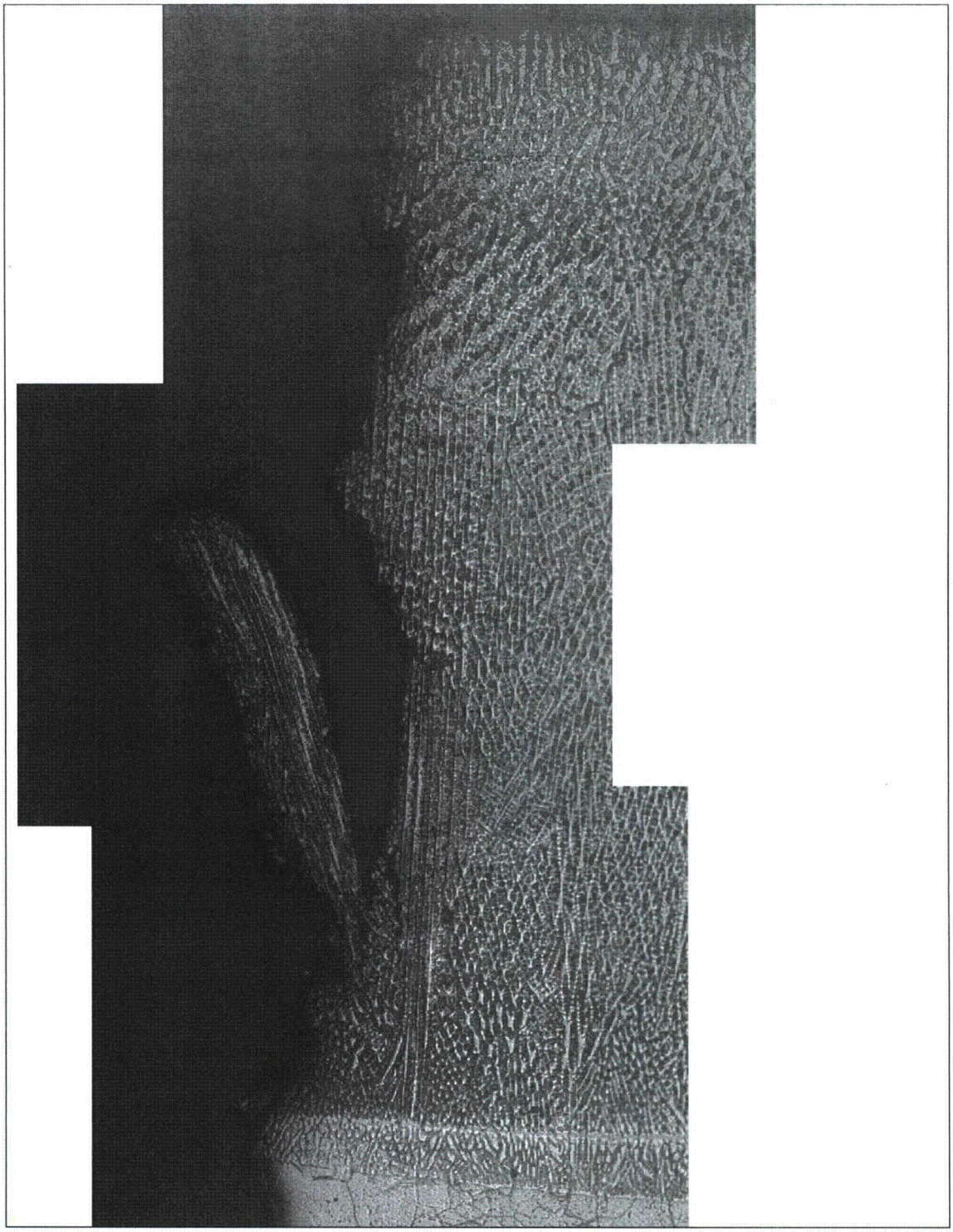

Figure 48 – A montage showing the edge of the axial crack in the Sample A2A weld. There was limited crack branching within the weld. The angled flap was likely pulled open when the crack surface was exposed in the lab. (190x Magnification)

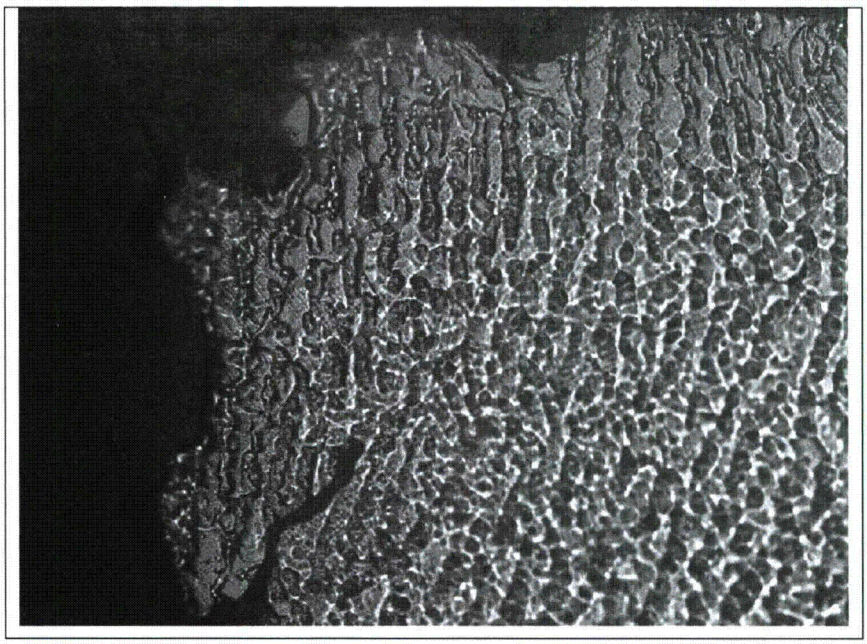

Figure 49 – A higher magnification view of Figure 48 near the wetted surface. In this region, the only branch was angled toward the wetted surface. (375x Magnification, Electrolytic Phosphoric-Nital Etch)

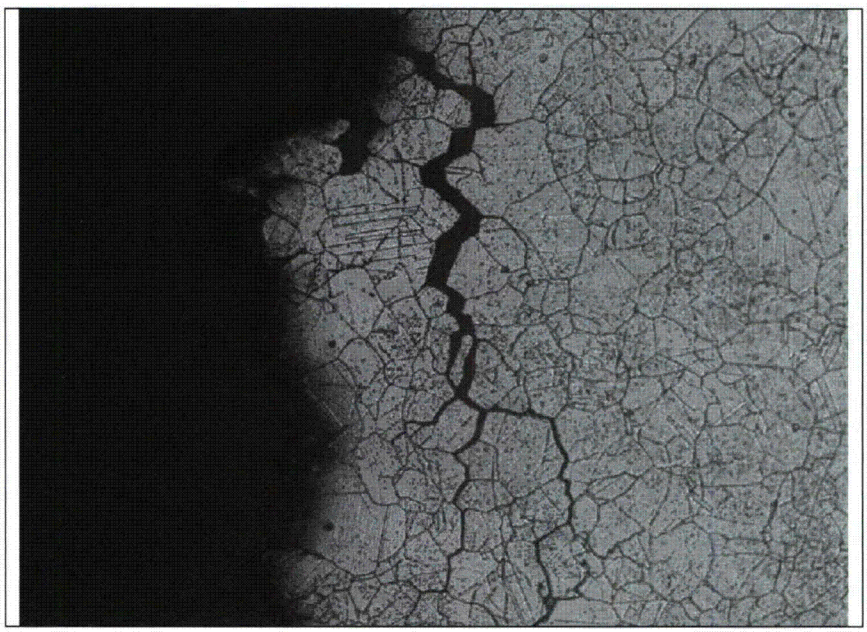

Figure 50 – An intergranular, branched crack that was connected to the axial crack in the Sample A2A tube material. (375x Magnification, Electrolytic Phosphoric-Nital Dual Etch)

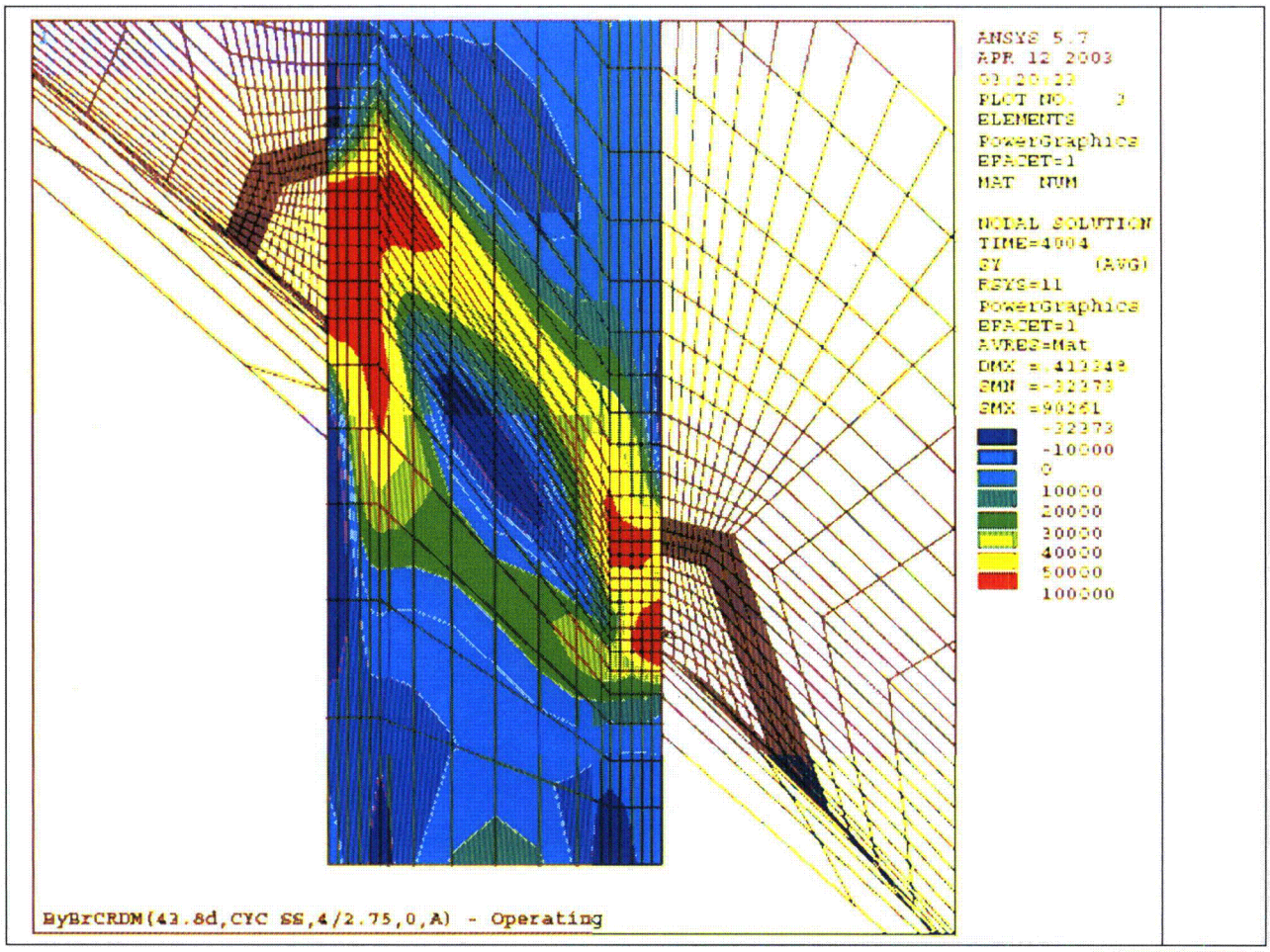


Figure 51 – A hoop stress plot from Reference 9 for the configuration that is applicable to the #68 CRDM penetration. The calculation included residual welding stresses and the stress from the operating pressure. The red areas highlight the high stress regions, which have calculated stresses between 50,000 to 100,000 psi. Note the high stress region at the downhill side of the weld corresponds to the approximate location of the axial indication in the #68 CRDM penetration.

## Laboratory Test Plan for Evaluations of a Crack Containing 'Boat' Sample from the #68 CRDM penetration on Byron Unit 2

A boat sample measuring approximately 1.5" long x 0.790" wide x 0.375" deep was removed from the #68 CRDM penetration on Byron Unit 2. The sample contained a portion of the UT and dye penetrant indications that were detected during Byron B2R13 outage inspections. Photos of the field dye penetrant results for the original indications and the boat sample excavation site are shown in Figures 1 and 2. The removed boat sample is shown in Figures 3 and 4. This document identifies the laboratory test plan developed for the indications in the removed boat sample. (Note: This test plan has been slightly modified from the 'Preliminary' test plan due to the smaller dimensions of the removed boat sample.)

(Note: The relevant results for each test plan step shall be documented by photographs.)

1. Perform low magnification visual and stereoscope inspections (up to 50x) of the external surfaces of the boat sample. Look for surface connected indications, anomalies and other distinguishing features that may be present.
2. Perform a fluorescent dye penetrant 'Zyglo' examination of the boat sample surfaces to determine the location of surface connected indications. Prior to performing the Zyglo exam, the sample will be ultrasonically cleaned in an iso-propanol bath to remove the remnants of the red dye penetrant exams that were performed in the field. The field NDE results from the boat sample excavation site should also be reviewed for potential crack locations.
3. Perform a scanning electron microscope (SEM) examination of the cut and non-cut surfaces of the of the boat sample. The sample will need to be re-cleaned by ultrasonic techniques prior to SEM exam. The purpose is to characterize any defects on the surface and to look for tight defects/cracking that may not have been detected by the Zyglo examination. These results should be compared to the field dye penetrant results for the boat sample excavation site.
4. Perform X-ray radiography exams at several orientations/angles to characterize flaws locations within the boat sample.
5. (Exelon Review Hold Point) Depending on the results of steps 1 thru 4, a sectioning plan will be developed to characterize microstructure, crack depth and crack morphology. The goal of the sectioning plan is to allow for completion of steps 6 thru 10. The sample sectioning should be performed with a diamond (or other thin) cutting wheel to minimize material loss. The on-site Exelon representative (or other Exelon designee) can remove the hold point. As the sectioning cuts are performed, the cut faces should be examined at low magnification for cracking and/or other defects.
6. Prepare a metallurgical mount through a portion of the surface connected linear indication. The mount orientation should be approximately perpendicular to the linear indication. The primary goals of the mount are to characterize the mode of crack propagation, evaluate the weld microstructure, and look for weld defects and other anomalies. If large inclusions or other anomalies are identified, they should be evaluated by SEM/EDS techniques. Prior to

performing metallurgical etching, the lab technician shall demonstrate the suitability of the etchant and etching procedure on a sample with a similar material chemistry. If necessary, multiple grind-polish-examine sequences can be performed to evaluate specific microstructure features. If multiple grinding sequences are performed, the amount of removed material should be measured and recorded.

7. Expose a portion of the linear indication that was detected by the field dye penetrant examination. Examine the exposed surface by scanning electron microscopy and semi-quantitative EDS techniques. The goals of this step are to characterize the crack surface features, identify an initiating region (if present), look for defects/anomalies, and characterize the composition of the oxidation/corrosion products of the crack surface. If there is heavy oxidation on the exposed crack surface, it may be necessary to clean the surface (after the EDS evaluations are completed).
8. It is anticipated that at least three additional metallurgical mounts will be prepared. The specific location and goals for the additional mounts will not determined until the results from the previous steps have been evaluated. It is expected that one of the mounts will evaluate the indication to that corresponds to the dye penetrant indication in the boat sample excavation.
9. Chemical Analysis: If sufficient material exists, a full chemical analysis will be performed on the tube and weld metal to allow for comparison to fabrication specifications. The facility should ensure that appropriate reference standards are available for the chemical analysis technique (e.g., ICP techniques). If the sample size is too small for a full chemistry, semi-quantitative EDS evaluations of the weld and base metals shall be performed on the metallurgical samples. EDS evaluations shall also be performed on any microstructural anomalies that were identified in the metallurgical mounts (e.g., large inclusions).
10. Perform Knoop micro-hardness traverses on areas of interest in the metallurgical mounts.

Additional Requirements:

- The lab facility shall allow for both Exelon and the NRC personnel to witness the lab evaluations.
- The lab facility shall be prepared to store the sample remnants for at least 1 year. The facility shall not dispose of the sample remnants without Exelon approval.

The initial laboratory report will cover the work that is identified in steps 1 thru 10. Depending on the lab results, additional materials characterization by advanced microscopy techniques could be considered (e.g., ATEM, TEM, X-ray diffraction).

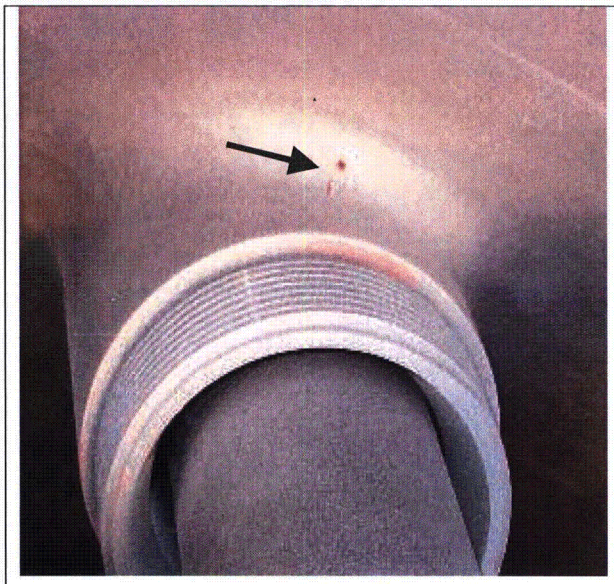

Figure 1 – A photo showing the original linear and rounded dye penetrant indications.

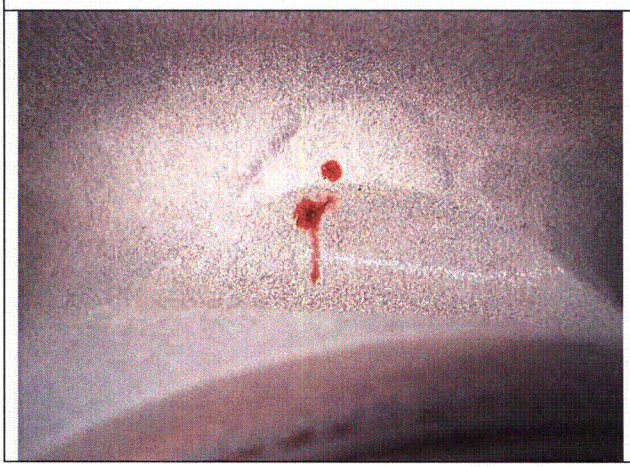

Figure 2 – A photo showing the dye penetrant indications at the boat sample excavation site.

Figures 3 and 4 – Photos showing the upper and lower sides of the removed boat sample.